Multifunctional composite membrane for proton exchange membrane fuel cells

Nguyen, Tien Hoa

2010

Nguyen, T. H. (2010). Multifunctional composite membrane for proton exchange membrane fuel cells. Doctoral thesis, Nanyang Technological University, Singapore.

https://hdl.handle.net/10356/42528

https://doi.org/10.32657/10356/42528

MULTIFUNCTIONAL COMPOSITE MEMBRANE FOR PROTON EXCHANGE MEMBRANE FUEL CELLS

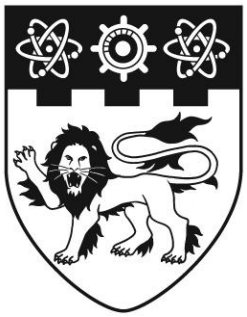

NANYANG TECHNOLOGICAL UNIVERSITY

MULTIFUNCTIONAL COMPOSITE MEMBRANE FOR PROTON EXCHANGE MEMBRANE FUEL CELLS

NGUYEN TIEN HOA

NGUYEN TIEN HOA

SCHOOL OF CHEMICAL AND BIOMEDICAL ENGINEERING

2010

2010

MULTIFUNCTIONAL COMPOSITE MEMBRANE FOR PROTON EXCHANGE MEMBRANE FUEL CELLS

NGUYEN TIEN HOA

School of Chemical and Biomedical Engineering

A thesis submitted to the Nanyang Technological University
in partial fulfillment of the requirement for the degree of
Doctor of Philisophy

2010

ACKNOWLEDGEMENT

I would first like to thank my supervisor, Associate Professor Wang Xin, for his encouragement, guidance and support over the past years. His expertise knowledge about fuel cells and his dedication to students help me grow as a professional. I am deeply grateful for his teachings and advice throughout the duration of this study. I would also like to thank Dr. Liu Yonghao for his assistance, allowing me to benefit the knowledge of electrochemical tests, membrane electrode preparation and fuel cell testing.

I send my thanks to the dedicated staff of School of Chemical and Biomedical Engineering, Nanyang Technological University for their help over the years.

I would like to thank all of my colleagues for their support in both my research and personal life Noel Christian, Wang Shuangyin, Yu Yaolun and Nguyen Truong Son.

Lastly, I want to especially thank my parents, Nguyen Nam and Pham Thi Hue, for their support throughout all of my life. I would like to express special thanks to my wife Pham Thi Lien, my sons Nguyen Tien Dat and Nguyen Tien Dinh for their great affection, devotion and moral support throughout my research career.

ABSTRACT

Novel proton exchange membranes (PEMs) based on (1) a porous polyimide matrix with high porosity, pore sizes on sub-micrometer scale and high mechanical strength and (2) a filling electrolyte having high proton conductivity that fills the pores of the substrate were prepared. In addition to the filling polymer, the host porous matrix affects the success of pore-filling as well as the performance of the composite membrane. Therefore, the selection and synthesis of the material for the host matrix is one of the main objectives in this study. Due to excellent properties of polyimide material compared to others, including high mechanical strength and no swelling following pore-filling, it is selected for fabricating the porous substrate to construct the composite membrane.

Firstly, in order to obtain an appropriate porous film, the morphology and property of porous films prepared from a polyimide precursor following a wet phase separation were investigated. Results indicated that besides cast solution, the film morphology strongly depends on the composition of non-solvent used to develop the porous structure. Experimentally, a spongy type structure is obtained when coagulating the cast film in a mixture of DMF and 1-butanol while the coagulation in water typically develops a film with a finger type. In addition, the pore size of the films is affected by the composition ratio between 1-butanol and DMF. Smaller pore size is obtained following the decrease of 1-butanol content. Moreover, the mechanical strength of the porous film depends on its morphology and pore size. A spongy type film possesses a higher strength compared to finger type one and a film with smaller pores shows higher strength.

Secondly, owning to a high viscosity of the filling electrolyte along with a small pore-size of the host matrix, completely filling the pores of the host matrix with an electrolyte is

critical to the preparation of a composite membrane. Apparently, the porous substrate with larger pores is more likely to be filled with an electrolyte than that with smaller ones. In addition, since most of the filling electrolytes are hydrophilic, the success of pore-filling also heavily depends on the hydrophilicity of the host matrix, with the hydrophilic substrate easier to be filled up than the hydrophobic one. This result indicated that the reason why a wet porous polyimide film with acetic anhydride trapped inside the pores in this study is successful for the filling with a Nafion-based electrolyte while the dry porous matrix is difficult to be filled up even though its pore sizes is bigger.

Lastly, the composite membranes constructed from a porous matrix of polyimide and a filling polymer such as SPSE, Nafion, and a mixture of Nafion and SAZBEA have been made, (designated as PI−SPSE, PI−Nafion and PI−Nafion−SAZBEA, respectively). Due to the filling of the electrolyte with high proton conductivity and the effective suppression of the swelling by the porous matrix with sub-micrometer pores, the composite membranes fabricated have shown a higher DMFC performance than those of Nafion-based membranes. In particular, when a solid proton conductor of sulfonic acid functionalized zeolite BEA nanocrystals (SAZBEA) was incorporated as a composite filler together with Nafion, this composite membrane has exhibited the best performance among all the membranes tested, including high proton conductivity, extremely low methanol crossover, dimensional stability, high durability and high maximum power density in single DMFC test. Moreover, with the presence of SAZBEA to maintain hydration at elevated temperatures, the composite membrane PI−Nafion−SAZBEA has great potential to maintain high proton conductivity and low methanol crossover at such temperatures. **Key words:** Film morphology, Porous polyimide film, Composite membrane, Direct methanol fuel cell.

TABLE OF CONTENTS

LIST OF ABBREVIATIONS

6FAP 2,2'-bis(4-aminophenoxy)hexafluoropropane

6FDA 2,2'-bis(3,4-dicarboxyphenyl) hexafluoropropane dianhydride

6FDA-6FAP polyimide based on 6FDA and 6FAP

AFC alkaline fuel cell

ASTM American Society for Testing and Materials

BAPB 4,4'-bis(4-aminophenoxy)biphenyl

BAPBDS 4,4'-bis(4-sulfophenoxy)biphenyl-3,3'-disulfonic

BAPF 9,9-bis(4-aminophenyl)fluorine

BAPS bis(4-aminophenyl) sulfone

BEA beta-type structure

BSPBs bis(3-sulfopropoxy)benzidines

BTDA benzophenone-3,3’,4,4’-tetracarboxylic dianhydride

BTDA–PPDA/ODA co-polyimide based on BTDA, PPDA and ODA

CLPE crosslinked polyethylene

co-SPIs sulfonated co-polyimides

DDI double de-ionized

DMA	N,N-dimethylacetamide
DMF	N,N-dimethylformamide
DMFC	direct methanol fuel cell
DMSO	dimethylsulfoxide
DSDA	3,3',4,4'-diphenylsulfonetetracarboxylic dianhydride
DSDSA	4,4'-diaminostilbene-2,2'-disulfonic acid
FDA	4,4'-(9-fluorenylidene)dianiline
FE−SEM	field emission scanning electron microscope
FT−IR	fourier transform infrared spectroscopy
GC	gas chromatography
Ludox	colloidal silica 30 (wt.%)
m-BAPPS	bis[4-(3-aminophenoxy)phenyl] sulfone
m-BAPS	bis[4-(3-aminophenoxy)phenyl]sulfone
MCFC	molten carbonate fuel cell
MDA	4,4'-methylene dianiline
m-DDS	4,4'-diaminodiphenylsulfone
MEA	membrane electrode assembly

MeOH	methanol
m-PDA	m-phenylene diamine
Nafion	sulfonated tetrafluoroethylene
NIGT	Nafion-Impregnated Gore-Tex
NNP	N-methyl-2-pyrrolidinone
NTDA	1,4,5,8-napthalenetetracarboxylic dianhydride
OCV	open circuit voltage
ODA	4,4'-oxydianline
ODPA	4,4'-oxydiphthalic anhydride
PAA	poly(amic acid)
PAFC	phosphoric acid fuel cell
PATBS	poly(acrylamide-tert-butylsulfonic acid)
PC	polycarbonate
p-DDS	4,4'-diaminodiphenylsulfone
PE	phenethyl
PEBEA	phenethyl functionalized zeolite BEA
PEM	proton exchange membrane

PEMFC proton exchange membrane fuel cell

PETMS phenethyl trimethoxysilane

PI polyimide

PI−Nafion composite membrane based on porous PI and Nafion

PI−Nafion−SAZBEA composite membrane based on porous PI, Nafion and SAZBEA

PI−SPSE composite membrane based on porous PI and SPSE

PMDA pyromellitic dianhydride

PPDA p-phenylenediamine

Pt/C Pt on carbon

PTFE polytetrafluoroethylene

PtRu/C Pt and Ru on carbon

PVSA poly(vinylsulfonic acid)

RT room temperature

SAZBEA sulfonic acid functionalized zeolite BEA nanocrystals

S-BPDA 3,3',4,4'-biphenyltetracarboxylic

S-BPDA−PPDA polyimide based on S-BPDA and PPDA

SDA	structure-directing agent
SEM	scanning electron microscope
SOFC	solid oxide fuel cell
S-PBDA−ODA	polyimide based on S-BPDA and ODA
S-PBDA−PPDA/ODA	co-polyimide based on S-BPDA, PPDA and ODA
SPES	sulfonated polyether sulfone
SPSE	sulfonated poly(styrene-ran-ethylene)
TEAOH	tetraethylammonium hydroxide
TEM	transmission electron microscopy
TGA	thermogravimetric analysis
THF	tetrahydrofuran
XRD	X−ray diffraction

LIST OF PUBLICATIONS ALL PHRASES AND FIGURES ARE COPIED FROM WITH PERMISSION OF PUBLISHERS

[1] T.H. Nguyen, X. Wang, Multifunctional composite membrane based on highly porous polyimide matrix for direct methanol fuel cells, Journal of Power Sources, 195 (2010) 1024-1030.

[2] T.H. Nguyen, C. Wang, X. Wang, Pore-filling membrane for direct methanol fuel cells based on sulfonated poly(styrene-ran-ethylene) and porous polyimide matrix, Journal of Membrane Science, 342 (2009) 208-214.

[3] T.H. Nguyen, X. Wang, Fabrication of the porous polyimide film as a matrix of the composite membrane of the direct methanol fuel cell, Separation and Purification Technology, 67 (2009) 208-212.

LIST OF FIGURES

LIST OF TABLES

LIST OF PUBLICATIONS

[1] **T.H. Nguyen**, X. Wang, Multifunctional composite membrane based on highly porous polyimide matrix for direct methanol fuel cells, Journal of Power Sources, 195 (2010) 1024-1030.

[2] **T.H. Nguyen**, C. Wang, X. Wang, Pore-filling membrane for direct methanol fuel cells based on sulfonated poly(styrene-ran-ethylene) and porous polyimide matrix, Journal of Membrane Science, 342 (2009) 208-214.

[3] **T.H. Nguyen**, X. Wang, Fabrication of the porous polyimide film as a matrix of the composite membrane of the direct methanol fuel cell, Separation and Purification Technology, 67 (2009) 208-212.

[4] Y. Liu, **T.H. Nguyen**, N. Kristian, Y. Yu, X. Wang, Reinforced and self-humidifying composite membrane for fuel cell applications, Journal of Membrane Science, 330 (2009) 357-362.

[5] S.T. Nguyen, H.M. Law, **T.H. Nguyen**, N. Kristian, S. Wang, S.H. Chan, X. Wang, Enhancement effect of Ag for Pd/C towards the ethanol electro-oxidation in alkaline media, Applied Catalysis B: Environmental 91 (2009) 507-515.

Chapter 1 Introduction

1.1 Background and Motivation

Over the past decades, the consumption of petroleum products as fuel for transportation and industrial activities has grown significantly due to the growth of population and industry in developing countries. As a speculation for next decades, the global demand on fuel will exceed the supply, and as a result, crude oil price will increase sharply and shortage of oil supply will occur, leading to an economic downturn and recession. In addition to high energy consumption, environmental concerns including climate change and global warming caused by burning fossil fuels take much attention at this time because they directly affect human beings.[1] Therefore, how to deal with carbon emissions, how to transit to less polluting energy sources and how to efficiently use energy will be the major challenges for future energy consumption. For years, internal combustion engines used to power most vehicles and industrial machines are well developed, cheap and powerful but they are inefficient (10-30%) and generate a lot of carbon emissions because of the low efficiency of fuel burning.[2] Recently, researchers have focused on developing electric vehicles based on battery to increase efficiency and reduce pollutants. [3] However, a battery cannot provide enough energy storage capacity to drive the vehicle for long distance and power heavy machines. In addition, to recharge the battery, it needs electrical power from power plants which also emit pollutants because of the burning of coal or other fuels.

To deal with such issues, fuel cells are considered as an alternative energy conversion device to combat environmental problems and reduce the reliance on fossil fuels. A fuel cell typically generates power by chemical reactions at electrodes instead of fuel

combustion as an internal combustion engine. As a result, less or no carbon emission is recognized for the fuel cell systems.[4] Among them, proton exchange membrane fuel cells (PEMFCs) is the most promising candidate as a sufficient and clean energy source for stationary, transportation and in particular, portable devices because they could generate more power density compared to others. [5] The high power density allows the manufactured fuel cell devices to be compact and lightweight while maintaining enough output to drive devices. The fuel using to feed PEMFCs is typically hydrogen and methanol. Hydrogen-fed PEMFCs need pure hydrogen supplied by a hydrogen storage or liquid hydrocarbon reformer creating directly pure hydrogen which is complicated and bulky to the fuel cell system, limiting to transportation and portable applications. Alternatively, the use of liquid fuel, such as methanol, offers the benefits of system simplicity and high power density because it remove that extra equipment [6] and direct methanol fuel cells (DMFCs) are regarded as one of the most potential power sources for portable applications in term of environmentally friendliness and high power density.

1.2 Problem Statement

The first issue of DMFCs is the poor kinetics of anodic methanol oxidation reaction at moderate temperature and catalyst poisoning caused by the intermediate species produced during the operation.[7] The development of catalysts with better activities and increasing operation temperature at elevated temperature are expected to enhance the kinetics of electrode reactions and decrease catalyst poisoning due to improve CO tolerance.[7, 8] Another big issue impeding the application of DMFCs is methanol crossover through the proton exchange membrane which not only leads to reduced fuel efficiency, but also lowers the output voltage because of the mixed potential effect at the cathode. [9-12] Therefore, the development of proton exchange membranes with high proton

conductivity, low methanol crossover, good mechanical strength and functional at elevated temperature is critical for the commercial application of DMFCs.[13-15]

Nafion is the most widely used membrane for PEMFCs for years because of its high proton conductivity, high mechanical strength and good chemical resistance. [16] Unfortunately, due to its high methanol permeability, Nafion membrane is unsuitable for DMFCs application.[17] Moreover, it only performs well at conditions of 80°C and 100% relative humidity. Once increasing operating temperature above 80°C, the membrane shows a poor performance because of severe methanol crossover and reduced proton conductivity due to lowered membrane humidity.[18] In spite of its poor performance, currently, Nafion is still used as the proton exchange membrane for DMFCs because no other commercialized polymeric material performs better and can replace it so far.[15]

To date, many efforts have been attempted to develop new proton exchange membranes with a lower methanol crossover while maintaining high proton conductivity and mechanical strength. These include the modification of Nafion membrane by introducing an inorganic material into its structure,[19-22] synthesizing entirely new polymer membranes not basing on Nafion[23, 24] and developing composite membranes called pore-filling electrolyte[25-30]. Combining an inorganic material such as SiO_2, TiO_2 with Nafion normally shows limited improvement in methanol crossover, at the cost of reduced proton conductivity.[21, 22, 31] Meanwhile, various sulfonated polymers have been synthesized and attempted for replacing Nafion for DMFCs. Unfortunately, none of them can meet the three requirements simultaneously, i.e., high proton conductivity, low methanol permeability and high mechanical strength.[23, 24] Alternatively, composite membrane is the most promising because it is typically constructed from a porous matrix with high mechanical strength and a high proton conducting filler. The porous matrix help

suppress membrane swelling, leading to high mechanical strength and significantly reduced methanol crossover while the filler serves as a proton conducting material. So far various materials have been studied as the porous matrix, including porous silica,[32] polytetrafluoroethylene (PTFE),[28, 33] crosslinked polyethylene (CLPE)[26, 34] and polyimide (PI).[29, 30, 35] It is believed that the porous PI is the best matrix to construct the composite membranes because of its high mechanical strength, chemical stability and in particular, no stretching while filling with an electrolyte.[27] Currently, most of the porous PI matrixes tried are taken from Ube Industries Japan, which show low porosity (~ 55 vol.%). They are not tailor made to suit the use in fuel cell applications and may not possess optimum properties.[29, 35] In addition to the porosity of the host matrixes, the proton conducting material or filler strongly affects the performance of resulted composite membranes. A variety of polymeric materials have been used as an electrolyte including sulfonated polyether sulfone (SPES),[29] polyperfluorosulfonic acid ionomer (Nafion),[36] poly(acrylamide-tert-butylsulfonic acid) (PATBS)[26, 34] and poly(vinylsulfonic acid) (PVSA).[28] Most of them show either lack of mechanical strength, or low stability. Among them, Nafion ionomer is still realized as the best electrolyte for preparing the composite membranes because of its compromise between methanol crossover, proton conductivity, chemical resistance and mechanical strength. Finally, the complete filling of the electrolyte into all the pores of the matrix is not trial and practically limits the application of this type of membrane.

1.3 Objectives

The main objective of this research is to develop a novel proton exchange membrane with structure integrity and suitable for the operation under high temperature and high methanol feeding concentration for DMFC application. To achieve this goal, the

composite membrane fabricated should have high mechanical strength, high proton conductivity, low methanol crossover, and dimensional stability during operation.

To fulfill the stated objectives, our approach is to first prepare a porous polyimide matrix with sub-microsize, high porosity and highly porous surface and then fill with a protonic electrolyte. The morphology of the matrix will be optimized to meet the three requirements for DMFC application and allow an easy infiltration of the electrolyte.

1.4 Outline

In chapter 3 of this thesis, the porous co-polyimide matrix of S-PBDA−PPDA/ODA was fabricated from a polyimide precursor of poly(amic acid) by immersing the cast film in the non-solvent bath which contains a mixture of NMP and 1-butanol with different ratios. The porous substrate was then attempted for Nafion infiltration to prepare the composite membrane. Unfortunately, the filling solution failed to penetrate into the porous matrix. In addition, the polyimide precursor, which contains non-solvent of 1-butanol, is not suitable for storage as it can form a gel gradually. Efforts to prepare a porous matrix easy to infiltrate by an electrolyte were presented in chapter 4 and chapter 5. First, porous polyimide matrixes with tunable pore sizes as well as porosities were prepared by using different cast solutions of S-PBDA−PPDA/ODA in DMF with or without non-solvent additives of 1-butanol and methanol, followed by coagulation in a non-solvent bath with various components of 1-butanol, DMF and water. The mechanical property of the porous film shows strong dependence on the morphology and the pore size. A porous film suitable for constructing a composite membrane was obtained, which consists of a spongy-type structure with a average pore size of about 0.5 (μm), a mechanical strength of 78.4 (MPa) and a highly porous surface. Using it as a host support matrix, in chapter 5, SPSE and Nafion were used as the electrolyte filler to construct the

composite membrane. While it was difficult to fill by Nafion, SPES was infiltrated completely into the porous matrix and the PI−SPSE composite membrane performed better than Nafion membrane. However, further improvement in the membrane performance is needed for real DMFC application. Research works to construct Nafion-infiltrated composite membrane were then conducted in chapter 6 and chapter 7. In chapter 6, the morphology of porous polyimide matrix BTDA−PPDA/ODA synthesized by a new method as well as its effect on Nafion filling was investigated. Using chemical imidization-based polyimide precursor, the wet porous films with different pore sizes were obtained. With the presence of trace acetic anhydride, this porous matrix is more hydrophilic and allows complete infiltration of Nafion ionomer even though its pore size is as small as 0.3 (μm). In chapter 7, the composite membrane PI−Nafion constructed from the porous matrix with pore size of 0.3 (μm) was characterized. This membrane outperformed Nafion as well as the PI−SPSE composite membrane. In chapter 8, further improvement has been made by using a mixture of Nafion and proton conducting zeolite nanoparticles as filler to construct the composite membrane PI−Nafion−Zeolite. Due to the blocking of the methanol pathway by zeolite, this membrane exhibited outstanding performance compared to others and it is expected to replace Nafion-based membrane as a proton exchange membrane for DMFCs. Finally, conclusions and recommendations for future study were presented at the end of the thesis.

Chapter 2 Literature Review

2.1 Principle of Fuel Cells

A fuel cell is an electrochemical device that converts chemical energy into electric energy. It works continuously without charging as long as fuel and oxidant are supplied. Different to an internal combustion engine, high energy efficiency, quiet operation and no carbon emission are well-known for fuel cell systems. Fuel cells are categorized by the type of electrolyte or separator, a conducting material that allows ionic charges to flow but prevents the transfer of chemical species. These include alkaline fuel cell (AFC), molten carbonate fuel cell (MCFC), solid oxide fuel cell (SOFC), phosphoric acid fuel cell (PAFC) and proton exchange membrane fuel cell (PEMFC). Among them, the PEMFC is the most promising candidate for power generation because of its system simplicity and high power density compared to others.[37] The feeding fuel in PEMFCs is typically hydrogen or methanol. Once operated, it is oxidized at the anode site to produce protons and electrons in the presence of catalysts. The protons are transported across the electrolyte to the cathode side while the electrons move through an external circuit to reach the cathode side, where the combination between the protons, electrons and oxygen will be occurred and water is formed.

Obviously, the output of PEMFCs is only power and water for hydrogen fuel, while power, water and carbon dioxide for methanol fuel (Figure 2.1). Experimentally, due to the faster kinetic of hydrogen oxidation than methanol oxidation, the power density of hydrogen-fed PEMFCs is much higher than methanol-fed PEMFCs or DMFCs.[38] To supply hydrogen fuel, but a heavy hydrogen storage attached to the system is needed that is unsuitable for its target application of mobile purposes.[5] Therefore, PEMFCs used methanol as fuel is realized to deal with such a problem because liquid methanol is easy

to supply and store in a compact tank, allowing to remove such a bulky container.

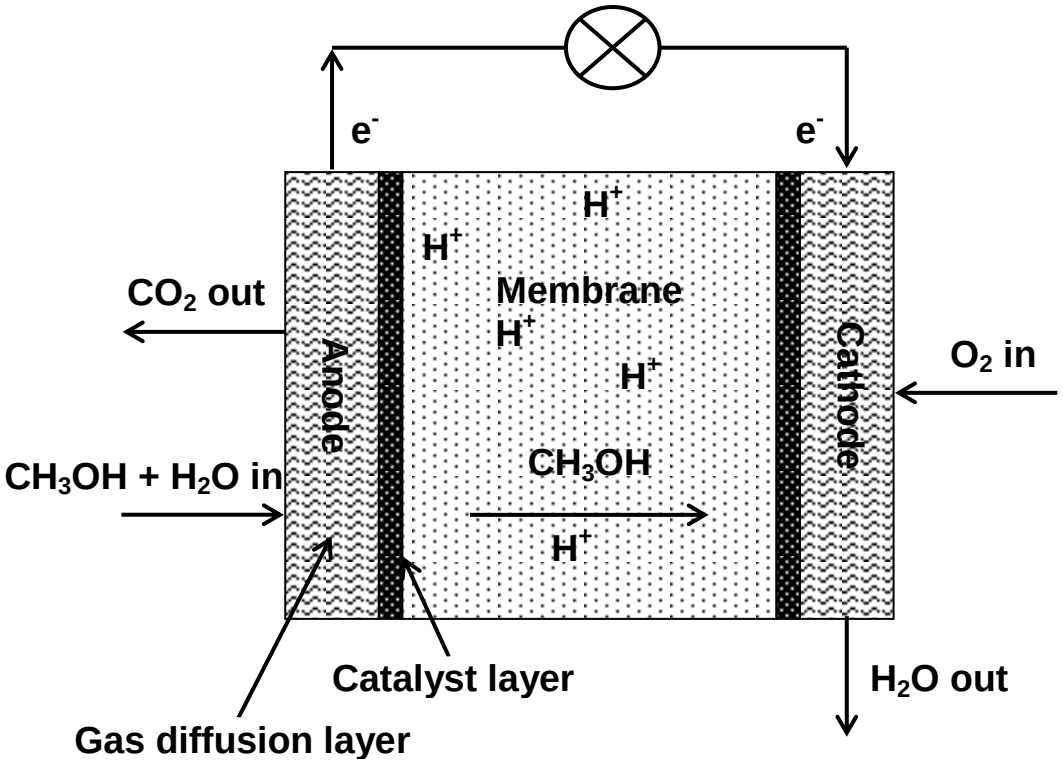

Anode reaction: $CH_3OH + H_2O \rightarrow CO_2 + 6H^+ + 6e^-$ ($E^\circ_{anode} = 0.02$ V)

Cathode reaction: $3/2O_2 + 6H^+ + 6e^- \rightarrow 3H_2O$ ($E^\circ_{cathode} = 1.23$ V)

Cell reaction: $CH_3OH + 3/2O_2 + H_2O \rightarrow CO_2 + 3H_2O$ ($E_{cell} = 1.21$ V)

Figure 2.1 Schematic and electrochemical reactions of a direct methanol fuel cell.

Again, due to combining poor kinetics of anodic reaction of methanol with catalyst poisoning caused by intermediate species such as CO, CHO, DMFCs have shown a low power density compared to the hydrogen fuel cells.[39, 40] In addition, methanol crossover, methanol transferring through the proton exchange membrane from the anode side to cathode, also contributes to further poor performance for DMFCs.[9, 41]

To deal with such issues, therefore, in addition to the improvement of catalyst activities for enhancing methanol oxidation,[42] a proton conducting membrane with high proton conductivity, low methanol crossover and high duration is strongly required for DMFCs before their commercialization.[15]

2.2 Proton Exchange Membranes for Direct Methanol Fuel Cells

2.2.1 Nafion Membrane

The heart of DMFCs is the membrane electrode assemblies (MEAs) which consist of a proton-conducted membrane sandwiching between two electrodes covered by catalyst layers. Nafion (Figure 2.2), which its structure is a polytetrafluoroethylene based polymer with sulfonic acid side chains, has been used as a proton exchange membrane for DMFCs for the past 50 years.[16]

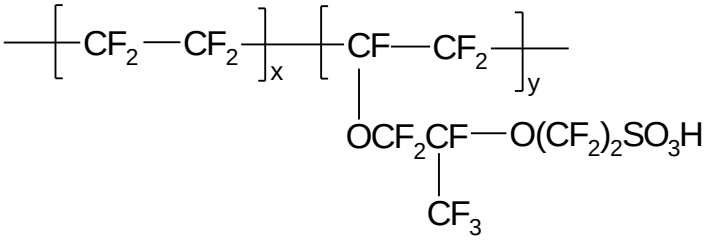

Figure 2.2 General structure of the Nafion membrane.

In addition to its high mechanical strength, the strong bonds between the fluorine and carbon also make it durable and resistant to chemical attacks. Moreover, Nafion is also an excellent proton conducting material because of the strong electron withdrawing of perfluorinated backbone. While well-suited for use in hydrogen-fed PEMFCs, Nafion is unsuitable for use in DMFCs because of its extremely high methanol permeability.[17, 43] The mechanism behind methanol and water crossover through a membrane is

straightforward if we understand its structure. As seen in Figure 2.3, the structure of Nafion-type membrane consists of hydrophobic backbones of fluorocarbon and hydrophilic side chains containing sulfonic groups. The hydrophilic regions around ionic clusters absorb a large amount of water, leading to the weak bonding between protons and sulfonic groups. Therefore, the protons can move freely in the structure and it becomes a good conductor after being well hydrated. Certain number of water molecules will be carried along with proton through the membrane from the anode side to the cathode side via electro-osmotic drag. In direct methanol fuel cell, a methanol solution is used to feed the cell. Due to the swelling of the membrane, more specially, the hydrophilic region of the membrane (the channel for methanol crossover) becomes larger, in the solution combining with the gradient of methanol concentration between two sides of the membrane, methanol accompanying water diffuse across the membrane. Methanol crossover is not only lowering the maximum power density but also reducing fuel efficiency.[12, 44] Efforts to develop appropriate PEMs for DMFCs have been continuing that the ideal membrane is impermeable to methanol, good proton conductivity and operating stably over a wide variety of temperatures.

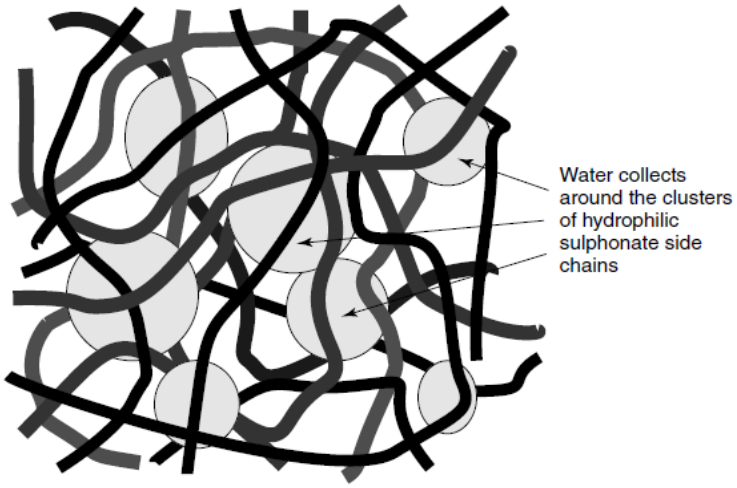

Figure 2.3 An illustration of well hydrated Nafion membranes.

To date, techniques improving PEMs fall roughly into three categories: (i) modifying the property of Nafion membranes; (ii) synthesizing entirely new PEM materials; (iii) developing composite membranes base on a highly porous matrix and an electrolyte with high proton conductivity.

2.2.2 Modified Nafion Membrane

The modification of the property of Nafion includes surface modification by coating a thin layer which is less permeable to methanol while still maintains proton conductivity, addition of additives into the membrane to react with methanol fuel to reduce methanol crossover and blending Nafion with other inorganic materials to form composite membranes. Palladium metal takes much attention for researchers as it is impermeable to methanol but not proton. Ma *et al*. used sputtering method to coat Pt/Pd-Ag/Pd layer on the surface of Nafion membrane.[27] The Pd alloy-coated Nafion had outperformed uncoated Nafion by generating a maximum current density in DMFC roughly 35% higher. Another method using ion exchange of chemical reaction to membranes was conducted by Kim *et al*.[45] The modified Nafion membrane showed less permeability to methanol and uptake more water than pure Nafion. In addition, DMFCs made with palladinized Nafion also generated roughly 40% higher maximum current density than Nafion membranes. In addition, a composite membrane has been made by introducing a nanosize of silica (SiO_2) into the structure of Nafion ionomer reported by Antonucci *et al*.[46]. Increasing working temperature up to 140°C and reducing methanol crossover is realized in this membrane.

2.2.3 Sulfonated Polymer-Based Membrane

In efforts for developing inexpensive and effective membranes for DMFCs, Xinhuai *et al*.[47] synthesized the sulfonated polyimide copolymers derived from 1,4,5,8-napthalenetetracarboxylic dianhydride (NTDA), 4,4'-diaminostilbene-2,2'-disulfonic acid (DSDSA), and other three common diamines, i.e., 4,4'-oxydianline (ODA), 4,4'-methylene dianiline (MDA), and 4,4'-(9-fluorenylidene)dianiline (FDA). The sulfonation degree of the copolymers is controlled by the molar ratio of DSDSA to the common diamines and the flexible, transparent, and mechanically strong membranes were synthesized. The membranes show good thermal stability, high proton conductivity at 70°C. At a higher temperature of about 140°C, the proton conductivity of the membranes was higher than those of Nafion membranes, indicating the potential application for high temperature DMFCs. Indeed, Okamoto *et al*.[48] had been synthesized two types of sulfonated co-polyimides (co-SPIs) from naphthalenetetracarboxylic dianhydride (NTDA), two types of sulfonated diamines of 4,4'-bis(4-sulfophenoxy)biphenyl-3,3'-disulfonic acid (BAPBDS) and bis(3-sulfopropoxy)benzidines (BSPBs), and common non-sulfonated diamines of 4,4'-diaminodiphenyl ether (ODA), m-phenylene diamine (m-PDA), 4,4'-bis(4-aminophenoxy)biphenyl (BAPB), 9,9-bis(4-aminophenyl)fluorene (BAPF), bis(4-aminophenyl) sulfone (BAPS), and bis[4-(3-aminophenoxy)phenyl] sulfone (m-BAPPS). Depending on the molar ratios and types of sulfonated to non-sulfonated diamines, the membranes with different properties were obtained. The co-SPI membranes have shown high proton conductivity in water and two times lower methanol permeability comparable to those of Nafion membranes. The co-SPI membranes have high potential as alternative membranes for DMFCs application.

2.2.4 Composite Membrane Based on Pore-Filling Electrolyte

Earlier 1990s in an effort developing the ion conducting membrane with low methanol permeability and high ion conductivity, composite membranes based on a porous matrix and an electrolyte filled into the pores was reported by Charles *et al*.[49, 50]. His team had successfully synthesized the Nafion-Impregnated Gore-Tex (NIGT) membrane by impregnating commercial porous polytetrafluoroethylene (PTFE, Gore-Tex) with an electrolyte of Nafion. The composite membrane had shown high mechanical strength, good ion transporting of $Ru(NH)_6^{3+}$, and particularly low cost compared to Nafion-based membrane. In 2000s, Yamaguchi *at al*.[28] had developed a new composite membrane for DMFCs by filling the porous PTFE with an electrolyte of a poly(vinylsulfonic acid/acrylic acid) (PVSA). The pore-filling membrane exhibited low methanol permeability because of effectively suppressing swelling of the PTFE substrate and thermal stability at 130°C due to the matrix durability, but proton conductivity was lower than Nafion 117 because of weak acidity of the electrolyte of PVSA.

In order to choose a proper matrix material for constructing composite membranes, Yamaguchi *at al*.[27] had been fabricated composite membranes used various porous matrixes including porous poly(tetrafluoroethylene) (PTFE), cross-linked high density polyethylene (CLPE), and polyimide (PI) filled with a high proton conductivity of a poly(acrylamine-tert-butylsulfonic acid) (PATBS). It found that the PTFE matrix showed a stretch from its original dimension by the filling polymer while no change in dimension was detected for CLPE and PI matrix. The prevention of substrate swelling from polymer filling strongly depends on the mechanical property of the porous matrix. Due to possessing a higher strength, PI and CLPE matrix prevented effectively the stretch following the polymer filling. In addition, a comparison between dry and swollen state of composite membranes, PTFE and CLPE composite membrane showed a large change in dimension between two states, while constant dimension was obtained for the PI

composite membrane. These results proved that the porous PI matrix is the best material as a porous substrate for preparing the composite membrane. Based on this material, an extremely low methanol crossover and highly durable composite membrane for direct methanol fuel cells was prepared by Yamaguchi *et al*.[29] The commercial porous polyimide with porosity of 55 (vol.%), 30 (μm) thick and a pore diameter of about 100 (nm) was filled up by an electrolyte of sulfonated polyether sulfone (SPES). The composite membrane constructed showed 300 times lower methanol permeability than those of Nafion 117 membrane, with a 30% methanol fed solution at 25°C. In addition, due to suppressing swelling of the rigid porous polyimide matrix, no dimensional change of the composite membrane was detected after soaking in the water, while Nafion membrane showed a 25% dimensional change. However, the composite membrane exhibited proton conductivity around one-fourth to one-third compared to Nafion 117 due to low porosity of the host matrix.

2.3 Methodology for Fabricating Porous Polyimide Film

2.3.1 Synthesis of Polyimide Precursor

The polycondensation of an organic dianhydride and a diamine is typically a method applied for the synthesis of polyimides.[51] This technique is suitable for both aliphatic and aromatic polyimides and the formation of polyimides is realized in a two-step reaction. In the first step (Figure 2.4) the nucleophilic groups of the amine attack the carbonyl groups of the dianhydride, which promotes the opening of the rings, yielding an intermediate poly(amic acid).

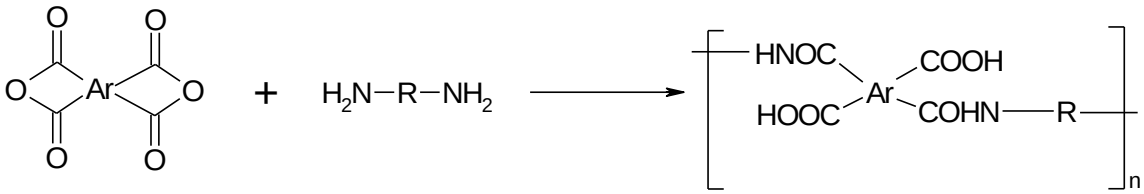

Figure 2.4 Polymerization reaction of dianhydrides and diamines.

In the second step the poly(amic acid) is converted to the corresponding polyimide through a cyclodehydration reaction promoted by thermal or chemical agents (Figure 2.5).

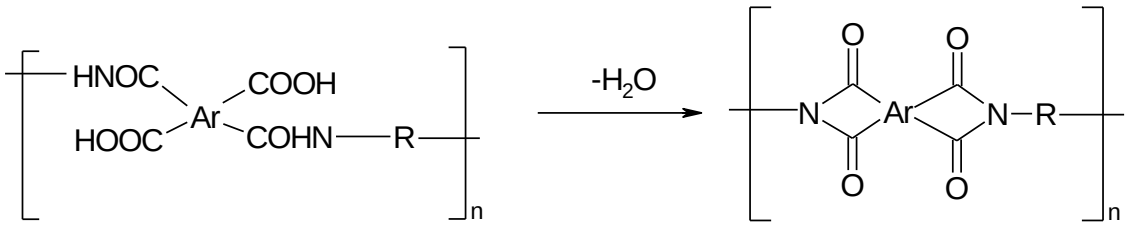

Figure 2.5 Cyclodehyration reaction of poly(amic acid) for forming corresponding polyimide.

Highly polar solvents such as N-methyl-2-pyrrolidinone (NNP), N,N-dimethylformamide (DMF), N,N-dimethylacetamide (DMA), and dimethylsulfoxide (DMSO) are suitable media to dissolve monomers as well as poly(amic acid)s. In addition, due to difficulty to dissolve aromatic dianhydrides in the solvent at low temperature, the addition of the solid dianhydride on the diamines solution has typically been used as the right way to synthesize the poly(amic acid)s because the diamines in large excess will favor the main reaction of poly(amic acid)s formation. Moreover, to achieve high molecular weight and avoid side reactions (Figure 2.6), the polycondensation reaction should be carried out with a high purity of solvents and reactants under rigorous stirring at moderate temperatures.

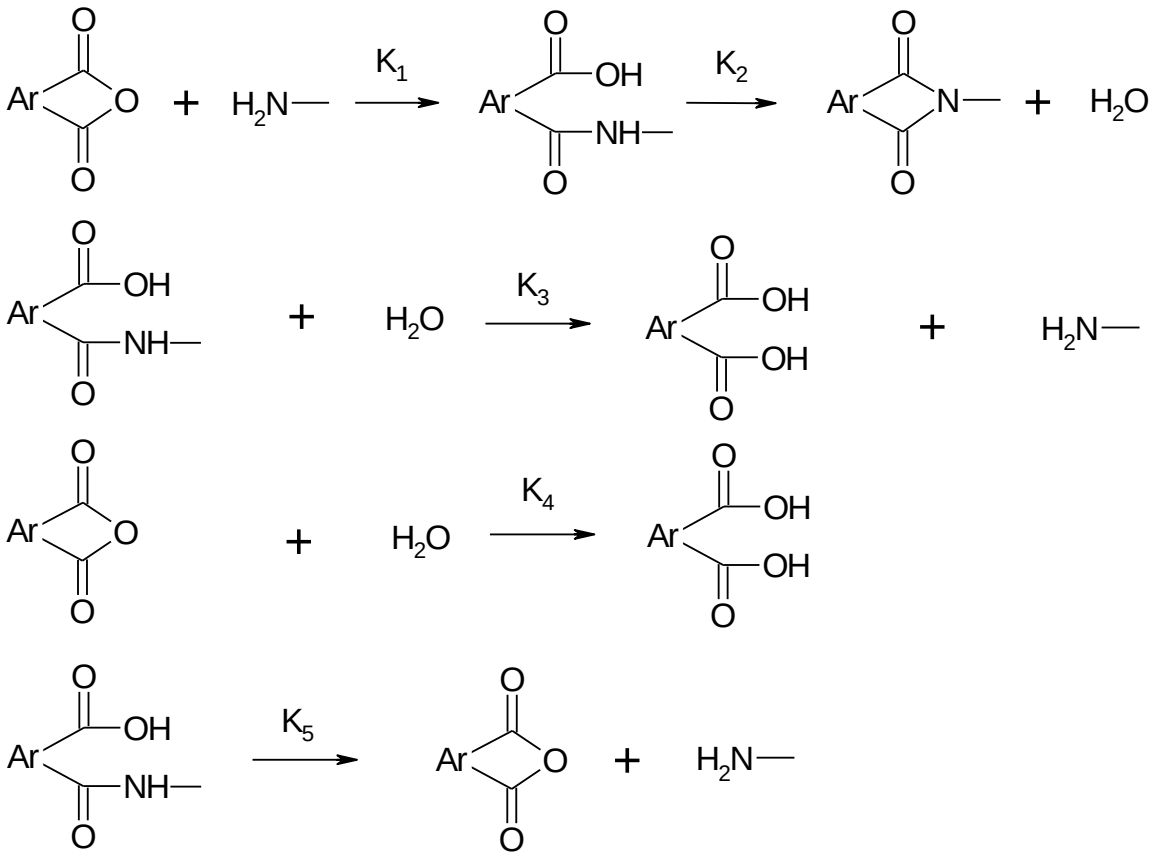

Figure 2.6 Possible side reactions during polyimide synthesis process.

The cyclodehydration reaction, converting a poly(amic acid) to corresponding polyimide, plays an important role in the synthesis of polyimides because it affects on the property of the resulted films. There are two methods employing to turn poly(amic acid) into polyimide, including thermal[52] and chemical imidization.[53] The thermal imidization is mainly employed for insoluble polyimides in which a multi-stage thermal cycle is typically employed to convert poly(amic acid) to corresponding polyimide because the trapped air, water, and solvent need time to evaporate out of the film. In addition, to complete thermal treatment the final reaction temperature should be above the ultimate T_g to remove all trapped water and solvents. On the other hand, due to the elimination of solvents and water at high temperatures, defects are more likely to form in the resulted films such as surface irregularities, micro-voids and polymer degradation, causing poor mechanical strength of the films. In addition, it is difficult to get 100% cyclodehydration

for thermal imidization because of the strong interaction between the poly(amic acid) and the solvent which prevents poly(amic acid) converting to polyimide form completely. To deal with such problems, therefore, the chemical imidization typically is applied for those which are totally dissolved in the solvent. The process is normally promoted by dehydrated reagents of acid anhydrides such as acetic, propinoic, n-butyric, benzoic, etc., in combination with organic bases like pyridine, triethylaminelutidine, or N-methylmorpholine. Different to thermal imidization, the conversion reaction can reach to up 100% for chemical imidization when the reaction is conducted at room temperature for 24h to 48h or only few hours if the chemical cyclodehydration reaction takes place at 100°C.

A polyimide precursor (PBDA−PPDA) of poly(p-phenylene biphenyltetracarboxamide acid) derived from 3,3',4,4'-biphenyltetracarboxylic dianhydride (S-BPDA) and p-phenylenediamine (PPDA) with high molecular weight were synthesized by Huang *at al*.[54]. The reaction is carried out with intense mechanical stirring in nitrogen media at -15 to 0°C for 48 to 72h. The corresponding polyimide after thermal treatment showed excellent mechanical properties such as tensile strength up to 900 MPa and E-modulus of 18 GPa. The PBDA−PPDA polyimide precursor is expected for use as casting solution to make the porous polyimide matrix. Other report by Mazoniene *et al*.[55] synthesized co-polyimide precursors from aromatic dianhydrides of pyromellitic (PMDA) and symmetric 3,3',4,4'-biphenyltetracarboxylic (S-BPDA), aromatic diamines of 4,4'-oxydianiline (ODA) and p-phenylenediamine (PPDA) and the solvent of anhydrous N,N-dimetylformamide (DMF) under strong stirring at 10-15°C for 6 to 12h. Results showed that the co-polyimide films of S-PBDA−PPDA/ODA synthesized from the ratio molar of S-BPDA:PPDA:ODA (1:0.75:0.25) exhibited a 35% higher ultimate strength and a 64% higher elongation at break at the ambient temperature than the reference polyimides of S-

PBDA−ODA. The high mechanical strength of these co-polyimides has potential to make porous substrates suitable for fabricating composite membranes. Meanwhile, Kawakami *et al.*[56] synthesized a soluble aromatic polyimide derived from 2,2'-bis(3,4-dicarboxyphenyl) hexafluoropropane dianhydride (6FDA) and 3,3'- or 4,4'-diaminodiphenylsulfone (m-DDS or p-DDS). The poly(amic acid) solution was converted into corresponding polyimide via the chemical imidization promoted by acetic anhydride and trimethylamine at 70°C for 24h. Under these conditions, the homogeneous solution with 100% conversion of soluble polyimide was obtained. In addition, other soluble polyimide was prepared from an aromatic diamine of bis[4-(3-aminophenoxy)phenyl]sulfone (m-BAPS) and three kinds of dianhydrides including 4,4'-oxydiphthalic anhydride (ODPA), pyromellitic dianhydride (PMDA) and 3,3',4,4'-diphenylsulfonetetracarboxylic dianhydride (DSDA) in a polar solvent of N-methyl-2-pyrrolidone (NNP) following traditional chemical two-step process. In the first step, an polycondensation reaction between a dianhydride and a diamine in NMP was employed to form a poly(amic acid). It was then converted into polyimide promoted by acetic anhydride and pyridine. This homogeneous solution can be used as a cast solution to fabricate porous polyimide films.

2.3.2 Porous Film Formation

The techniques used to develop the porous film from a homogeneous solution of polyimide precursors are typically to rely on three basis procedures following.[57]

Phase separation by cooling. This technique was applied for polymer solutions which are a homogeneous phase at high temperatures but show a miscible gap at lower temperatures. The thermal precipitation process forming the porous film is presented by the phase diagram (Figure 2.7).

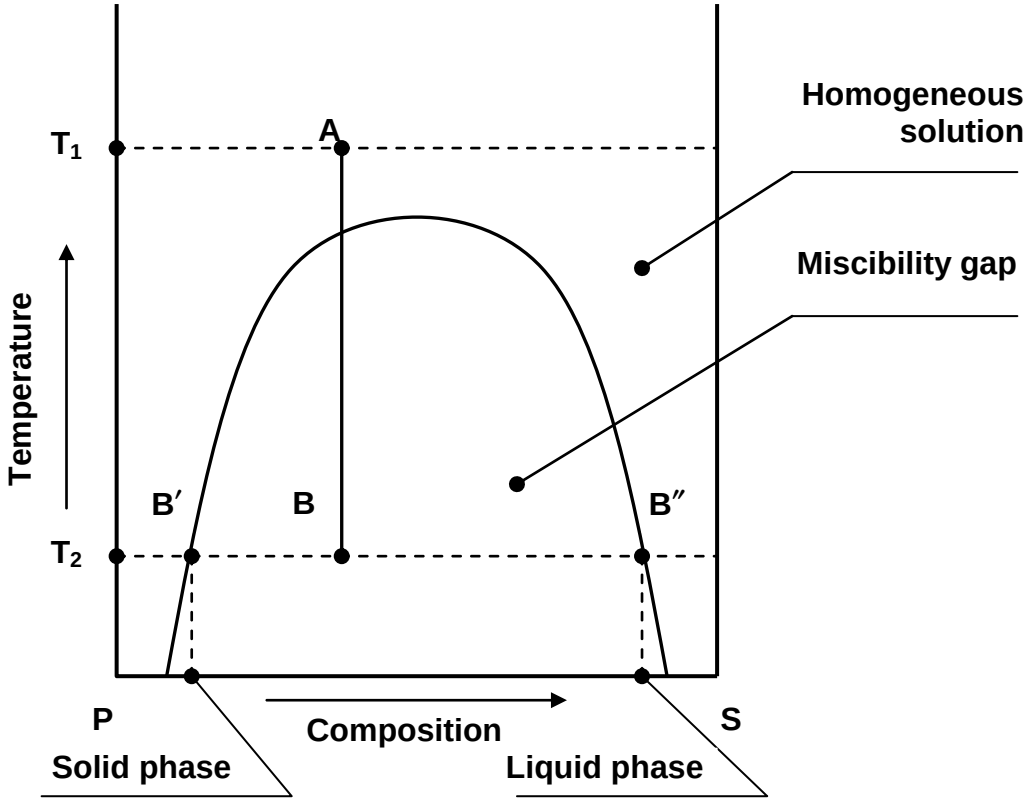

Figure 2.7 Three-phase diagram showing phase separation by cooling.

The pure polymer and solvent shown by the points P and S, respectively and line P-S describes mixtures of these two components. When a homogeneous solution with the composition at point A and at temperature T_1 is cooled down to T_2 as indicated by point B, it will separate into two different phases indicated by the points B' called polymer-rich phase and B" for polymer-poor phase. The polymer-rich phase containing large amount of solid polymer will develop the matrix of the porous film, while the polymer-poor phase containing a lot of solvent will form the pores of the resulted film. Due to the cooling to be uniform throughout the cast film, the resulted film is being isotropic. In addition, the pore size of the porous films can be controlled by changing the solvent as well as polymer in the solution. Moreover, the morphology of the porous film heavily depends on the cooling rate in the process, where the film with open structure is for cooling slowly and a much finer structure for rapid cooling.

Phase separation by solvent evaporation. This method typically applies for homogeneous polymer solutions dissolving completely in the two different solvents, which one solvent is volatile and well-soluble polymer such as methylene and acetone and other named non-solvent is more likely to precipitate polymer like water and alcohol. Once the volatile solvent in the solution evaporates, the composition of the mixture will change from at point A, which is a homogeneous phase, to heterogeneous phase at point B, where the solution is separated into a polymer-rich phase (B') forming the matrix structure and a polymer-poor phase (B'') creating the pores of the film (Figure 2.8).

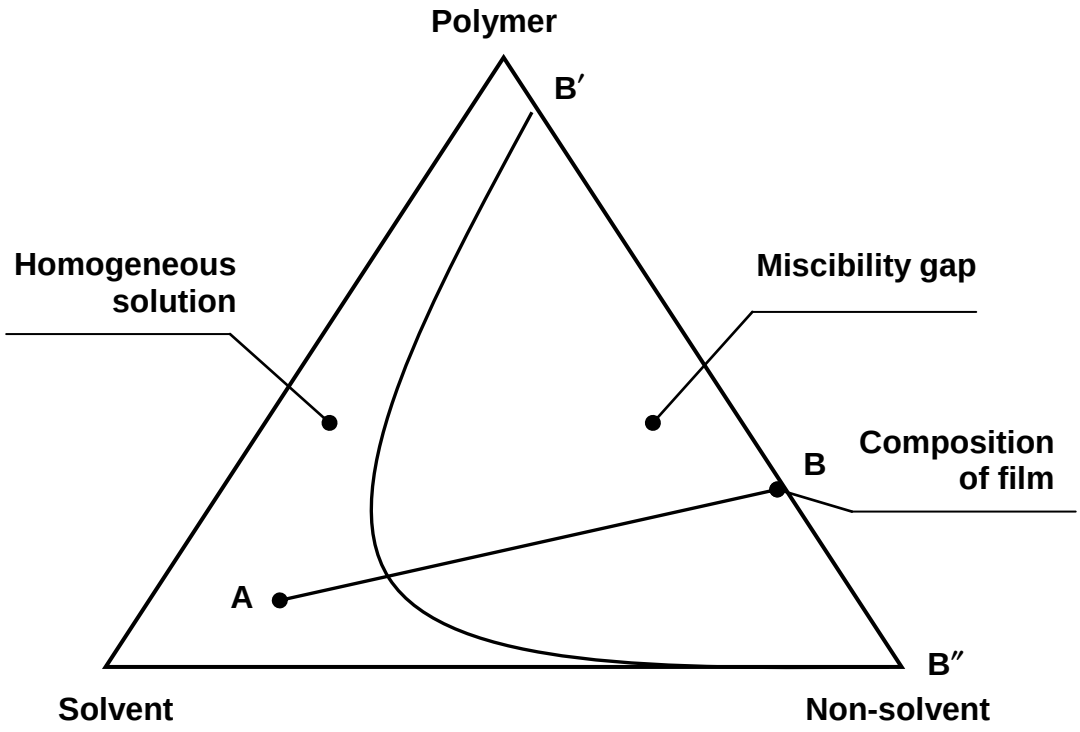

Figure 2.8 Three-phase diagram showing phase separation by solvent evaporation.

The compatible capability of the non-solvent to the polymer plays an important role in determining for the film morphology. As the non-solvent is completely incompatible with the polymer, the result film is being finely micro-porous and open. In contrast a partially

compatible non-solvent containing in the solution, the pores are more likely to be collapsed when the solvent is evaporated. The porous film formed is being dense, leading to a low porosity and semi-porous surface.

Wet phase separation by addition of non-solvent. This technique developed first by Loeb-Sourirajan called wet phase inversion, so far remains dominant to fabricate micro-porous films for reverse osmosis, ultrafiltration and gas separation applications.

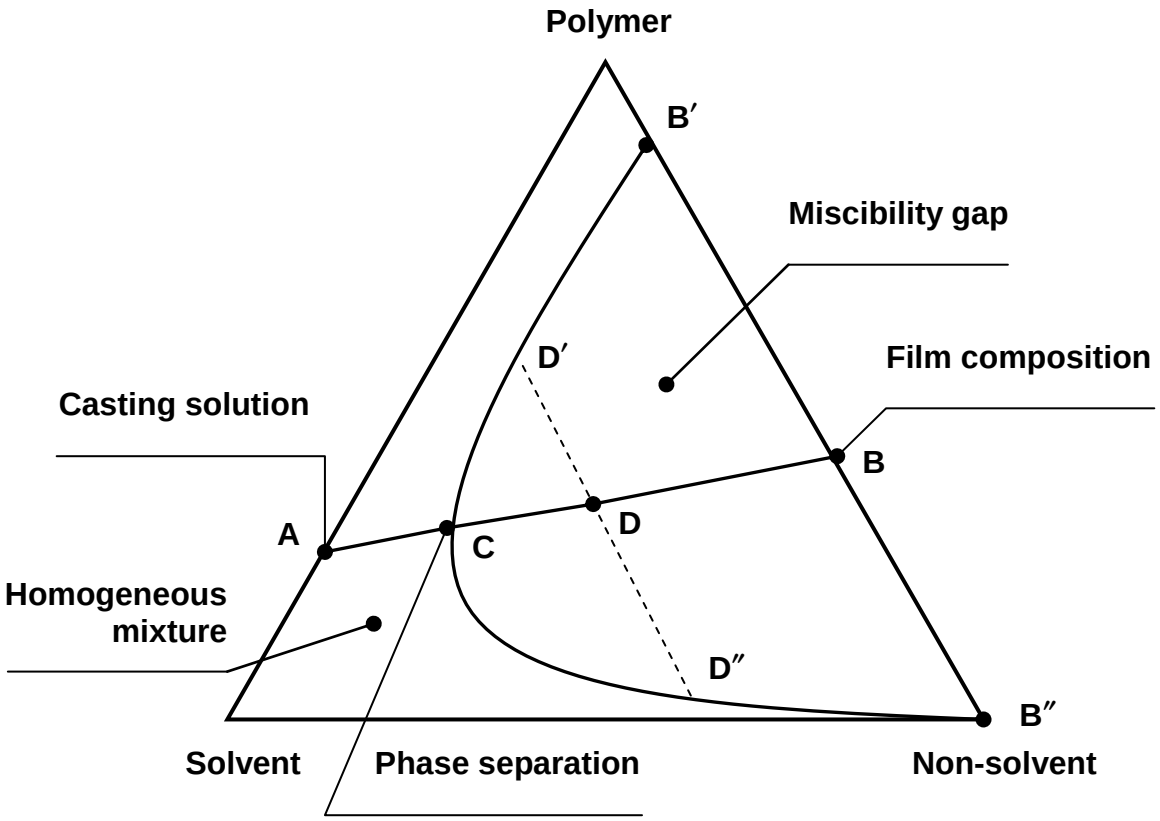

Figure 2.9 Three-phase diagram to show phase separation by adding a non-solvent.

By changing the composition of the polymer solution as well as non-solvent, the porous film with different morphologies and pore sizes will be obtained. As can be seen in Figure 2.9, the homogeneous polymer solution at point A is immersed in the non-solvent, typically water or alcohol. Immediately, there is the exchange between solvent and non-

solvent in which solvent is removing from the mixture while the non-solvent is entering into the liquid film. As the result, the composition of the system will reach the miscibility gap at point C, where two separate phases are formed, including a polymer-rich phase at upper boundary of the miscibility gap and a polymer-poor phase at lower boundary. When the polymer solution continues to lose solvent and gain non-solvent, the polymer concentration in the polymer-rich phase is being high enough to become solid represented by point D. The further exchange of solvent and non-solvent will reach the final composition of the film at point B, which determines the overall porosity of the film. Here, there are two phases which is a solid phase represented by point S forming the matrix of the final film and a liquid phase represented by point L forming the pores of the film after the evaporation of non-solvent.

Shimizu *et al*.[58] reported the formation of porous films by coagulating the polyimide liquid film synthesized by a chemical imidization of 6FDA-6FAP in different solvents such as tetrahydrofuran (THF), N,N-dimethylacetamide (DMA), acetone, N-methylpyrrolidone (NMP), N,N-dimethylformamide (DMF) and dimethylsulfoxide (DMSO) in the non-solvent of water. The porous formation mechanism was investigated by a ternary system in polyimide/solvent/water. It found out the morphology of the films has depended on the demixing between solvent and water. With an instantaneous demixing between the water and solvents of DMA, NMP, DMF and DMSO, the result films consist of a porous top layer and a finger-type structure. In contrast, due to a delayed demixing between the water and solvents of THF and acetone, the formation films compose of a semi-porous top layer and a spongy-type structure. Meanwhile, the influence of the non-solvent additives such as methanol, ethanol and 1-butanol contained in the cast solution on the morphology of the films was investigated by Taketani *et al*. The cast solution was a polyimide precursor of 6FDA-6FAP dissolved in NMP containing

a non-solvent additive of methanol, butanol, or octanol with different amounts. The formation of porous films was carried out by immersing the liquid film into the non-solvent bath of water. In this study, the film structure greatly depends on the butanol content in the cast solution, which the structure of the films prepared from the solution without butanol showed a porous top layer and a finger-type sub-layer, while the film fabricated from the solution containing 42.5 (wt.%) butanol exhibited a spongy-type structure. However, when using the solution containing 25.5 (wt.%) butanol, on the other hand, the resulted films consist of a porous top layer and a cylinder-type structure. These results can be explained by the different transport rates of butanol during liquid-liquid de-mixing. Other than that, the morphology of the films is also affected by the composition of additive. With a 29 (wt.%) methanol in the cast solution, the porous films showed the straight cylinder micro-pores while less ordered cylinder is obtained for the porous films prepared from cast solutions containing 25.5 (wt.%) butanol and 9 (wt.%) octanol. The mechanism behind the change of pore shape of with various non-solvent additives was unknown so far, but one can confirm that the exchange rate between the solvent and non-solvents clearly controls the film morphology. In addition, an investigation of the morphology of porous polyimide films prepared by coagulating the cast film in the non-solvent containing solvent of NMP was reported by Matsuyama *et al.*[59] The cast solution was a polyimide precursor of (N,N'-(1,4-phenylene)-3,3',4,4'-benzophenonetetracarboxylic) dissolved in N-methylpyrrolidone (NMP) and the non-solvent bath contains a mixture of water and NMP with different ratios. As water content in the bath is decreasing, the structure of porous films turned from a finger into spongy type because the present of solvent of NMP in the non-solvent bath caused the delayed de-mixing, which the spongy type structure is in favor. In addition, it found the pore size of the spongy films is increasing when decreasing the water content in the coagulation

bath. The pore size can grow until the polymer-rich phase is solidified and with a lower amount of water, the delayed de-mixing was occurred and the polymer concentration of the polymer-rich phase was lower. Therefore, it takes a longer time to separate phase and bigger pore sizes are obtained.

Chapter 3 Fabrication of the Porous Polyimide Film as a Matrix of the Composite Membrane for Direct Methanol Fuel Cells

3.1 Introduction

"High energy, lightweight, power source has great market potential in various portable applications. The PEMFCs, particularly DMFCs have been proposed as a leading candidate for these applications. However, before DMFCs can be considered for commercial applications, certain key issues need to be addressed. First, the current system is still considered too heavy due to the requirement of additional materials to provide structure stiffness. Second, due to slow anodic reaction kinetics, the DMFCs shows inferior performance compared to hydrogen fuel cell systems. Finally, the Nafion based membrane used currently in the DMFCs has high methanol permeability, resulting in lower fuel utilization and electric potential.[6, 60]

Large research efforts have been succeeded in efficient methanol oxidation catalyst development.[61-65] However, the methanol crossover from the anode to the cathode is still a main problem needed to be improved so far.[12, 44, 66-68] Numerous efforts have been made to modify Nafion based polymers[8, 69] or synthesize alternative membranes[23, 24, 70] with an objective to develop membranes with low methanol crossover while still maintaining high proton conductivity and mechanical strength. Most of the results show a certain level of reduction in methanol permeability but the proton conductivity and mechanical strength are also sacrificed to certain degree, which limits their use in real situations. To date, there have been no reports of the successful application of new membranes in practical DMFC applications.[69]

One solution to solve these problems is to fabricate a porous polymer matrix and then fill it with a highly proton conductive electrolyte.[27, 30, 34] This offers the possibility to decouple the mechanical and electrical properties of the composite membrane. Such a matrix should be mechanical strong and will not change its dimension while filling with proton conductive electrolyte and when the composite membrane contacts with methanol or water. A reduced overall system weight can then be expected by eliminating the need for external stiffness and strength. Another advantage of using the composite membrane structure is the possibility of fabricating a very thin film to reduce the resistance of membrane in operation. The choice and synthesis of this porous matrix is critical and then is the objective of this chapter.

Various porous substrates have been used as a matrix such as porous polytetrafluoroethylene (PTFE),[28] crosslinked polyethylene (CLPE),[26] and polyimide (PI).[30] Yamaguchi's group has been proved the porous PI is the best substrate to prepare the composite membrane because of the following reasons:[27] (i) this material has high mechanical strength and no stretching while filling with electrolytes; (ii) as the major component of the porous structure is still hydrophilic polyimide material, it is compatible with filling electrolyte, e.g. Nafion ionomer, which the infiltration will be much more efficient; (iii) as polyimide is totally inert to methanol and methanol crossover is mainly through the polymer electrolyte filler, the fact that composite membrane mechanically prevents the electrolyte from swelling can lead to decreased methanol crossover; (iv) polyimide film itself is widely used for electrical and electronic appliances.

In this study, we report the successful synthesis of a novel porous film of polyimide with a high porosity consisted of a porous top surface and a spongy type structure by a wet

phase inversion process based on phase separation in a ternary system of polyimide/solvent/non-solvent. The porous polyimide of film was co-polymerized among 3,3',4,4'−biphenyltetracarboxylicdianhydride (S-BPDA), p-phenylenediamine (PPDA) and 4,4'-oxydianiline (ODA) monomers. The morphology and porosity of the porous film were controlled by adding the non-solvent of 1-butanol in the casting solution of poly(amic acid) of N-methylpyrrolidone (NMP)-soluble S-BPDA−PPDA/ODA and by varying the weight ratio between 1-butanol and NMP in the non-solvent bath as well as coagulation time. For a potential application in DMFCs, the experimental conditions that will render high mechanical strength were also adopted.

3.2 Experimental Details

3.2.1 Starting Materials

S-BPDA (97 wt.%), PPDA (99.9 wt.%), ODA (97 wt.%), NMP (anhydrous), and 1-butanol (99 wt.%) were purchased from Sigma−Aldrich. The PPDA, ODA, and NMP were used for the synthesis of polymer as received, while the S-BPDA was heated at 280°C for 6h before using.

3.2.2 Synthesis of Poly(amic acid) S-BPDA−PPDA/ODA

S-BPDA was dissolved in the solution of two aromatic diamines of PPDA and ODA in NMP with a mechanical overhead stirrer. The molar ratio of S-PBDA, PPDA, and ODA was 1:0.75:0.25 respectively and total solid content of monomers was calculated to be 18 (wt.%). Polymerization reaction was carried out in nitrogen environment at a temperature of 10°C with vigorous stirring for 48h to obtain a poly(amic acid) solution.[55, 71]

3.2.3 Preparation of Porous Polyimide Film

Porous polyimide film of S-BPDA–PPDA/ODA was fabricated by a wet phase inversion technique.[72, 73] The composition of polymer in casting solution used for the preparation of the porous film was controlled at 14 (wt.%) by added 1-butanol to the poly(amic acid) solution above. The resulted casting solution then contains 14 (wt.%) of co-polymer content, 57 (wt.%) of NMP and 29 (wt.%) of 1-butanol. The solution was cast on glass plates using a spin coating machine (SCS G3, Cookson Electronics) to obtain films around 20 (μm) thick. Immediately after casting, the film was coagulated by immersing in a non-solvent bath containing different ratios of NMP and 1-butanol for several hours, washed with methanol and then water, dried in air for few hours, and finally treated in a vacuum oven at 350°C for 1h to remove all the solvents and completely convert poly(amic acid) into corresponding polyimide. For comparison purpose, a non-porous film was also prepared by thermal conversion of the casting film without any coagulation treatment.

3.2.4 Material Characterization

3.2.4.1 Fourier Transform Infrared Spectroscopy (FT–IR)

The chemical conversion of films from poly(amic acid) to polyimide was examined by FT–IR spectra of transparent thin films taken with a Perkin–Elmer FT–IR Spectrum X Spectrophotometer (FTS3100).

3.2.4.2 Scanning Electron Microscope (SEM)

The morphology of porous films was observed with a Scanning Electron Microscope (SEM JSM–6390LA, JEOL). The thin films were coated with Pt/Pd by Auto Fine Coater (JFC–1600, JEOL) before observation.

3.3 Results and Discussion

3.3.1 Synthesis and Characterization of Co-polyimides S-BPDA–PPDA/ODA

The polycondensation reaction of an organic dianhydride and a diamine was employed for the synthesis of polyimide, which consists of two steps.[51] In the first step, the nucleophilic attack of the amine group to the carbonyl group of the dianhydride leads to the opening of the rings yielding an intermediate poly(amic acid) (stage 1). The poly(amic acid) was thermally converted to the corresponding polyimide through a cyclodehydration reaction in the second step (stage 2), as shown in Figure 3.1.

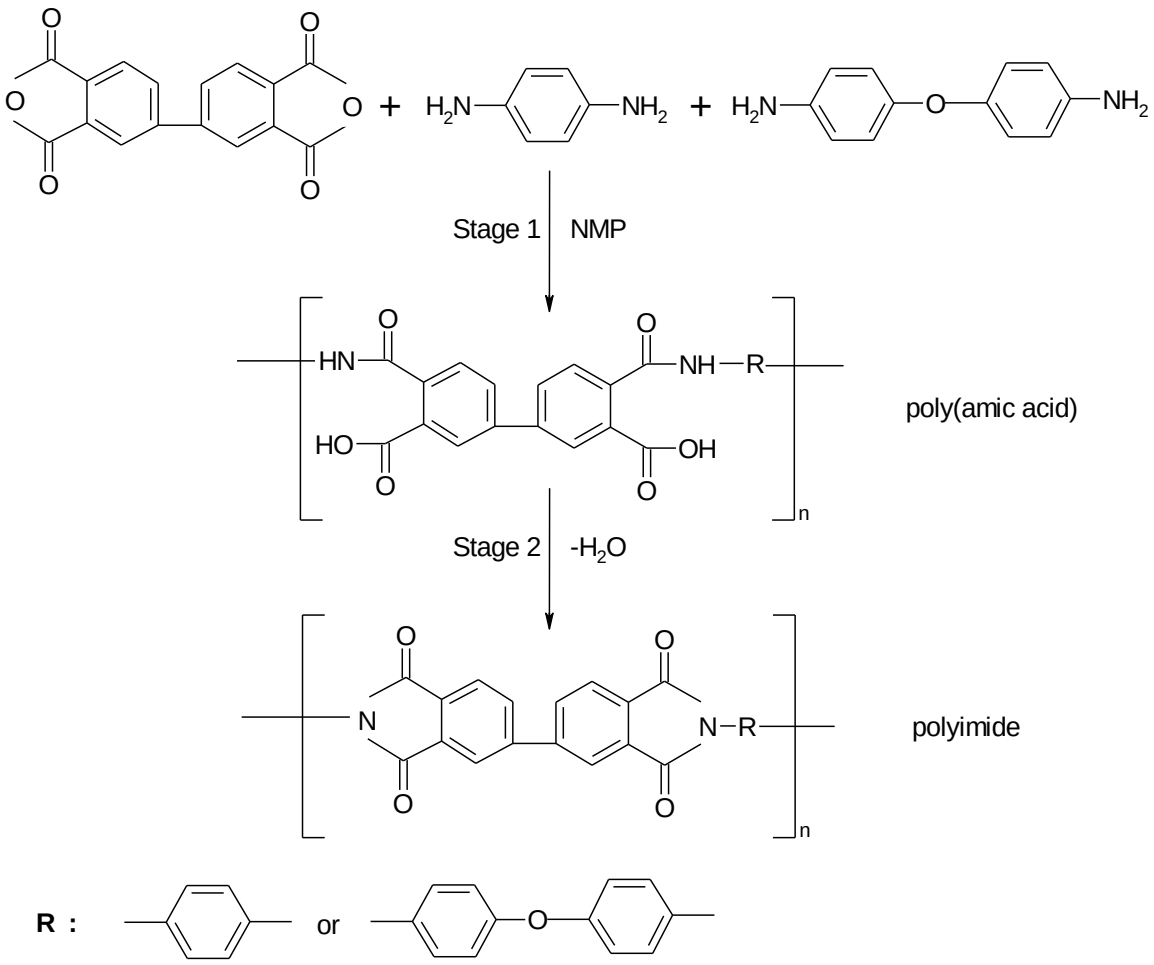

Figure 3.1 Two-stage synthesis of polyimide S-BPDA–PPDA/ODA.

To be used as a support matrix of the composite membrane for DMFC, the key requirement is that the porous polyimide must be mechanically strong and stiff in structure,[27] so our first efforts were then focused on this part. Mechanical properties of films are affected by molecular weight of polyimide. A higher molecular weight of polyimide favors the formation of films with higher mechanical strength.[54] To get a high molecular weight, intense mechanical stirring, low reaction temperature (10°C) and long reaction time (48h) were used during the polymerization in this work. A low reaction temperature was reported to be favorable for suppressing the side reaction (Figure 3.2) and producing high molecular weight product in the condensation between dianhydride and diamines.

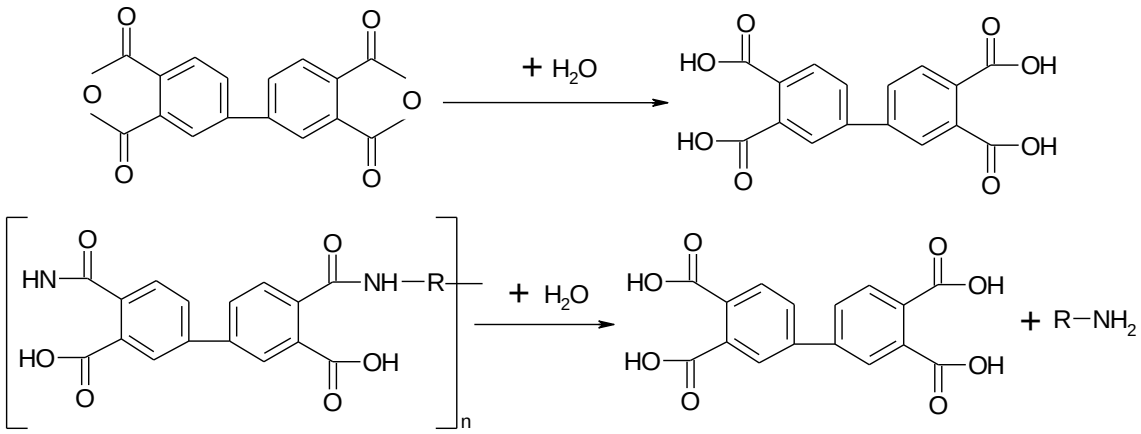

Figure 3.2 Side reactions in the synthesis of polyimide in the presence of water.

In addition to reaction temperature, the solid content of casting solution plays an important role in affecting the mechanical strength of porous films.[74] Especially, the precipitation pathway entering the two phase region of the phase diagram must be above the critical point at which the bimodal and spinodal lines intersect in the ternary system (Figure 3.3).

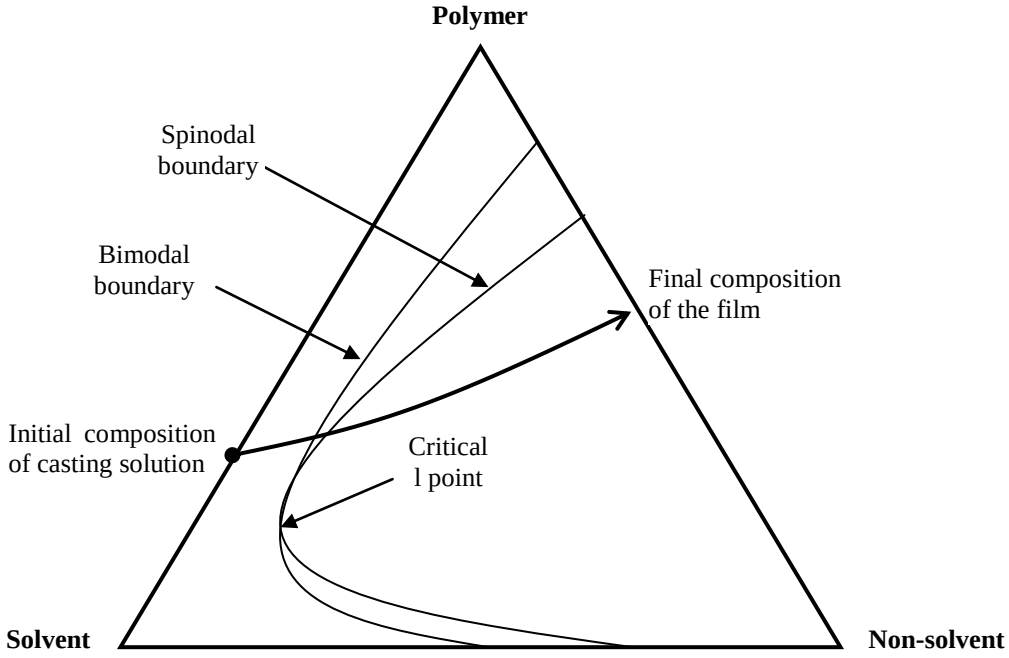

Figure 3.3 Three-component phase diagram showing the formation of porous film by adding a non-solvent.

This is very important because it means that precipitation will occur as a liquid droplet in a continuous polymer-rich phase. Films formed in such regions inhered good strength of resulted films. If dilute casting solutions are used, in which the precipitation pathway enters the two phase region of the phase diagram below the critical point, precipitation produces polymer gel particles in continuous liquid phase. Such formed films are then weak in strength and powdery. With that in mind, we chose the polymer composition of the casting solution at about 14 (wt.%). Such composition lies in the region of liquid droplet that forms porous films with high mechanical strength. For comparison purpose, we also synthesized poly(amic acid) at room temperature and with diluted casting solution (below 10 wt.%). The resulted films are brittle and exhibit poor mechanical properties. In contrast, the film of S-BPDA–PPDA/ODA co-polyimide that synthesized at low temperature of 10°C with the solid content of polymer of 14 (wt.%) shows excellent mechanical properties. As a last measure to improve the strength, co-polyimide

film was synthesized in this work by choosing PPDA and ODA as co-diamine source. It is reported by C. Huang *et al.*[54] the film of S-BPDA–PPDA/ODA had a 35% higher ultimate strength and a 64% higher elongation at break at the ambient temperature than the reference polyimide (S-PBDA–PPDA), and also retained the strength and exhibited a 200% higher elongation at a temperature of 200°C.

Converting poly(amic acid) into corresponding polyimide followed heat treatment was proved by FT–IR spectra shown in Figure 3.4.

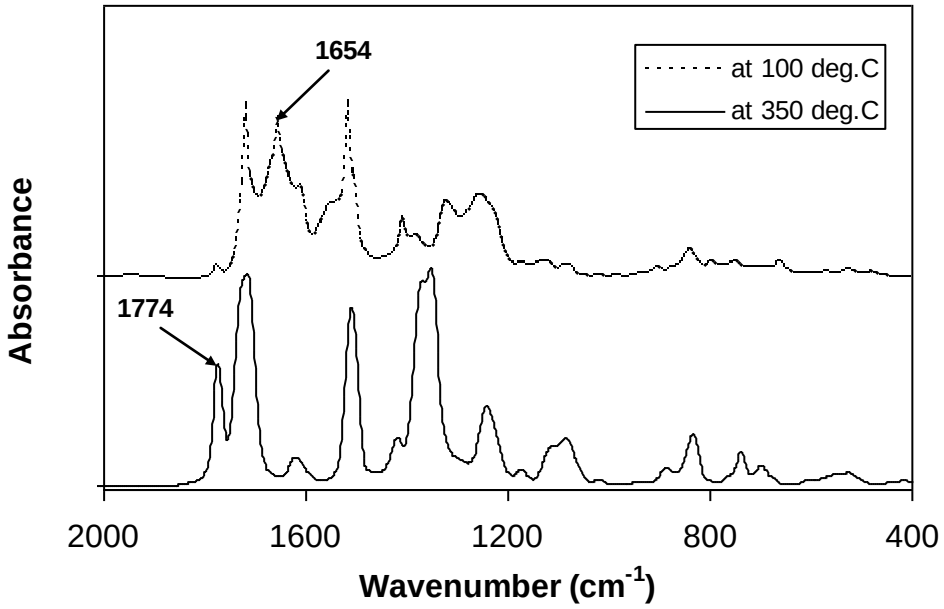

Figure 3.4 FT–IR spectrum of the cast film S-BPDA–PPDA/ODA treated at different temperatures.

Apparently, the success of the imidization process of the film treated at 350°C for 1h was identified by the disappearance of absorption peak of amide carbonyl group at 1,654 (cm^{-1}) and by the appearance of the band near 1,774 (cm^{-1}) which is related to the symmetric stretch of C=O of an imide group.[75] Film treated at 100°C still shows the adsorption peak of amide carbonyl group and there is minimal peak at 1,774 (cm^{-1}). According to

these FT−IR spectra results, one can conclude that the imidization process is completed after 1h at 350°C.

3.3.2 Formation and Morphology of Porous Polyimide Film

Other than mechanical strength, porosity is another key property for the porous polyimide film to be used as a support matrix of the composite membrane for DMFCs. Both thermodynamic and kinetic factors affect the film forming process. In a wet phase inversion process, the thermodynamics of the polymer solution provide information on the overall porosity of the final film, while the pore size and its distribution are controlled by kinetic factors. That means the mass transfer, expressed by the exchange rate of solvents and non-solvents at the interface between the polymer solution and coagulation solution, determines the structure of film.

Solvents used in the synthesis of a poly(amic acid) solution play very important roles in determining the final morphology of the porous film. Some reports have shown that the films prepared with tetrahydrofuran (THF) or acetone as solvent have a spongy porous sub-structure. In contrast, films prepared using N−methylpyrrolidone (NMP), N,N−dimethylacetamide (DMA), N,N−dimethylformamide (DMF), or dimethylsulfoxide (DMSO) as solvent exhibit a finger type structure after coagulating in water.[58] Those results were explained from kinetics by the interaction between a solvent and a non-solvent in the coagulation process. In the case of the THF or acetone, the low affinity of solvent and non-solvent mixture caused a delayed de-mixing so that the film consisted of a dense or semi-porous top layer and a sponge type sub-structure. Alternately, the high affinity of NMP, DMA, DMF, or DMSO with non-solvents caused an instantaneous de-mixing between the solvent and non-solvent.

In this study, we try to make the porous polyimide film with a spongy type sub-structure which we believe is a better structure as the matrix to fabricate a pore-filling electrolyte membrane.[72] Obviously, THF and acetone are not suitable for the synthesis of the polyimide film because of their low boiling point. We selected the NMP as the solvent which shows a good solubility for the polymer and 1-butanol as the non-solvent. In addition, to delay de-mixing between the NMP and 1-butanol at interface, we added the 1-butanol to both the casting solution and coagulation bath. Such a delayed de-mixing will facilitate the formation of porous films with spongy structure.

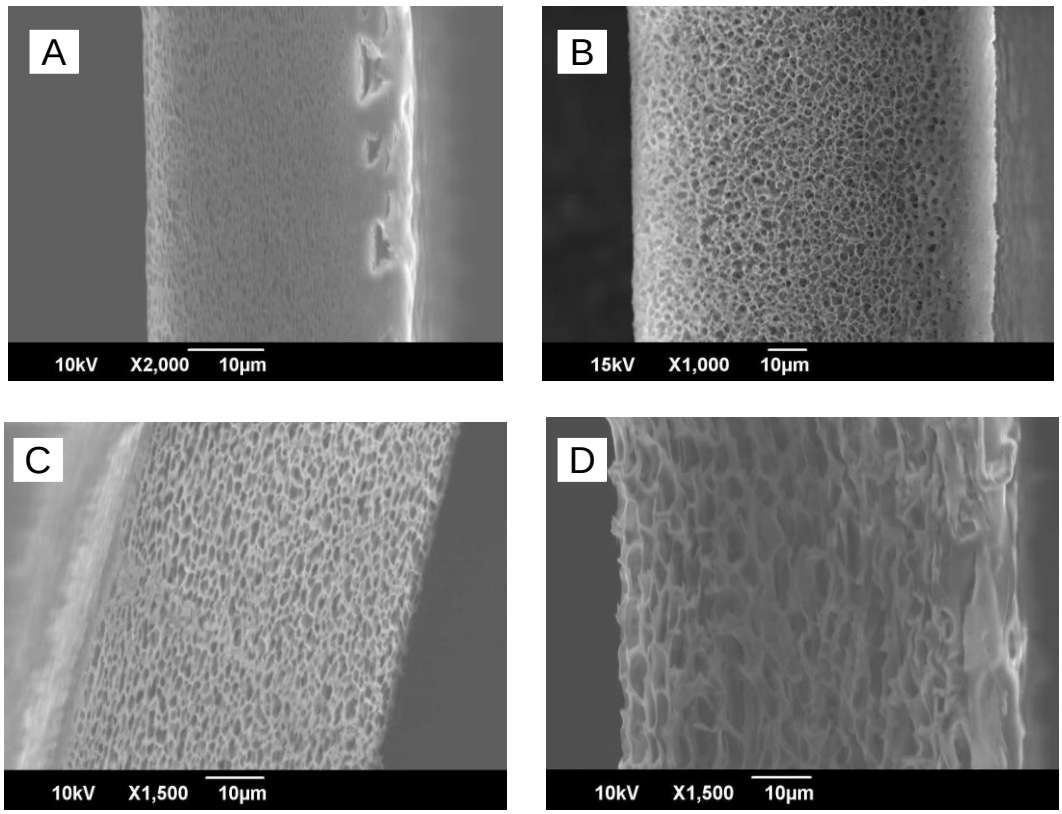

Figure 3.5 SEM images of the cross section of porous polyimide films S-BPDA–PPDA/ODA prepared by coagulating the cast films in non-solvent bath contained different amount of NMP and 1-butanol for 30 min at room temperature: (A) 1-butanol:NMP (w/w)=100:0, (B) 66.7:33.3, (C) 33.3:66.7 and (D) 50.0:50.0.

To form the porous film by wet phase inversion method as in this study, the pore size of the porous film strongly depends on the amount of non-solvent of 1-butanol in the coagulation bath, where the pore size increases with the decrease of 1-butanol content. As can be seen in Figure 3.5, with 100 (wt.%) 1-butanol in non-solvent bath, the porous polyimide film exhibited the dense pore , while bigger pore size was obtained with a lower 1-butanol content of 66.7, 50.0, and 33.3 (wt.%). The casting film precipitated and solidified immediately when the solvent of NMP was absent in the coagulation bath. The resulted porous film consisted of a dense porous surface and a spongy structure with a very small pore size. In contrast, since there is more time for phase separation and solidification when the coagulation bath contains solvent of NMP, the porous polyimide film formed possesses a larger pore size and the pore size of the porous film increases when decreasing 1-butanol content. The casing film coagulated in the bath containing 66.7 (wt.%) 1-butanol and 33.3 (wt.%) NMP shows a uniform and fine pore-size, which is thought to be suitable as a support matrix for composite membranes.

The development of pores in the membrane also depends on the length of coagulation time in the coagulation bath. The scanning electron microscopy images of the cross-sectional structure of S-BPDA−PPDA/ODA co-polyimide films fabricated with different length of coagulation time, forming of porous film was complete from top to bottom after coagulation for 30 min in the bath (Figure 3.6). The film exhibits a dense porous top layer and a spongy type sub-structure. When the cast film of the polymer solution was exposed to the precipitation medium, the top surface began to precipitate first which resulted in a micro-porous surface structure. This precipitated surface layer then became a barrier that slowed the mass transfer of solvent and non-solvent between the sub-surface and coagulation bath. The result is the slower precipitation from the top to the bottom of the film and different porosity developed in the sub-surface compared with the top layer.

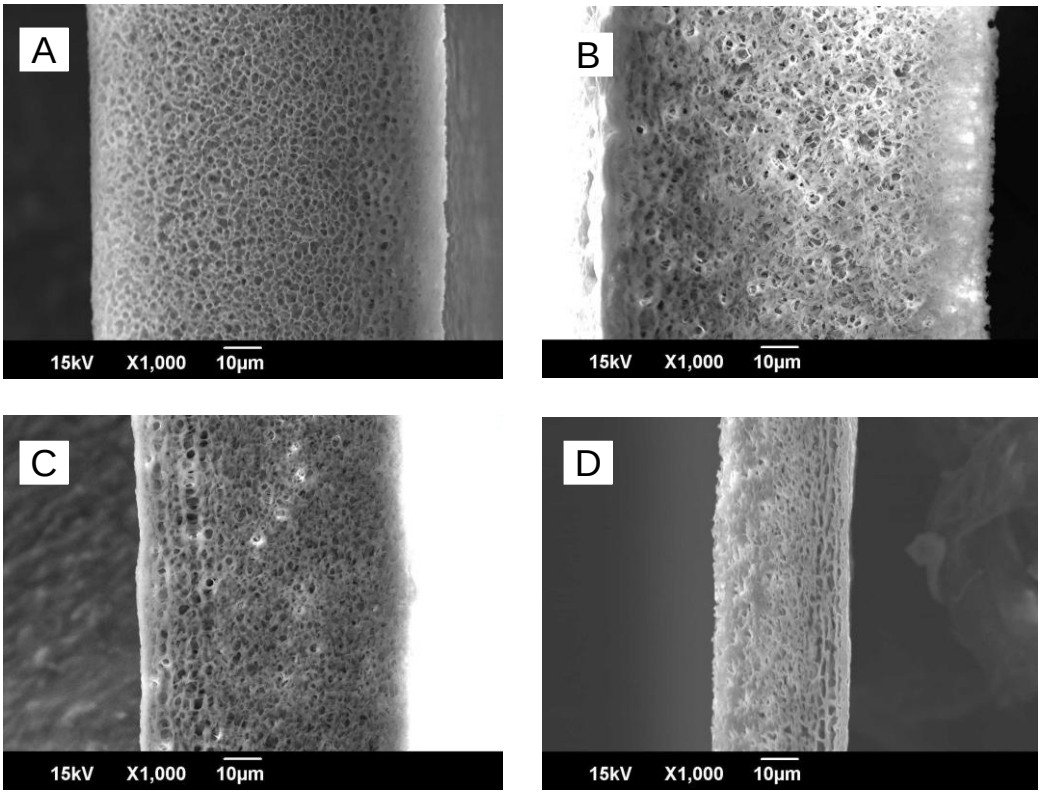

Figure 3.6 SEM images of cross section of porous polyimide films SBPDA–PPDA/ODA coagulated in a mixture of 33.3 (wt.%) DMF and 66.7 (wt.%) 1-butanol for : (A) 30 min, (B) 60 min, (C) 120 min and (D) 240 min.

It is found that, the thickness of porous films decreases with the increase of the coagulation time. After coagulation for 240 min, the thickness of film is reduced by half. This result indicates that the film was dissolved by the mixture of 33.3 (wt.%) NMP and 66.7 (wt.%) 1-butanol if exposed too long in the coagulation bath.

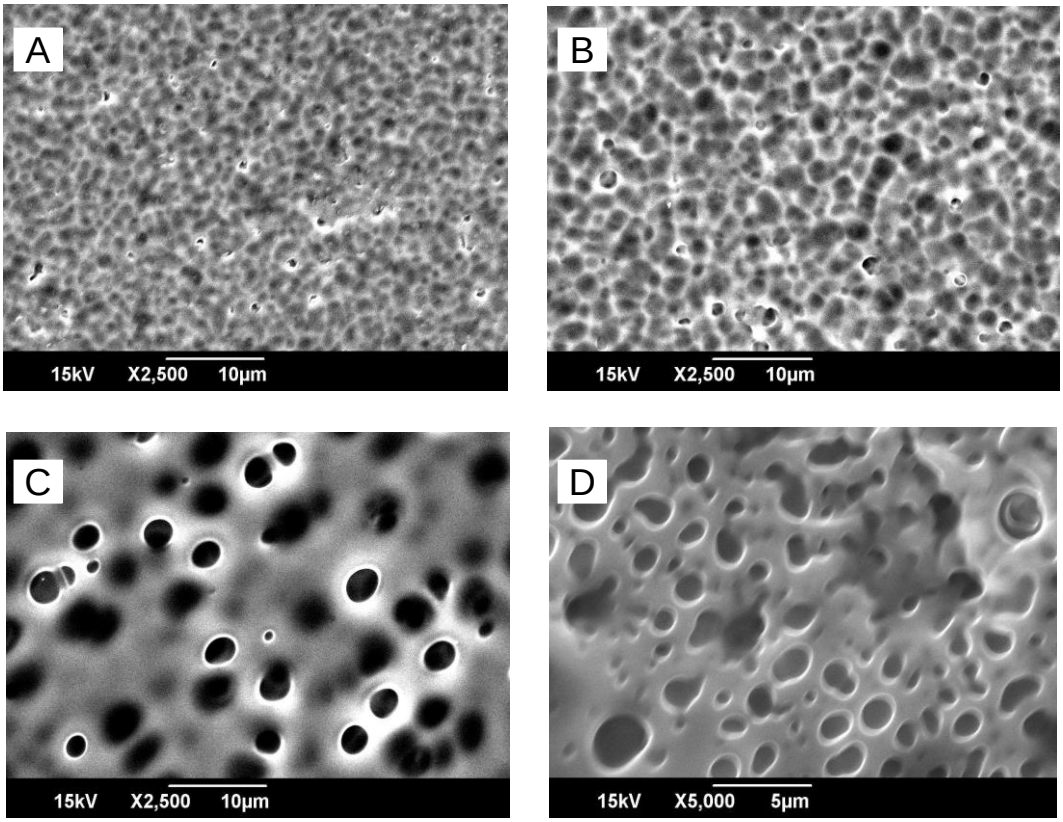

Figure 3.7 SEM images of top layer of porous polyimide films SBPDA–PPDA/ODA coagulated in a mixture of 33.3 (wt.%) DMF and 66.7 (wt.%) 1-butanol for : (A) 30 min, (B) 60 min, (C) 120 min and (D) 240 min.

SEM images in Figure 3.7 shows the top surface of films after coagulation for the difference of time. It can be seen that the dense porous surface layer was dissolved in the non-solvent bath for long time treatment and the resulted film exposes sub-surface layer with larger pore size.

The SEM images of the cross-section of the porous film after 30 min coagulation and a non-porous film were shown in Figure 3.8. Both films contain same amount of the polymer, but the thickness of porous film was increased as many as five times compared with non-porous film (100 µm vs. 20 µm), from which the porosity of film was estimated at ~80 (vol.%).

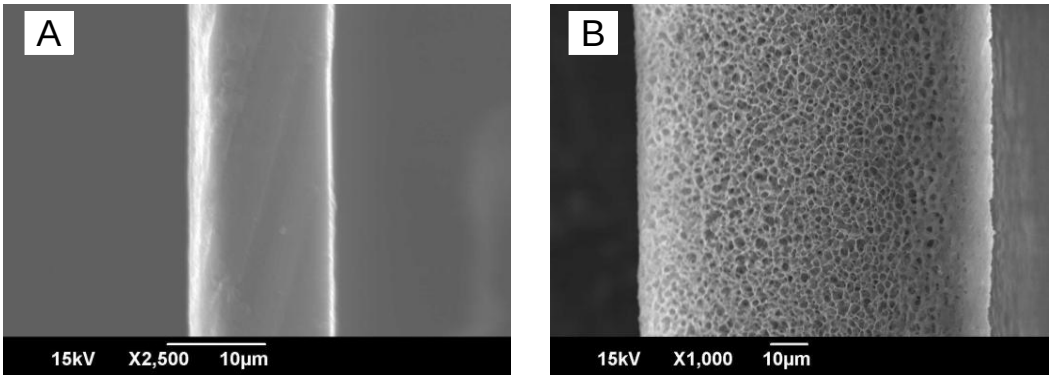

Figure 3.8 SEM images of the cross section of polyimide films S-BPDA–PPDA/ODA: (A) non-porous film and (B) porous film.

3.4 Conclusion

The porous co-polyimide film was prepared with a spongy structure by using a wet phase inversion process derived from a polyimide precursor of S-BPDA–PPDA/ODA. Factors affecting the mechanical strength of the membrane and porosity were discussed. By tuning the parameters, a spongy type porous film with high mechanical strength and porosity was obtained. The porous film consisted of a thin top porous layer and a spongy type sub-structure. The top surface of the membrane had dissolved after pore structure developed completely. Micro-pores in the structure connected to each other were suitable to make a multifunctional composite membrane by filling a proton conducting electrolyte. With a porosity of ~80 (vol.%), this porous film is suitable as a support matrix of a multi-functional composite membrane by filling protonic electrolytes in the micropores of the matrix."

Experiments were conducted to infiltrate the porous polyimide film with a proton conductive electrolyte of Nafion to make composite membrane. Unfortunately, it was very difficult for Nafion filling up all the pores of porous matrix. In addition, the cast solution containing 1-butanol was unstable and become a gel during storage.

In the next chapter, we attempted to prepare new porous polyimide matrixes which can be easily infiltrated with hydrophilic electrolytes such as Nafion, sulfonated poly(styrene-ran-ethylene) to make composite membranes workable as a proton exchange membrane for DMFCs. In addition, the stability of cast solutions over time was also considered.

Chapter 4 Effects of Solvent and Non-solvent on the Morphology of S-PBDA–PPDA/ODA Porous Polyimide Films Based on Wet Phase Separation

4.1 Introduction

The composite membrane based on pore-filling electrolyte is considered as one of the promising proton exchange membranes replacing Nafion-based membranes for DMFCs.[76, 77] However, the difficulty of infiltration of an electrolyte into the host porous matrix and a low porosity of commercialized polyimide substrates are resisted such a membrane widely use for the real DMFCs application.[29, 78] Therefore, efforts to synthesize a good porous matrix suitable for making a composite membrane take much attention at this time.

The wet phase inversion method is one of the major phase separation techniques to fabricate a porous polymeric film because such a method can be applied with a wide range of polymer solutions and it is easy to control pore size and porosity of the film, which could allows the fabrication of the porous films with different morphologies.[59, 79] In the process, a homogeneous polymer solution is normally cast on a suitable support and is subsequently immersed in a non-solvent bath, which typically contains water, lower alcohols, or their mixtures. Phase separation occurs because of the diffusion of non-solvent into the cast film and of solvent out of it. During this process, a polymer-rich phase and a polymer-poor phase are formed, which are turned into the film matrix and the film pores respectively. The morphology of the film is significantly affected by the physico-chemical properties of polymer/solvent/non-solvent interaction.

In this study, aiming to look for a porous matrix with a high porosity, high mechanical strength, and easiness to be filled up by an electrolyte, the pore-forming behavior of the S-BPDA–PPDA/ODA polyimide films was investigated by using different cast solutions and coagulating in a non-solvent bath with various compositions. The non-solvent bath contains water, 1-butanol, or a mixture of DMF and 1-butanol with different ratios. The cast solution is a poly(amic acid) of S-BPDA–PPDA/ODA dissolved in DMF with or without non-solvent additive of methanol or 1-butanol.

4.2 Experimental Details

4.2.1 Synthesis of Cast Solution of Poly(amic acid) S-BPDA–PPDA/ODA

S-BPDA was dissolved in a aromatic diamine solution containing PPDA, ODA and dimethylformamide (DMF) with a molar ratio of S-BPDA:PPDA:ODA (1:0.75:0.25). The polymerization reaction was carried out with strong stirring by a mechanical stirrer in nitrogen environment to exclude moisture at room temperature for 24h to complete the condensation reaction. Finally, a polyimide precursor of poly(amic acid) solution was obtained.[55]

4.2.2 Preparation of Porous Polyimide Film

In order to study the influence of non-solvent additive on the morphology of porous films, in addition to a cast solution of poly(amic acid) as synthesized, methanol or 1-butanol was added to the initial polyimide precursor to prepare cast solutions containing non-solvent additive. The total solid content of all cast solutions was maintained at 16 (wt.%). The porous PI film was fabricated by a wet phase inversion based technique. First, the solution was cast on a glass plate by Spin Coating Machine (SCS G3, Cookson Electronics) with a spin speed of 1,000 rpm and a spin time of 60s. Then, the cast film

was coagulated immediately in a non-solvent bath, which contains water, 1-butanol, or a mixture of 1-butanol and DMF with various ratios, at room temperature for 15 min to develop porous structure, followed by aging in methanol for 5 min and then in water, and subsequently drying in the air for 12h. Finally, the porous film was dried and cured by heating in a vacuum oven in four stages: at 100^{o}C for 1h, 200^{o}C for 1h, 300^{o}C for 1h, and 350^{o}C for 30 min.

4.2.3 Film Characterization

4.2.3.1 Field Emission Scanning Electron Microscope (FE-SEM)

The morphology of the porous film was observed by Field Emission Scanning Electron Microscope (FE-SEM: JSM−6390LA, JEOL). The film was fractured by dipping in liquid nitrogen and then coated with Pt/Pd by Auto Fine Coater (JFC−1600, JEOL) before observation.

4.2.3.2 Fourier Transform Infrared Spectroscopy (FT−IR)

The thermal imidization of the film from poly(amic acid) to polyimide was examined by FT−IR spectra of transparent thin films taken by a Perkin−Elmer FT−IR Spectrum X spectrophotometer.

4.2.3.3 Mechanical Strength

The mechanical property of the porous PI film was measured under ambient condition for dry state by a Universal Materials Machine (Instron 5543, Instron Corp.) following Standard Test Method for Tensile Properties of Thin Plastic Sheeting ASTM D 882-02. The test samples were prepared in 5 (mm) width and 100 (mm) length with 5 test specimens for each specific porous film. The testing speed was 1 (mm/min) and initial

gage length was 50 (mm). The curve of tensile stress versus strain was generated until the film was fractured.

4.2.3.4 Film Porosity

The porosity of the porous film Φ_p (%) was estimated using the following Equation 4.1.

$$\phi_p = \left\{1 - \frac{\left(\frac{w_{sub}}{\rho_{sub}}\right)}{V_{sub}}\right\} \times 100 \qquad (4.1)$$

where w_{sub}, ρ_{sub}, and V_{sub} are the porous substrate weight, polyimide density, and volume respectively.

4.3 Results and Discussion

4.3.1 Poly(amic acid) Synthesis and Thermal Imidization Process

The polycondensation reaction of an organic dianhydride and a diamine was typically employed for the synthesis of a poly(amic acid) solution.[55] Briefly, as shown in Figure 4.1, the reaction of an aromatic dianhydride (S-BPDA) with aromatic diamines (PPDA and ODA) forms dimethylformamide soluble poly(amic acid) as the PI precursor (stage 1), which is thermally converted to a PI (stage 2).

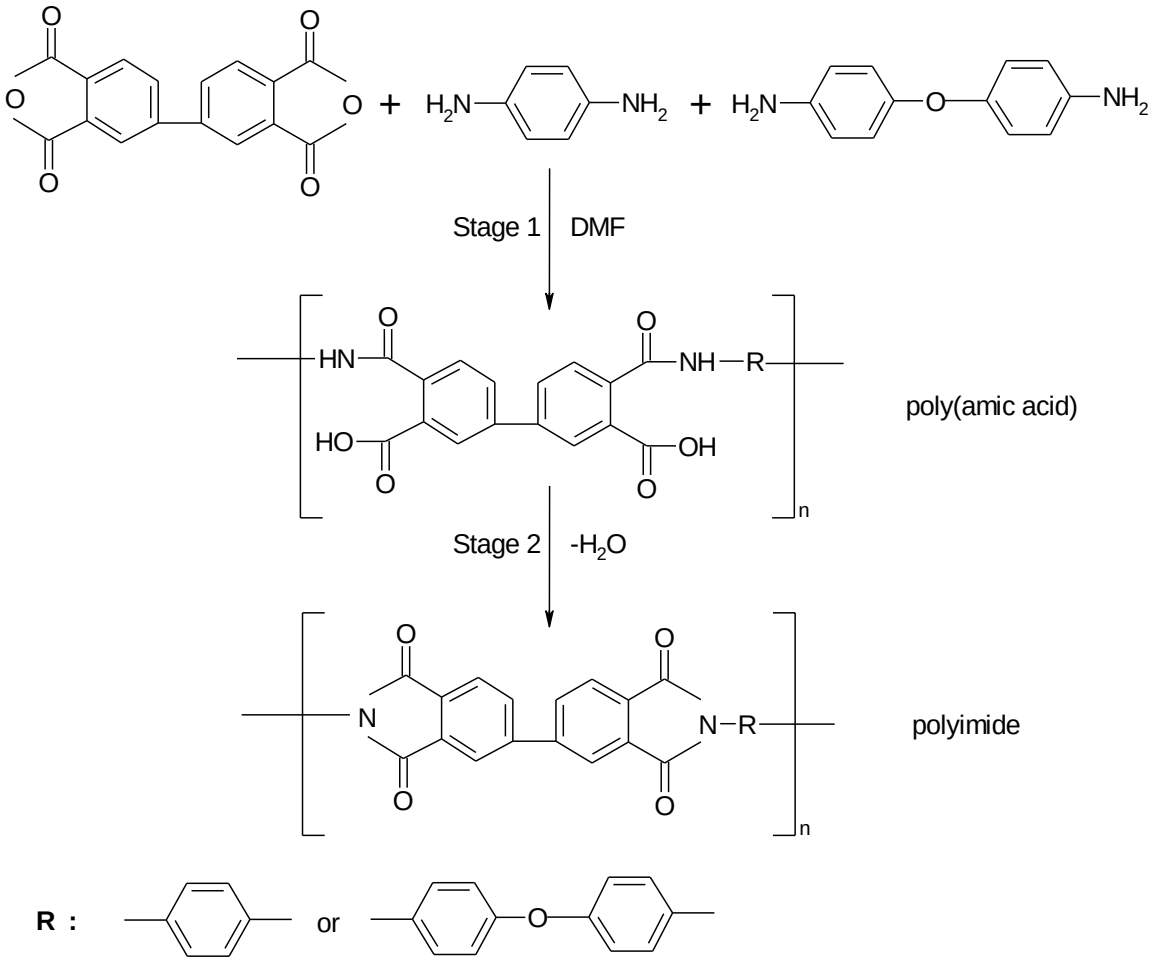

Figure 4.1 Two-stage synthesis of polyimide S-BPDA–PPDA/ODA.

The thermal imidization of the PI film was proven by FT–IR spectra of the poly(amic acid) and polyimide shown in Figure 4.2, where the disappearance of amide carbonyl absorption at 1,654 (cm^{-1}) and by the appearance of imide absorption at 1,776 (cm^{-1}).[55] According to these results, it can be conclude poly(amic acid) converted into polyimide completely after treated in vacuum oven at 350°C for 30 min.

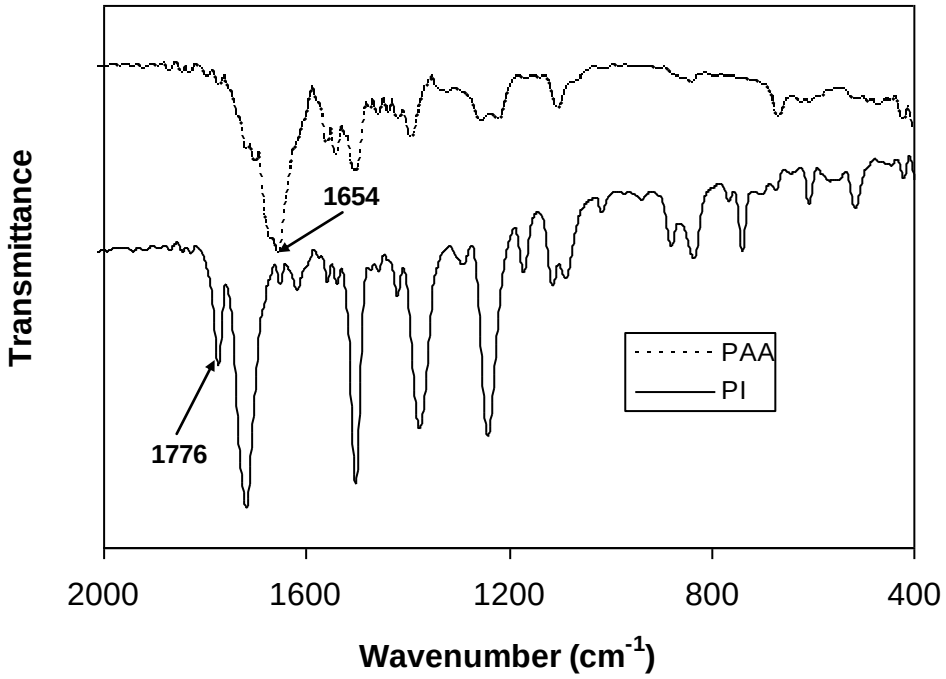

Figure 4.2 FT–IR spectra of poly(amic acid) (PAA) S-BPDA–PPDA/ODA and corresponding polyimide (PI).

4.3.2 Factors Affecting on Morphology of Porous Polyimide Film

It is well known that, both the thermodynamic and kinetic factors have significant influences on the porous film forming process. In a wet phase inversion process, the thermodynamic properties of the polymer solution provide some information on the overall porosity (ε), but not on the pore size and its distribution, which are mainly determined by kinetic effects, expressed as the exchange rate of the solvent and non-solvent at the interface between the polymer solution and the coagulation bath. During the precipitation process, polymer solution compositions are thermodynamically unstable. As more solvent leaves the casting solution and non-solvent enters the solution, it spontaneously separate into two phases, which are polymer-rich and polymer-poor phases.[80] At some point, the viscosity of the polymer-rich phase is high enough for the

precipitated polymer to be regarded as a solid. Once the precipitated polymer solidifies, further bulk movement of the polymer is hindered. Based on this phase separation knowledge, different pore size and different morphology of the film can be realized.

Many reports have confirmed solvent dissolved monomers play an important role for successful synthesis of poly(amic acid) as well as determining the properties of the resulted porous film, where highly polar solvents are preferred for synthesizing poly(amic acid)s and subsequently forming a good porous matrix.[51, 81, 82] Therefore, a solvent DMF was selected because it dissolves easily a wide variety of polymers, and the casting solution based on this solvent precipitates rapidly when the cast film was immersed in a non-solvent bath to give a highly porous film.[58] In this study, the influence of the coagulation bath composition on the porous film property was conducted by using different coagulants as a non-solvent to develop porous films, including water, 1-butanol, and mixtures of 1-butanol and DMF with various ratios. When exposing the cast film to the coagulation bath, phase separation occurred, where the pores can grow until the matrix phase, the polymer-rich phase, is solidified. Here the pore size can be controlled by changing the DMF/1-butanol ratio, where the pore size of the porous film increases with the decrease of 1-butanol content in the coagulation bath, as shown in Figures 4.3, 4.4 and 4.5 or porous films prepared from the cast solution containing no non-solvent, 1-butanol, and methanol additives respectively.

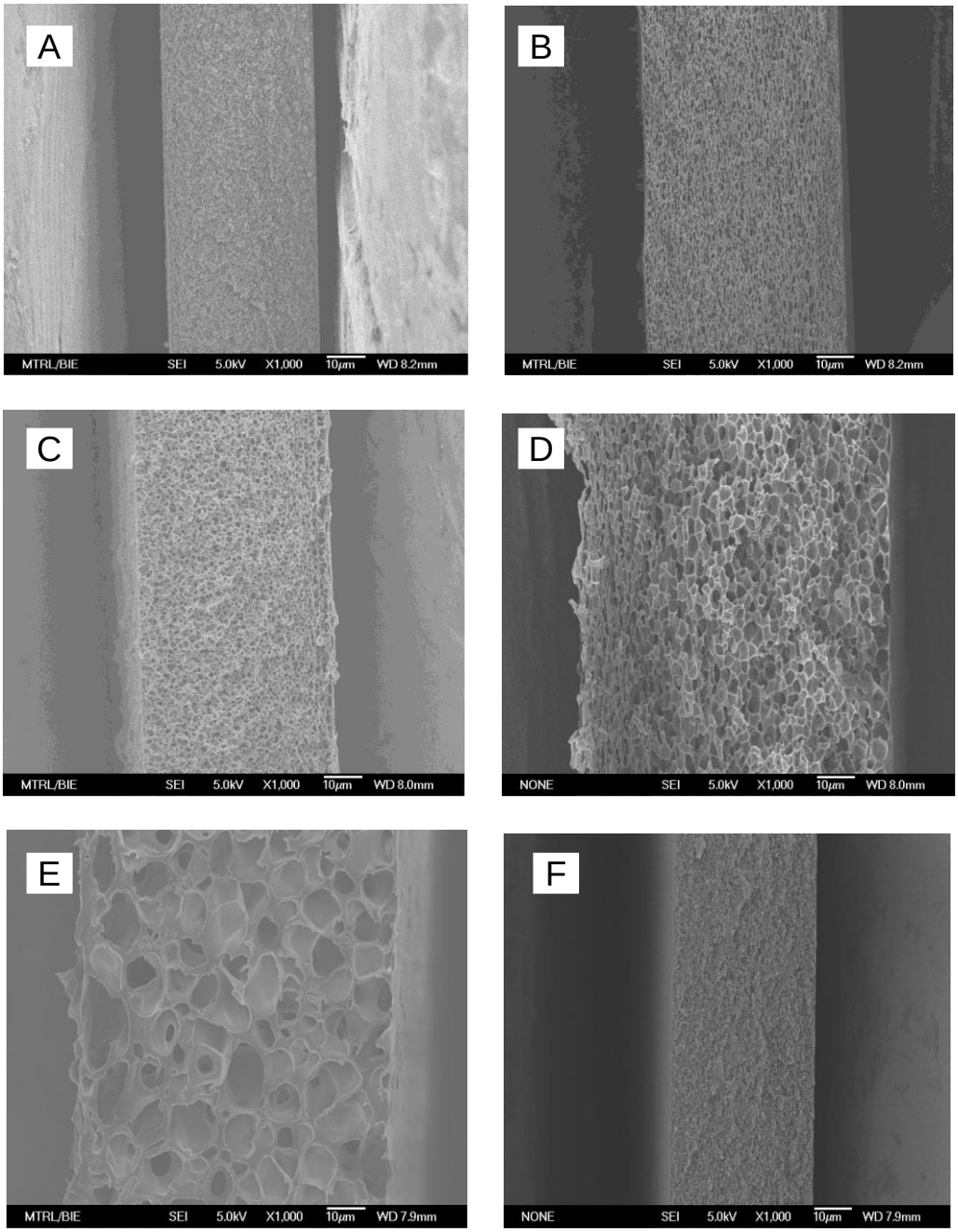

Figure 4.3 FE–SEM images of the cross sections of the porous polyimide film of S-PBDA–PPDA/ODA prepared from the cast solution without non-solvent additive by coagulating the cast film in the non-solvent bath with different compositions: (A) 1-butanol, (B) 1-butanol:DMF (vol.%:vol.%) of 90:10, (C) 80:20, (D) 70:30, (E) 60:40 and (F) water.

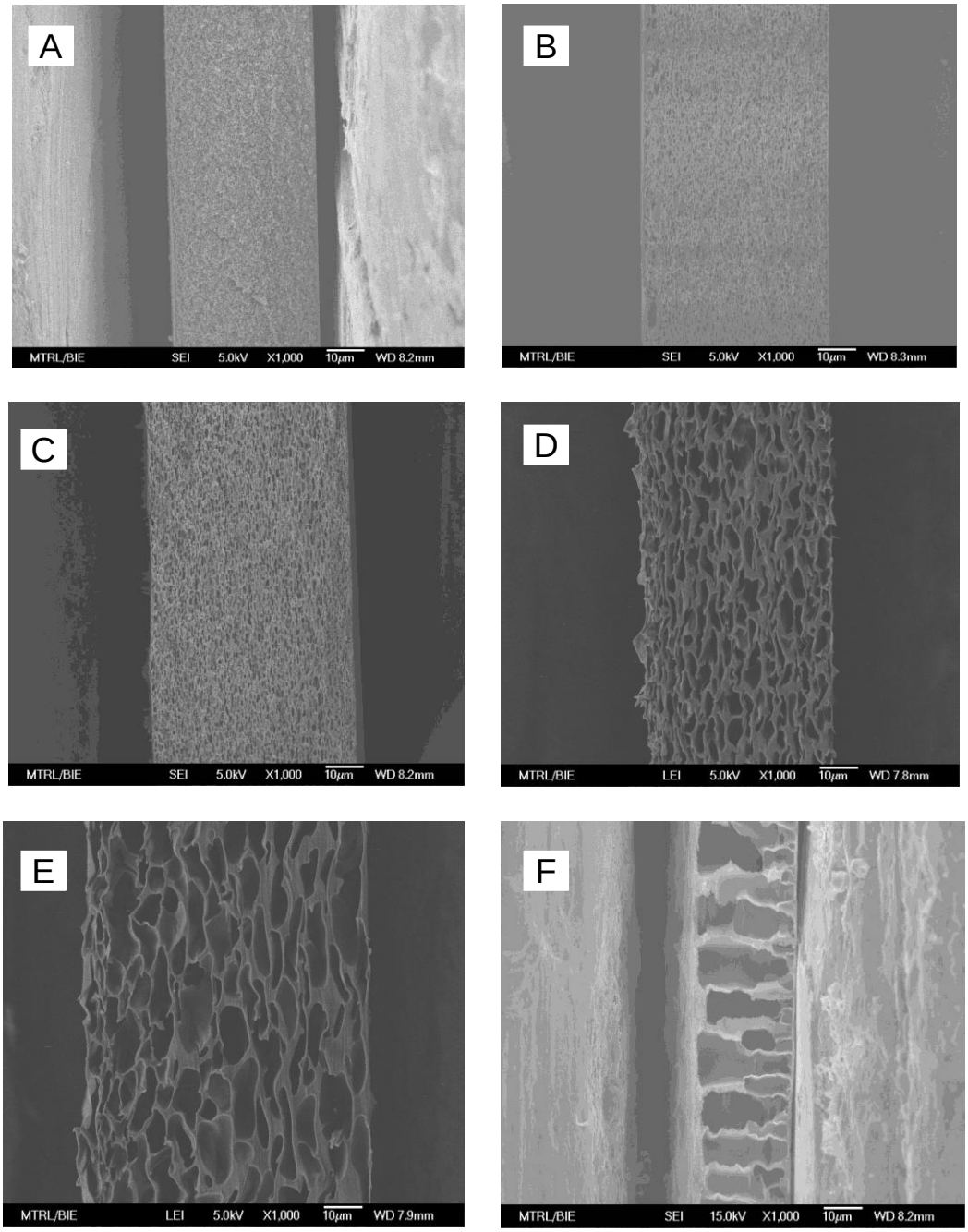

Figure 4.4 FE–SEM images of the cross sections of the porous polyimide films of S-PBDA–PPDA/ODA prepared from the cast solution containing 1-butanol additive by coagulating the cast film in the non-solvent bath with different compositions: (A) 1-butanol, (B) 1-butanol:DMF (vol.%:vol.%) of 90:10, (C) 80:20, (D) 70:30, (E) 60:40 and (F) water.

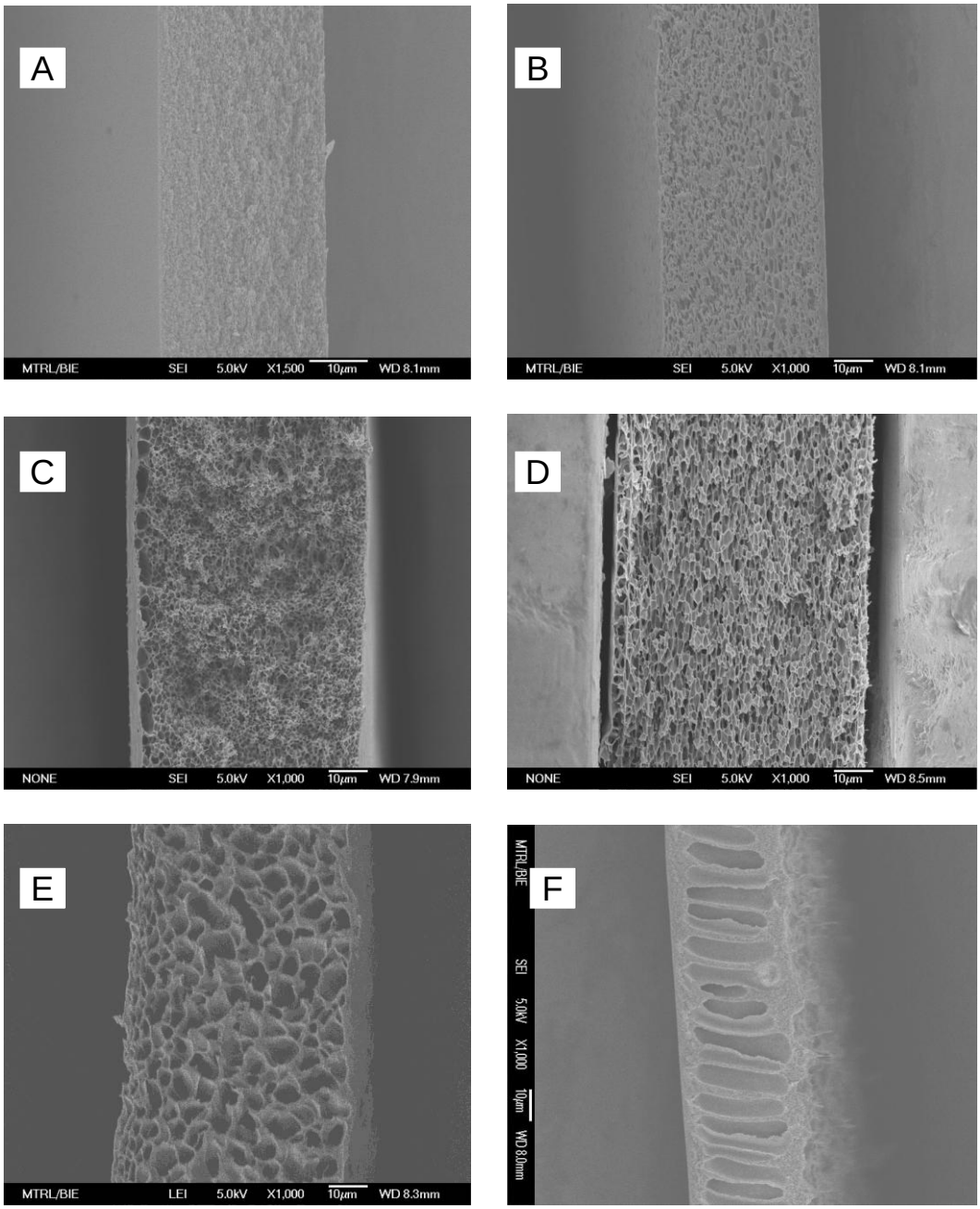

Figure 4.5 FE–SEM images of the cross sections of the porous polyimide films of SPBDA–PPDA/ODA prepared from the cast solution containing methanol additive by coagulating the cast film in the non-solvent bath with different compositions: (A) 1-butanol, (B) 1-butanol:DMF (vol.%:vol.%) of 90:10, (C) 80:20, (D) 70:30, (E) 60:40 and (F) water.

Apparently, this trend does not depend on the non-solvent additive contained in the cast solution and the porous polyimide films prepared with high ratio of 1-butanol (90%, v/v and 100%, v/v) exhibit pore size smaller than 1 μm, while much bigger pore size is obtained with the low 1-butanol ratio of 60%, 70% and 80% (v/v). With lower 1-butanol content, the rates of solvent removal from the cast film and 1-butanol entering the cast film are also slowed, and the polymer concentration of the polymer-rich phase is also lower. Therefore, there is a longer time until the film solidifies and bigger pores can be developed. In other words, the casting film immediately becomes precipitated when solvent DMF is absent or has low concentration in the coagulation bath, causing rapid diffusion of 1-butanol into the film. As a result, the precipitated polymer is easily solidified and the resulting structure of the porous film is uniformly porous.[74]

While pore size is affected by the content of DMF in the coagulation bath, the morphology of porous films depends on the specific cast solution. The pore shape in the porous film is spongy type when the cast film without additive was coagulated in the non-solvent bath of any composition of water, 1-butanol, or a mixture with various ratios of 1-butanol and DMF (Figure 4.3). Alternatively, the cast solution containing additive of 1-butanol or methanol renders films with a spongy type when coagulated in the coagulation bath of 1-butanol and its mixture with DMF and a finger-type structure when coagulated in water, as shown in Figures 4.4 and 4.5. Apparently, in this case, alcohol transport during liquid-liquid demixing controlled the morphology of resulted films. With the cast solution containing no non-solvent additive, a delayed demixing occurred in all types of non-solvents, In contrast, for cast films containing non-solvent additives of 1-butanol and methanol, exchange rate between solvent and non-solvent increases when coagulating in water due to inducement of additives, leading to the formation of finger type structure, while delayed de-mixing can still occur when coagulating in 1-butanol and its mixtures

with DMF.[81] Moreover, the structure of the porous film prepared from a methanol-containing cast film exhibits a uniform finger type, commonly called cylinder-type structure (Figure 4.5(F)). This result can be explained by the high affinity of methanol with water than 1-butanol.

4.3.3 Mechanical Property of Porous Polyimide Film

To be used as a porous matrix of composite membrane for DMFC, the key requirement is that the porous polyimide substrate must be mechanically strong, stiff in structure, and highly porous.[27] To achieve that, we use co-polyimide S-PBDA–PPDA/ODA which combines flexible ODA monomeric unit and rigid PPDA monomer for the synthesis of porous PI film. It is reported that the ultimate strength and tensile modulus of this co-polyimide is greater than those of the reference polyimides of S-PBDA–PPDA and S-PPDA–ODA.[55] In addition to the composition of the polymer, the solid content of cast solution plays an important role in affecting the mechanical strength of resulted porous films. As described in previous chapter, if dilute casting solutions are used, in which the precipitation pathway enters the two phase region below the critical point, precipitation produces polymer gel particles in continuous liquid phase. Such formed membranes are then weak in strength. Therefore, we have chosen the polymer composition of the casting solution at about 16 (wt.%) of solid content, which allows the precipitation to occur as a liquid droplet in a continuous polymer-rich phase and ensures high mechanical strength of the resulted porous film. As expected, the mechanical strength of all the porous PI films with different morphologies is high, as seen in Figure 4.6. Particularly, the mechanical strength of the porous film with spongy-type structure is higher compared to those of cylinder and finger type (78.4 vs. 45.1 and 42.2 MPa) (Table 4.1), because macrovoid-containing films can easily lose their strength, leading to mechanical weakness.[72]

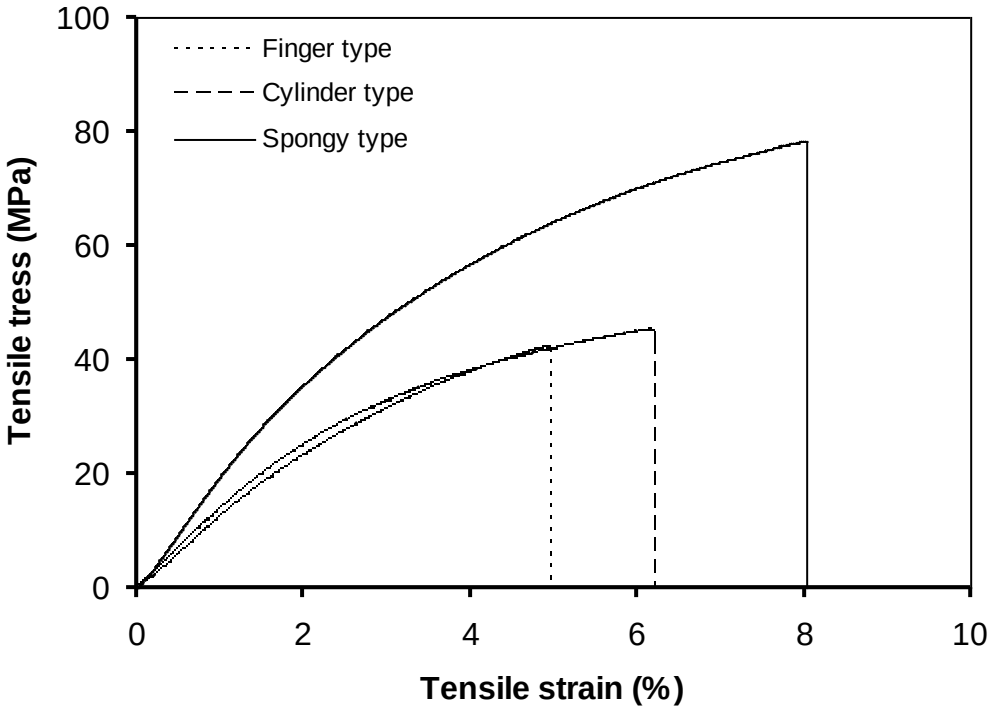

Figure 4.6 Tensile stress-strain curves of the porous polyimide film S-BPDA−PPDA/ODA with different morphologies.

In addition to mechanical strength, the porosity of the porous matrix strongly affects the performance of the resulted composite membrane. A higher porosity is preferred because much electrolyte could be contained in the resulted membrane. The film porosity can be estimated by Equation 4.1 and results were also shown in Table 1. Apparently, the spongy-type structure film exhibits a higher porosity compared to both finger and cylinder type. The high porosity of the spongy type could be explained by its fine structure which leaves more space in the porous film.

Table 4.1 Effect of the morphology on porosity and mechanical strength of porous polyimide films S-BPDA–PPDA/ODA.

Morphology of PI film	Finger	Cylinder	**Spongy**
Porosity (vol.%)	55	57	**80**
Mechanical strength (MPa)	42.2	45.1	**78.4**

Other than that, the porous surface of polyimide matrixes is also critical for the success of electrolyte infiltration, where the matrix with a highly porous surface will be easier to be filled up by electrolytes compared to a dense porous surface film.[83] The top surfaces of spongy films prepared from different cast solutions were shown in Figure 4.7. As can be seen, the surface of the film prepared from the cast solution without non-solvent additive is more porous compared to those preparing from the cast films containing an additive of methanol or 1-butanol. Obviously, due to the presence of non-solvents in the cast film, the exchange rate between solvent and non-solvent at the interface is slowed down, which makes the top surface of the formed film less porous. In contrast, instantaneous de-mixing between solvent and non-solvent occurs for the cast film without additive, forming the porous film with open and porous top layer.

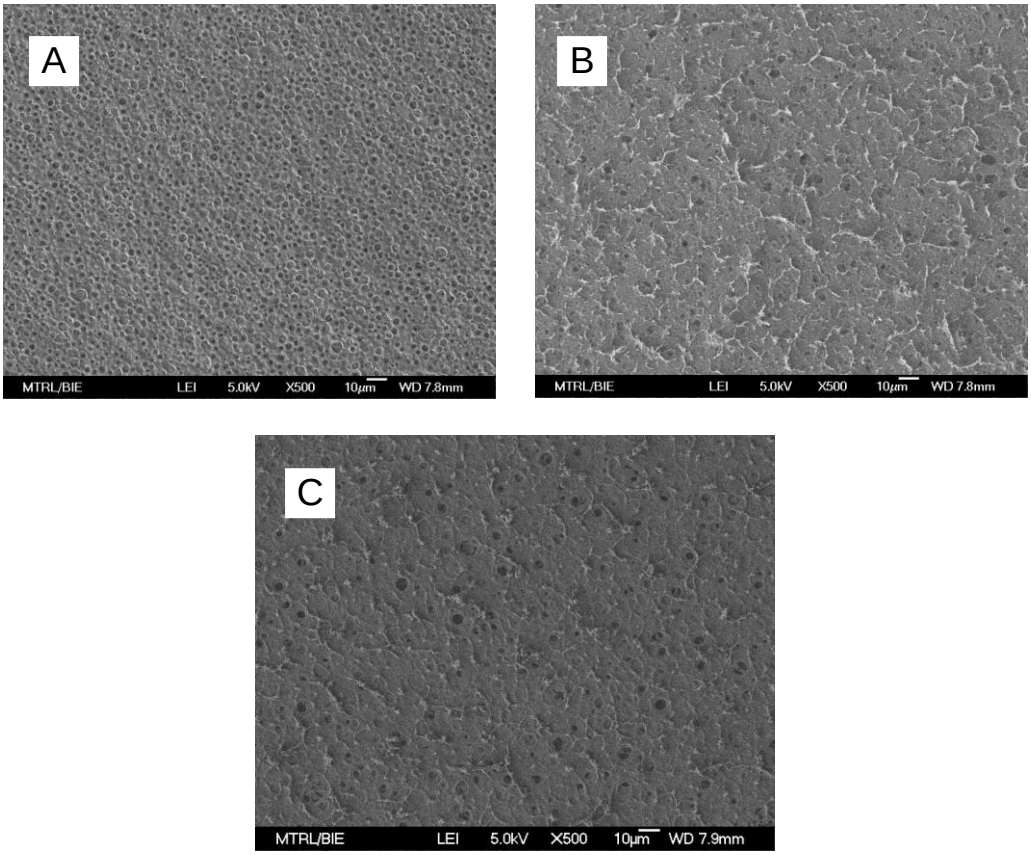

Figure 4.7 FE−SEM images of top layer of the porous polyimide film S-BPDA−PPDA/ODA prepared by coagulating in a non-solvent bath of 80 (vol.%) 1-butanol and 20 (vol.%) DMF from different cast solutions: (A) no additive, (B) methanol additive, and (C) 1-butanol additive.

4.4 Conclusion

Porous polyimide films of S-PBDA−PPDA/ODA with different pore sizes and morphologies based on a wet phase inversion technique were prepared. The film morphology does not depend on various volume ratios between 1-butanol and DMF in the coagulation bath, but the pore size of the porous film is affected by this change, where it increases with the decrease of 1-butanol content. Meanwhile, the porous film morphology can be controlled by non-solvent additive contained in the cast solution. A spongy type was obtained when the cast film without additive was coagulated in water, while finger

type and cylinder type were achieved for the cast film containing additive of 1-butanol and methanol, respectively. In addition, porosity and mechanical strength of the porous PI film were significantly dependent on its morphology, which are higher for a spongy type compared to the cylinder and finger structure. The porous polyimide film prepared from the cast solution without additive by coagulating the cast film in a mixture of 1-butanol and DMF of 80:20 (v/v.%) consisted of a spongy type sub-layer with uniform and sub-micrometer pore size and a highly porous top layer. In addition, with a high porosity of 80 (vol.%), and high mechanical strength of 78.4 (MPa), such a porous PI film is considered as the best support matrix for constructing a composite membrane by infiltrating an electrolyte into the pores of the matrix.

In the next chapter, experiments were conducted to infiltrate the porous polyimide film with proton conductive electrolytes like sulfonated poly(styrene-ran-ethylene), Nafion, sulfonated polyimide to make the composite membrane, and characterize its performance as a proton exchange membrane for DMFCs, including proton conductivity, methanol crossover, mechanical strength and DMFC cell performance.

Chapter 5 Pore-Filling Electrolyte Membrane for Direct Methanol Fuel Cells Based on Sulfonated Poly(Styrene-*ran*-Ethylene) and Porous Polyimide Matrix

5.1 Introduction

"The DMFCs are one of the most potential power sources for portable devices because of their clean energy source, high energy density and system simplicity.[2, 4] Nafion membrane is the most use as proton exchange membrane for DMFCs due to its high proton conductivity, highly mechanical strength, and good chemical resistance.[16] However, because of its high methanol permeability, crossover of liquid methanol fuel from the anode side to cathode, it is limitation to be used Nafion membrane for DMFCs application.[84] Methanol crossover causes the decrease of DMFCs open circuit voltage called mixed potential, loss of methanol fuel, and catalyst poisoning.[12] To date, many membranes have been developed in aims to replace the Nafion membrane for DMFC application such as the modification of Nafion membrane by introducing inorganic materials into Nafion structure,[19, 85] sulfonated polyimides,[24, 86] sol-gel type organic-inorganic hybrids.[87] Unfortunately, these membranes do not satisfy all criteria for DMFC membranes including low methanol permeability, high proton conductivity, chemical resistance, dimensional stability between dry and wet state, and high mechanical strength.

Yamaguchi *et al*. first proposed the concept of pore-filling electrolyte membrane in an attempt to meet all these requirements.[25, 28] This membrane consists of two parts: a porous substrate to provide mechanical strength and a filling polymer that infiltrates the pores of the support matrix to provide proton conductivity. High mechanical strength

would allow for a reduced overall system weight by eliminating the need for external stiffness and strength. It also limits the swelling of the filling electrolyte. As methanol crossover is mainly through the polymer electrolyte filler, the fact that composite membrane mechanically prevents the electrolyte from swelling can lead to decreased methanol crossover due to the confined passage.

Based on Yamaguchi's reports,[27] the porous polyimide (PI) film is realized as one of the good matrixes to make a composite membrane because it shows no excess swelling of the filling polymers and negligible dimensional changes between dryness and wetness. However, due to low porosity of commercial porous polyimides and difficulty to fill up their pores, it is not tailor made to suit the use in fuel cell applications and may not possess optimum properties.

Following a success of fabricating porous polyimide films of S-BPDA–PPDA/ODA with different pore sizes and morphologies in the previous work, in the study, a proton conducting material of poly(styrene-ran-ethylene) (SPSE) or Nafion ionomer was used to construct composite membranes by infiltrating the electrolyte into the porous matrix. The choice of SPSE or Nafion is based on its high proton conductivity and good compatibility with the porous substrate. However, due to high methanol crossover limits its direct application as a proton exchange membrane for DMFCs. While the composite membrane PI–SPSE has been successfully fabricated, Nafion was failed to fill the porous matrix to make the composite membrane PI−Nafion. The PI–SPSE composite membrane prepared from a good porous PI matrix had shown outstanding properties such as a high mechanical strength, low methanol crossover, high proton conductivity, high maximum power density, and less dimensional change between dry and swollen states. Improved fuel cell performance was also demonstrated with this composite membrane.

5.2 Experimental Details

5.2.1 Fabrication of Composite Membrane PI−SPSE

The porous polyimide film was washed by soaking in ethanol for 1h at room temperature and then dried in a vacuum oven at 60°C for 30 min. The filling polymer was prepared from SPSE solution (Sigma−Aldrich, 5 wt. %) or 5 (wt.%) Nafion solution (Gashub, Singapore). It is first dried at 60°C until the solvent is evaporated completely. The obtained pure polymer is then dispersed again in a mixture of absolute ethanol and DMF (volume ratio 2:1) under ultrasonication to form a 5 (wt. %) of filling solution. The clean porous PI substrate was extended over a round glass plate by a membrane caster; after that, the solution made above was poured on the surface of the porous film. The glass plate was put in an oven at 60°C for 24h and finally dried in a vacuum oven at 150°C for 12h. After that, the obtained composite membrane was treated with a commonly used pretreatment procedure using hydrogen peroxide and sulfuric acid solutions described as follows:[17] they were first boiled in a 3 (wt.%) H_2O_2 aqueous solution for 1h, rinsed in boiling double deionized (DDI) water repeatedly. Then, they were boiled in 0.5M H_2SO_4 for 1h, rinsed in boiling DDI water again. Finally, the membrane is boiled for 1h in DDI water and allowed to cool. The hydrogen peroxide served to oxidize any small molecule contaminants that might block the ion conduction channels. Sulfuric acid solution revert all acidic sites to the proton form. After those pretreatments, membranes were stored in DDI water and were ready for testing.

5.2.2 Characterization of Membrane

5.2.2.1 Field Emission Scanning Electron Microscope (FE−SEM)

The morphology of the composite membrane was observed by JEOL Field Emission Electron Microscope JSM−6700F. For cross-section observation, samples were fractured under cryogenic conditions using liquid nitrogen. All samples were coated with gold by Auto Fine Coater before FE−SEM images were taken.

5.2.2.2 Water Uptake

Samples of the membranes were weighed (W_1) after the immersion in DDI water at 80°C for 24h. Then samples were weighed (W_2) after drying in a vacuum oven at 80°C for 24h. Water content (ΔW) was calculated according to Equation 5.1.[28]

$$\Delta W(wt.\%) = \frac{W_1 - W_2}{W_2} \times 100 \quad (5.1)$$

5.2.2.3 Dimensional Stability

Membranes around 2.5 (cm) in diameter were stored in a vacuum oven at 80°C for 24h and the dimension was measured before (L_1) and after (L_2) the samples were soaked in deionized water at 80°C for 24h. The dimensional change (ΔL) was calculated using Equation 5.2.[28]

$$\Delta L(\%) = \frac{L_2 - L_1}{L_1} \times 100 \quad (5.2)$$

5.2.2.4 Proton Conductivity

The proton conductivity of the membrane in the through-plane direction was measured using a potentiostat with built-in frequency response analyzer (Autolab, Netherlands) in a home-made cell.[88, 89] The cell consists of two Teflon blocks attached with platinum foil electrode (1.2×1.2 cm) and platinum lead. The pretreated membrane (1.5×1.5 cm)

was sandwiched between these two Teflon blocks held in place with Teflon screws. The impedance measurements were carried out with frequency range from 250 (kHz) to 150 (kHz). The proton conductivity of the membrane was calculated using the equation $\sigma = L/RS$, where σ, L, R, and S denote the ionic conductivity, thickness of the membrane, resistance of the membrane, and surface area of the electrode, respectively.

5.2.2.5 Methanol Permeability

The methanol permeability of the membranes was determined using the two compartment diffusion cell technique.[17, 21] One compartment (V_A = 62 mL) was filled with a solution of methanol (8 vol.%) and 1-butanol (0.2 vol.%) in deionized water. The other compartment (V_B = 62 mL) was filled with 1-butanol (0.2 vol.%) in deionized water. The pretreated membrane was kept between the two compartments, and these two compartments were kept under stirring conditions during an experiment. The methanol flux establishes across the membrane due to the methanol concentration difference in compartment A and B. V_A and V_B were chosen sufficiently large that a pseudosteady-state condition prevailed during these experiments, after an initial transient. Moreover, the methanol concentration in the receiving compartment was always negligible compared to compartment A, while the concentration in compartment A was almost unchanged during the experiment. Based on the above assumption, the flux of methanol was constant, and the methanol permeability (P) is given by Equation 5.3.

$$P = \frac{V_B L}{A C_A} \frac{dC_B}{dt} \qquad (5.3)$$

where A is the membrane area, L is the membrane thickness, dC_B/dt is the slope of the straight line (C_B versus time), C_B was measured at different time intervals during the

experiment using Gas Chromatography (GC-Agilent 6890N) fitted with a flame ionization detection. The samples (1μL) were drawn from the receiving solution by robotic arm automatically; 1-butanol was used as an internal standard.

5.2.2.6 Mechanical Strength

Testing was performed using testing machine (Instron 5543) following Standard Test Method for Tensile Properties of Thin Plastic Sheeting ASTM D 882-02. The samples were prepared in 5 (mm) width, 100 (mm) length, and 50 (μm) thick with 5 test specimens for each membrane. The testing speed was 10 (mm/min) and initial gage length was 50 (mm).

5.2.2.7 Single Cell DMFC Performance

To minimize the influence from the electrode variation, commercial electrodes (Gashub, Singapore) were used for the membrane electrode assembly (MEA) fabrication and performance test. The electrode consists of a PTFE treated (20 wt.%) carbon paper substrate, a microporous layer with carbon loading of 1.2 (mg/cm^2), and a catalyst layer. The catalyst layer in anode contains 40 (wt.%) PtRu/C and Nafion, with total metal loading of 2.0 (mg/cm^2) (Pt:Ru = 1:1), while that in cathode contains 40 (wt.%) Pt/C and Nafion, with Pt loading of 2.0 (mg/cm^2). MEA with an active electrode area of 5 (cm^2) was obtained by pressing the cathode and anode onto each side of a pretreated Nafion 1135 membrane or composite membrane at 140°C and 2.0 (MPa) for 1min (Hydraulic 3912, Carver, Inc.). The MEA was then assembled into a DMFC single cell. The I-V curves were obtained by the following procedure: (1) a single cell was activated by 1M MeOH with 1.0 (mL/min) for 3h at 70°C with no oxygen flow at the cathode; (2) oxygen was introduced with a flow rate at 0.2 (L/min) until the oxygen back pressure reached 0.3

(MPa); and (3) the single cell polarization curves were collected after the operation conditions of the single cell was stable for 30 min.[21, 22] The operation conditions were as follows: anode fuel 1M MeOH; flow rate, 1.0 (mL/min); oxygen back pressure, 0.3 (MPa); and flow rate, 0.2 (L/min). The temperature of the cell was at 70°C. All single cell tests were conducted three times, and the results presented here are the average data.

5.3 Results and Discussion

5.3.1 Preparation of Composite Membrane PI−SPSE

To fabricate a composite membrane with high performance for DMFCs based on pore-filling electrolyte method, the porous PI matrix preferentially should have pore size on the sub-micrometer scale or less to efficiently suppress swelling and enhance proton conduction of the composite membrane.[90] On the other hand, to successfully infiltrate the electrolyte into the porous substrate, the pore size of a support matrix must be big enough to facilitate infiltration. Other than the pore size effect, for a polymer electrolyte to successfully fill the pores of a host substrate, the viscosity and contact angle on the host substrate of the filling solution must be low.[78, 91] Therefore, to facilitate the subsequent polymer infiltration, we re-dispersed SPSE or Nafion in a mixture of DMF and ethanol to lower the viscosity and also decrease the contact angle between the porous film and filling polymer. During the filling process, the gravity force dragged polymer solution into the pores of the porous PI film and after evaporating solvents, the electrolyte could plug completely the micro-pores.[36]

In this study, the porous matrix S-BPDA−PPDA/ODA formed by coagulating the cast film in the non-solvent bath of 1-butanol/DMF ratio of 80:20 prepared in the previous work was selected as a porous host matrix for constructing the composite membrane by

filling with an electrolyte. Such a porous substrate exhibited a highly porous structure with porosity of about 80 (vol.%) and mechanical strength of 78.4 (MPa) consisting of a spongy type sub-layer with a pore size of ~1 (μm) and a top porous surface as shown in Figures 5.1(A) and 5.2(A).

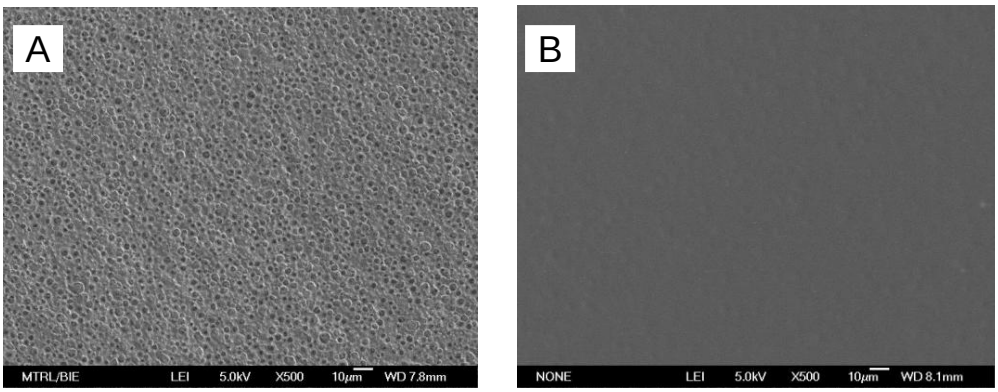

Figure 5.1 FE−SEM images of (A) top surface of the porous polyimide film prepared with 1-butanol:DMF=80:20 and (B) top surface of corresponding composite membrane PI−SPSE.

As can be seen in Figure 5.2(C), electrolyte filling was unsuccessful for Nafion, where Nafion ionomer formed separate layer instead of filling up all pores of the porous matrix. Alternatively, as shown in Figure 5.2(B), the pores of the host matrix were completely filled by the electrolyte of SPSE, no pores can be observed on the cross-section images. In addition to pore size effect, i.e., a porous matrix with bigger size is easier to fill by an electrolyte than those with smaller pore, the viscosity of a filling solution and contact angle between the matrix and solution also play important roles in the filling process. Due to having zero contact angle and very low viscosity, the filling solution of SPSE is easy to penetrate into the pores. In contrast, the filling solution of Nafion forms a small contact angle with the host matrix of PI, therefore, it is difficult to infiltrate Nafion into the porous substrate.

In addition, a smooth morphology was also observed on the top surface, as shown in Figure 5.1(B), indicating that SPSE was distributed uniformly in the composite membrane.

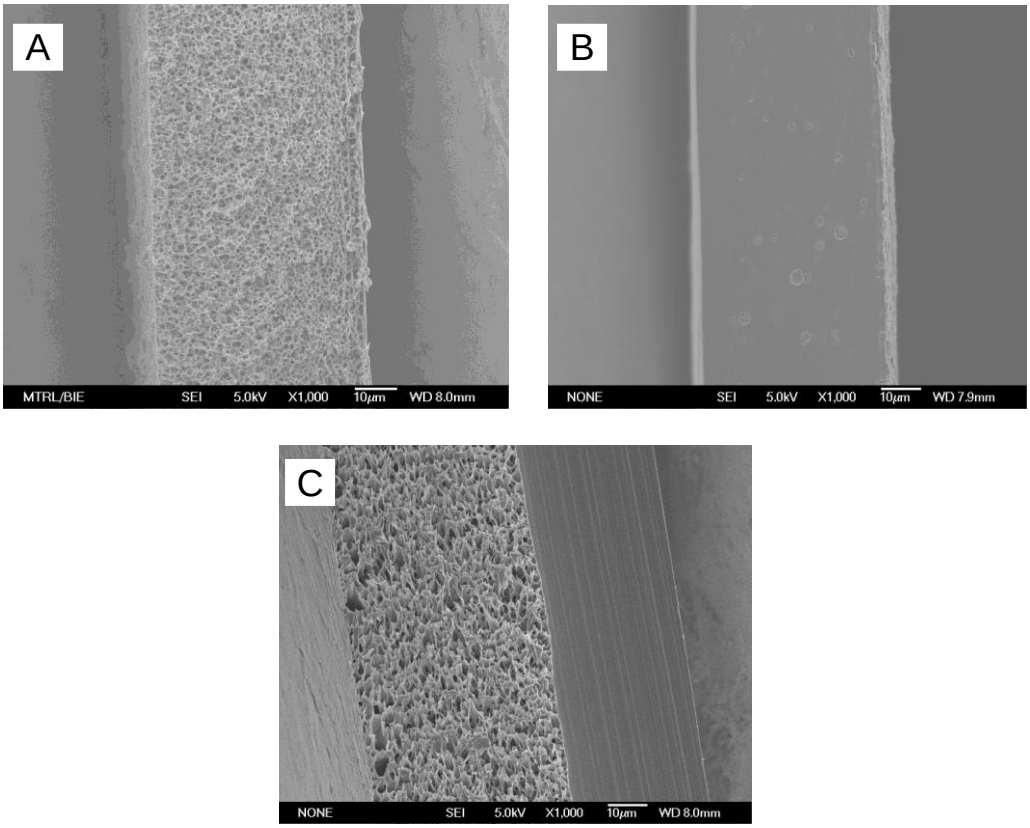

Figure 5.2 FE−SEM images of cross-section of (A) porous PI film prepared with 1-butanol:DMF=80:20, (B) corresponding composite membrane PI−SPSE and (C) PI−Nafion.

5.3.2 Water Uptake and Dimensional Change of Membrane

The dimensional stability of the membrane is one of the important properties for practical operation of a fuel cell. Since carbon electrodes do not swell and change in dimension from any water uptake, less damage to the structure integrity of the MEA and improved durability can be expected for those membranes with smaller change in dimension.[25] Table 5.1 shows the comparison of the PI−SPSE composite membrane with Nafion 1135

and SPSE membrane. After being soaked in water at 80°C for 24h, the PI−SPSE composite membrane shows much lower dimensional change (~1/3 of Nafion 1135) and water uptake (~1/2 of Nafion 1135), although pure SPSE membrane itself shows similar properties as Nafion. We have conducted similar experiments in 1M and 5M methanol at room temperature. In both cases, the dimensional change is less than 4% and no dependence on the concentration is observed, while Nafion 1135 and SPSE membranes show strong dependence on methanol concentration. It can be concluded that the strong PI matrix in the composite membrane can effectively suppress the membrane from swelling and prevent the membrane from absorbing excess water, although the volumetric ratio of PI is only 20%

Table 5.1 Physical Properties of composite membrane PI–SPSE, Nafion 1135 and SPSE membrane.

Membrane	Thickness (μm)	Water content (%)	Dimensional change (%) H_2O (80°C)/1M MeOH/5M MeOH	Tensile strength (MPa)
Nafion 1135	89	24.80	17.0/12.7/18.6	35.2
PI–SPSE	**80**	**11.26**	**5.9/3.7/3.8**	**84.6**
Pure SPSE	105	29.20	18.5/20.6/29.5	31.2

5.3.3 Mechanical Strength of Membrane

Mechanical strength of membranes affects the manufacturing condition and durability of MEA. Higher mechanical strength allows the fabrication of thinner membranes with smaller resistance. As shown in Table 5.1, the composite membrane possessed much

higher mechanical strength compared to Nafion 1135 and pure SPSE membranes (84.6 MPa vs. 35.2 MPa and 31.2 MPa), because of the reinforcing effect of the PI matrix.

5.3.4 Methanol Permeability of Membrane

The methanol crossover from the anode to the cathode not only leads to a lowered fuel utilization, but also lowers the cathodic potential as a result of concurring of oxygen reduction and methanol oxidation on the cathode side. In the pore-filling electrolyte membrane, the pores of the porous PI matrix were completely filled with SPSE polymer. The suppressed water absorption and less dimensional change may indicate less methanol crossover though the membrane. Indeed, as shown in Table 5.2, the measured methanol permeability of the composite membrane is 20 times lower than Nafion 1135 membrane (2.46×10^{-6} cm^2/s vs. 1.25×10^{-7} cm^2/s).

Table 5.2 Electrochemical Properties of composite membrane PI–SPSE, Nafion 1135 and SPSE membrane.

Membrane	Proton conductivity σ (S/cm)	Methanol permeability P (cm^2/s)	Mass flux of methanol (mol/cm^2s)	Selectivity ϕ=σ/P (S s/cm^3)
Nafion 1135	0.062	2.46×10^{-6}	4.32×10^{-7}	2.52×10^{4}
PI−SPSE	**0.091**	**1.25×10^{-7}**	**2.88×10^{-8}**	**7.28×10^{5}**
Pure SPSE	0.105	2.80×10^{-6}	4.47×10^{-7}	3.75×10^{4}

5.3.5 Proton Conductivity of Membrane

The proton conductivity of the membrane is particularly important for fuel cell performance. Two types of cell geometry were reported in the literature regarding the conductivity measurements, namely, in-plane[18, 92] and through-plane measurements.[88, 89, 93] The in-plane conductivity measurements are known to be relatively insensitive to the contact resistance at the current carrying electrodes, but do not reflect the real conductivity of ionic motion through a membrane in a fuel cell. When the membrane is isotropic, the difference between the in-plane and the through-plane conductivity would be small. However, when the membrane is anisotropic, such as multilayer membrane or pore-filling membrane as in this work, the difference would be expected to be large.[93] In this study, the through-plane conductivity for fully hydrated membranes at room temperature is determined and the results are shown in Table 5.2. The proton conductivity of PI−SPSE composite membranes is higher (0.091 S/cm) than the Nafion 1135 membrane (0.062 S/cm) but lower than the pure SPSE membrane (0.105 S/cm) because the pure SPSE possesses a higher ion exchange capacity (0.15 meq/g) than Nafion based membranes (0.10 meq/g) and the high porosity of PI support matrix (80%) minimizes the adverse effect of the non-conducting PI on the conductivity of the resulting PI−SPSE composite membrane. Table 5.2 also shows the selectivity factor (ϕ), a commonly used quantity to describe a membrane's performance in DMFC, which is defined as the ratio between the proton conductivity and the methanol permeability.[21] The selectivity of the composite membrane is much higher than that of the Nafion 1135 membrane (7.28×10^5 S s/cm^3 vs. 2.52×10^4 S s/cm^3).

5.3.6 DMFC Single Cell Performance

The single cell performances of the MEAs based on the commercial Nafion 1135 membrane and PI−SPSE composite membrane are presented in Figure 5.3. As expected, the MEA with the PI−SPSE composite membrane shows a higher performance than that with Nafion 1135 membrane, because of its slightly higher proton conductivity and reduced methanol crossover. Particularly, the PI−SPSE membrane shows a higher open circuit voltage (OCV) than Nafion 1135 membrane (0.70V vs. 0.60V) although they have similar thickness. The OCV of a MEA is closely related to the methanol crossover. Higher methanol crossover leads to a lower OCV. The higher OCV for PI−SPSE membrane then validates that the PI−SPSE composite membrane in the MEA suppressed methanol crossover, consistent with the ex-situ methanol permeability measurement.

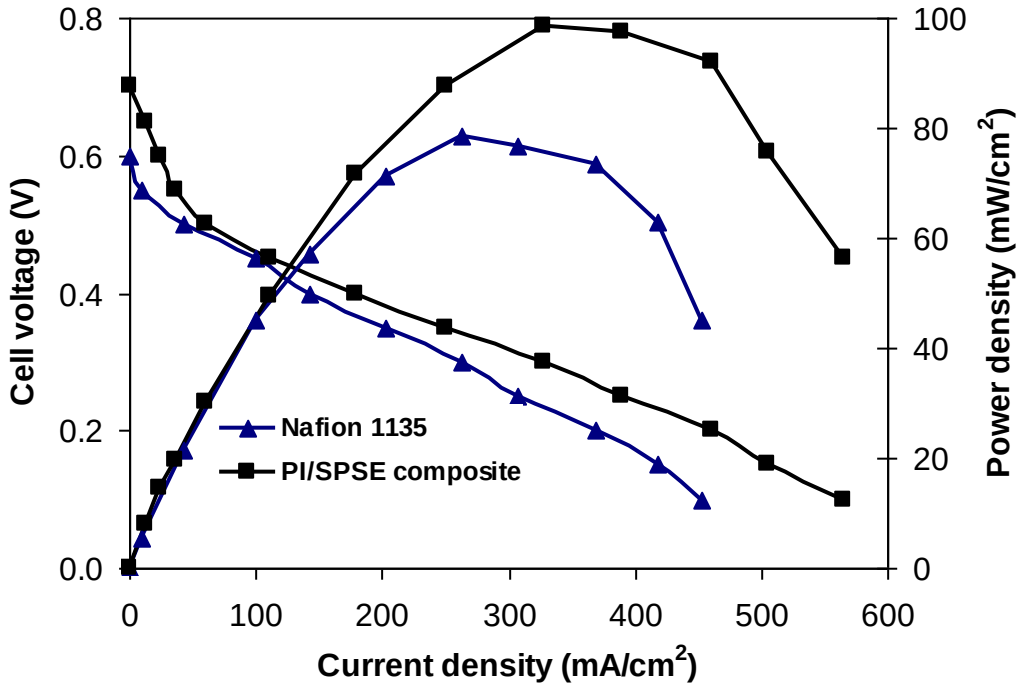

Figure 5.3 DMFC single cell performance of composite membrane PI−SPSE and Nafion 1135 at 70°C with 1M CH_3OH.

5.4 Conclusion

The composite membrane PI−SPSE was made by successful infiltration of SPSE in all the micro-pores of a porous PI matrix. Due to the complete inertness to methanol and the very high mechanical strength of the polyimide matrix, the PI−SPSE composite membrane shows excellent properties compared to Nafion 1135 membrane, such as lower in dimensional change, higher in mechanical strength and proton conductivity, and twenty times lower in methanol crossover. The improved performance of the DMFC with PI−SPSE composite membrane is also demonstrated, as evidenced by a 16.7% higher OCV and a 25% higher maximum power density than the Nafion 1135 membranes."

However, to meet the requirements for a practical application in DMFCs, further improvement in the properties of the composite membrane is needed. To achieve that, it is necessary to look for other electrolytes which show chemical stability as well as high proton conductivity and mechanical strength. The author realized that Nafion is a good candidate as an electrolyte because its properties satisfy the above requirements. Unfortunately, we have failed to infiltrate Nafion into the porous PI matrix in this work instead of SPSE. In the next step, our research focused on filling the porous PI matrix with Nafion to make the composite membrane with a higher performance.

Chapter 6 Investigation on the Morphology of Chemical Imidization-Based Porous Polyimide Film by Wet Phase Inversion

6.1 Introduction

The composite membrane based on pore-filling electrolyte is considered as the best proton exchange membrane for DMFC application to overcome drawbacks of Nafion-based membranes because it can suppress efficiently methanol crossover while maintaining high proton conductivity and mechanical strength.[28, 94] Depending on the right selections of components of porous matrix and electrolyte, it allows to prepare the composite membrane with high performance for DMFCs.[25, 34] Porous polyimides had been proved as the suitable support matrix to fabricate composite membrane because of its high mechanical strength and no stretching after electrolyte filling.[27] Unfortunately, commercial porous polyimides have low porosity from 50 (vol.%) to 55 (vol.%) that the composite membranes made from those matrix show low proton conductivity because less amount of electrolyte can be contained.[29] Among various proton conducting materials, Nafion is a good candidate for filling up the pores of the matrix because it has good chemical stability, high proton conductivity and mechanical strength, particularly, it is commercially available and widely used.[16] But it is difficult to infiltrate Nafion into the micro-pores of the porous polyimide matrix due to small pore size of the host matrix and high viscosity of filling solutions. So far, there is limitation to use these commercialized materials to make composite membranes. In our previous work, although we had successfully synthesized the porous polyimide film of SPBDA−PPDA/ODA with a fine pore size and high porosity, we failed to completely fill this dry porous PI matrix with polyperfluorosulfonic acid (Nafion). Instead, it can only be filled with sulfonated poly(styrene-ran-ethylene) (SPSE), which has high proton conductivity itself but low

mechanical strength, and the composite membrane PI−SPSE prepared may not be optimal for the real DMFC application. Therefore, the preparation of a porous matrix film with a sub-micropore and high porosity while maintaining high mechanical strength and then allowing the easy infiltration of electrolyte will be our tasks.

In this finding, a soluble co-polyimide derived from a polyimide precursor of PPDA, ODA and benzophenone-3,3',4,4'-tetracarboxylic dianhydride (BTDA) was prepared using chemical imidization promoted by acetic anhydride and pyridine. Then, a wet phase inversion method was applied to fabricate porous polyimide films by coagulating the cast film in the non-solvent of a mixture of 1-butanol and DMF. The morphology of the film was investigated by changing a volume ratio of 1-butanol and DMF in the non-solvent bath as well as coagulation time. The aim of this study is to synthesize a porous polyimide matrix which has sub-micrometer pore, high porosity, and easy to be filled up with Nafion to make a composite membrane suitable for real DMFC application. Other than that, the ability to control the thickness and pore size of matrix will be beneficial for fabricating composite membranes with optimum properties.

6.2 Experimental Details

6.2.1 Starting Materials

BTDA (96 wt.%,), PPDA (99.9 wt.%), ODA (97 wt.%), N,N-dimethylformamide anhydrous (DMF), and 1-butanol (99.9 wt.%) were purchased from Sigma−Aldrich. Materials were used as received.

6.2.2 Synthesis of Polyimide Precursor BTDA−PPDA/ODA

A poly(amic acid) solution of 18.0 (wt.%) co-polymer in DMF was synthesized in a glass flash with a mechanical stirrer and nitrogen inlet and outlet. First, PPDA and ODA were completely dissolved in DMF, then BTDA was added at a molar ratio of BTDA−PPDA/ODA (1:0.75:0.25). The poly-condensation reaction was carried out for 24 h at room temperature under a nitrogen atmosphere to form a poly(amic acid) solution. Then, a mixture of acetic anhydride and pyridine (volume ratio 2:1) was added slowly to the obtained poly(amic acid) and the resulting polymer solution was held at 60°C for 24h to obtain a polyimide precursor solution with a 16 (wt.%) solid content.[53, 56]

6.2.3 Preparation of Porous Polyimide Film

The porous polyimide film was fabricated by a wet phase inversion based technique.[58, 72] First, the PI precursor was cast on round glass plate by Spin Coating Machine (SCS G3, Cookson Electronics) with a spin speed of 900 rpm and a spin time of 30s. Then, the cast film was coagulated immediately in a non-solvent bath at room temperature for different length of coagulation time to develop a porous structure, followed by ageing for 5 min in pure methanol and 5 min in DDI water. The non-solvent solutions were mixtures of 1-butanol and DMF at various ratios. Finally, the porous PI film was dried in the air and ready for observing its morphologies. The thickness of films can be easily controlled by varying the spin speed during the film casting.

6.2.4 Film Characterization

6.2.4.1 Fourier Transform Infrared (FT−IR)

The chemical imidization of the transparent thin film from poly(amic acid) to polyimide structure was examined by FT−IR spectra taken by a Perkin−Elmer FT−IR Spectrum X spectrophotometer.

6.2.4.2 Field Emission Scanning Electron Microscope (FE−SEM)

The morphologies of both surface and cross-section of the porous matrix were observed by JEOL Field Emission Electron Microscope (JSM−6700F). For cross-section observation, samples were fractured under cryogenic conditions using liquid nitrogen. All samples were coated with gold by Auto Fine Coater (JFC−1600) before images were taken.

6.2.4.3 Porosity of Porous Polyimide Film

The film porosity, ϕ_p (vol.%), which the fraction of the total film volume that is porous, was estimated using the following Equation (6.1).[27]

$$\phi_p = \left\{1 - \frac{w_{PI}}{\rho_{PI}.V_{PI}}\right\} \times 100 \qquad (6.1)$$

where w_{PI}, $\rho_{PI,}$ and V_{PI} are the weight, density, and volume of porous PI substrate, respectively.

6.2.4.4 Mechanical Strength

The mechanical property of the porous PI film was measured under ambient condition for dry state by a Universal Materials Machine (Instron 5543, Instron Corp.) following Standard Test Method for Tensile Properties of Thin Plastic Sheeting ASTM D 882-02. The test samples were prepared in 5 (mm) width and 100 (mm) length with 5 test specimens for each specific porous film. The testing speed was 1 (mm/min) and initial gage length was 50 (mm). The curve of tensile stress versus strain was generated until the film was fractured.

6.3 Results and Discussion

6.3.1 Synthesis and Characterization of Polyimide Precursor BTDA–PPDA/ODA

The disadvantage of thermal imidization for converting poly(amic acid)s into polyimides is incomplete conversion and the decrease in molecular weight, which cause lower mechanical strength of the resulted polyimide film.[71] To avoid this effect, chemical imidization, which use chemical agents as catalysts for cyclodehydration reaction, is employed.[53] In this study, a polyimide precursor was obtained by a two-step chemical imidization method, with the synthesis route shown in Figure 6.1. In the first step, poly(amic acid) is formed from the reaction of aromatic dianhydride (BTDA) with aromatic diamine (PPDA and ODA). In the second step, the poly(amic acid) is chemically converted to a polyimide structure with the presence of promoted agents of acetic anhydride and pyridine. The mechanism of polyimide formation from poly(amic acid) at the presence of catalysts (acetic anhydride and pyridine) at mild temperature (60°C) involves a mixed anhydride intermediate of an iminolactone and then the imide linkages, which thermodynamically favors polyimide formation.[95]

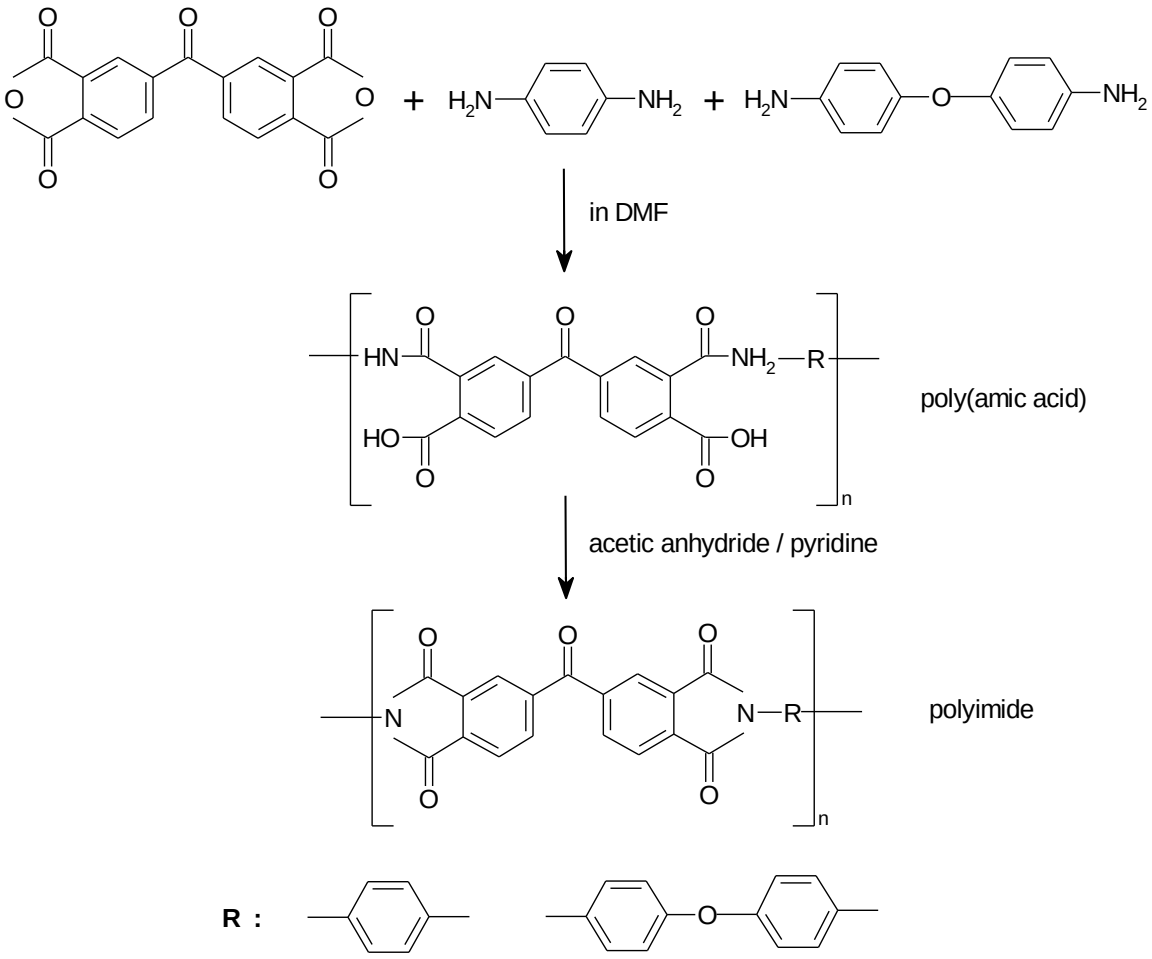

Figure 6.1 Synthesis scheme of polyimide precursor BTDA−PPDA/ODA based on chemical imidization.

The structures of the poly(amic acid) and polyimide were confirmed by FT−IR. As can be seen in Figure 6.2, the major peaks at 1,660 (cm^{-1}) assigned to amide disappear completely after the chemical imidization. Instead, an imide ring absorption peak appears at 1,775 (cm^{-1}); it is attributed to stretching of the carbonyl group of imide. According to FT−IR spectra results, it can conclude that the chemical imidization process was completed by promoting agents at 60°C for 24h.

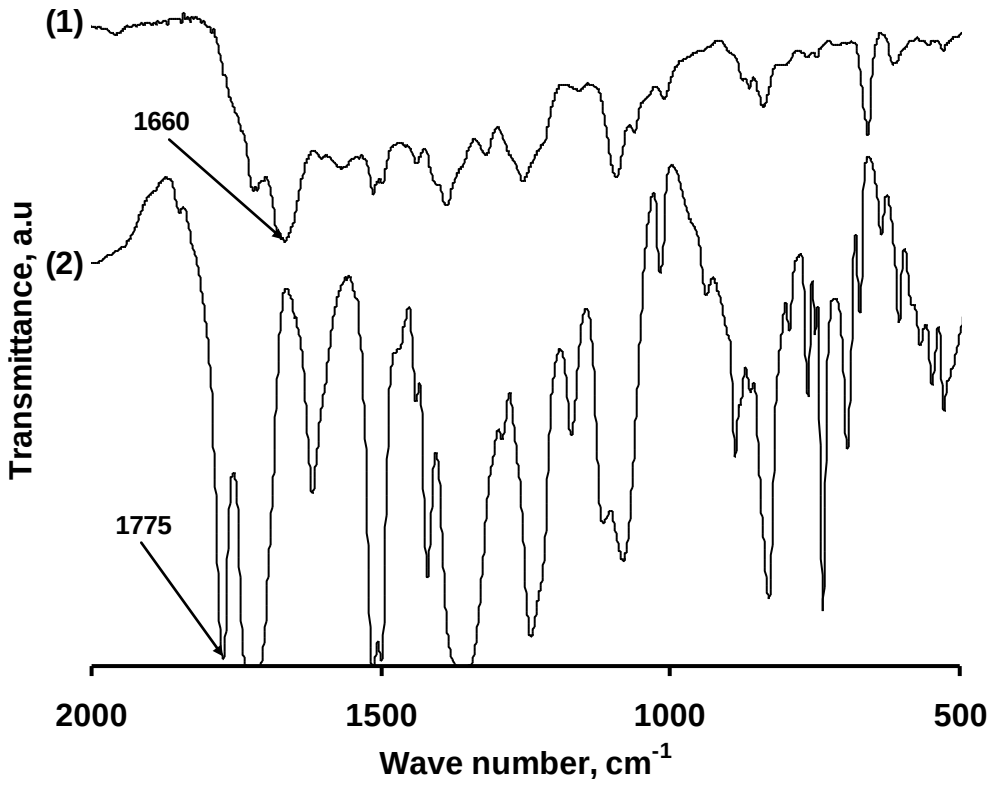

Figure 6.2 FT−IR spectra of (1) poly(amic acid) and (2) corresponding polyimide BTDA−PPDA/ODA.

To make the porous matrix from a liquid cast film by wet phase separation, the solid content of polyimide precursors is one of the main factors determining the mechanical strength of the resulted films. Experimentally, polyimide concentration of the casting solution must be high enough, such that the precipitation pathway of the cast film enters the two phase region of the phase diagram lying above the critical point, as shown in Figure 6.3, where the porous film formed will be high in mechanical strength. Alternatively, if the precipitation pathway goes below the critical point, the formation porous film is powdery and weak in strength.[80] With that in mind, the polyimide solid content of the cast solution in this study is maintained at about 16 (wt.%), which is expected to make porous films with high strength.

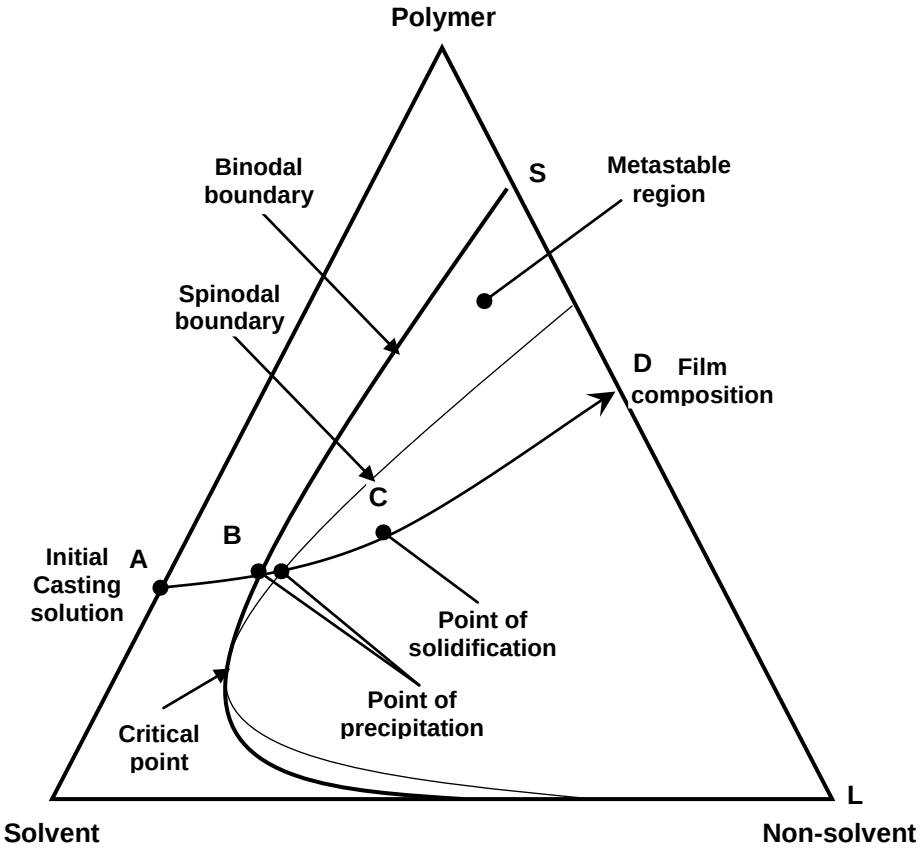

Figure 6.3 Three-component phase diagram for the formation of a porous film by additional non-solvent.

6.3.2 Morphology and Property of Porous Polyimide Film

In this study, an attempt is made to make porous PI film with sub-micrometer in pore size, high porosity and mechanical strength, which can be filled up by Nafion completely. Since preliminary results show that the sponge type structure possesses higher mechanical strength than the finger type at high porosity, DMF was selected as solvent and 1-butanol as the non-solvent to develop porous structure. Such a solvent dissolves a wide variety of polymers, and casting solution based on this solvent precipitates rapidly when immersed in non-solvent, favoring the formation of a highly porous film with a spongy-type structure.[58] To study the effect of non-solvent on the morphology of the porous film

and select a good matrix for the composite membrane, various ratios of 1-butanol to DMF was used to develop porous films. Here the pore size can be controlled by changing the solvent/non-solvent ratio. The pore size of porous films increases with decrease of the 1-butanol content in a coagulation bath. The pores can grow until the matrix phase, polymer-rich phase, is solidified.[59] Pore size of porous films prepared at different ratios of 1-butanol and DMF can be estimated from FE−SEM cross-section images (Figure 6.4) and the results are shown in Table 6.1.

Table 6.1 Physical properties of porous polyimide film BTDA−PPDA/ODA with different pore sizes.

DMF : 1-butanol (v/v. %)	Porosity (vol. %)	Pore size (μm)	Mechanical strength (MPa)
0 : 100	50	< 0.1	106.6
10 : 90	52	< 0.1	102.9
20 : 80	55	< 0.1	96.1
30 : 70	**80**	**~ 0.3**	**93.3**
40 : 60	83	~ 1	45.1
50 : 50	85	~ 5	37.1

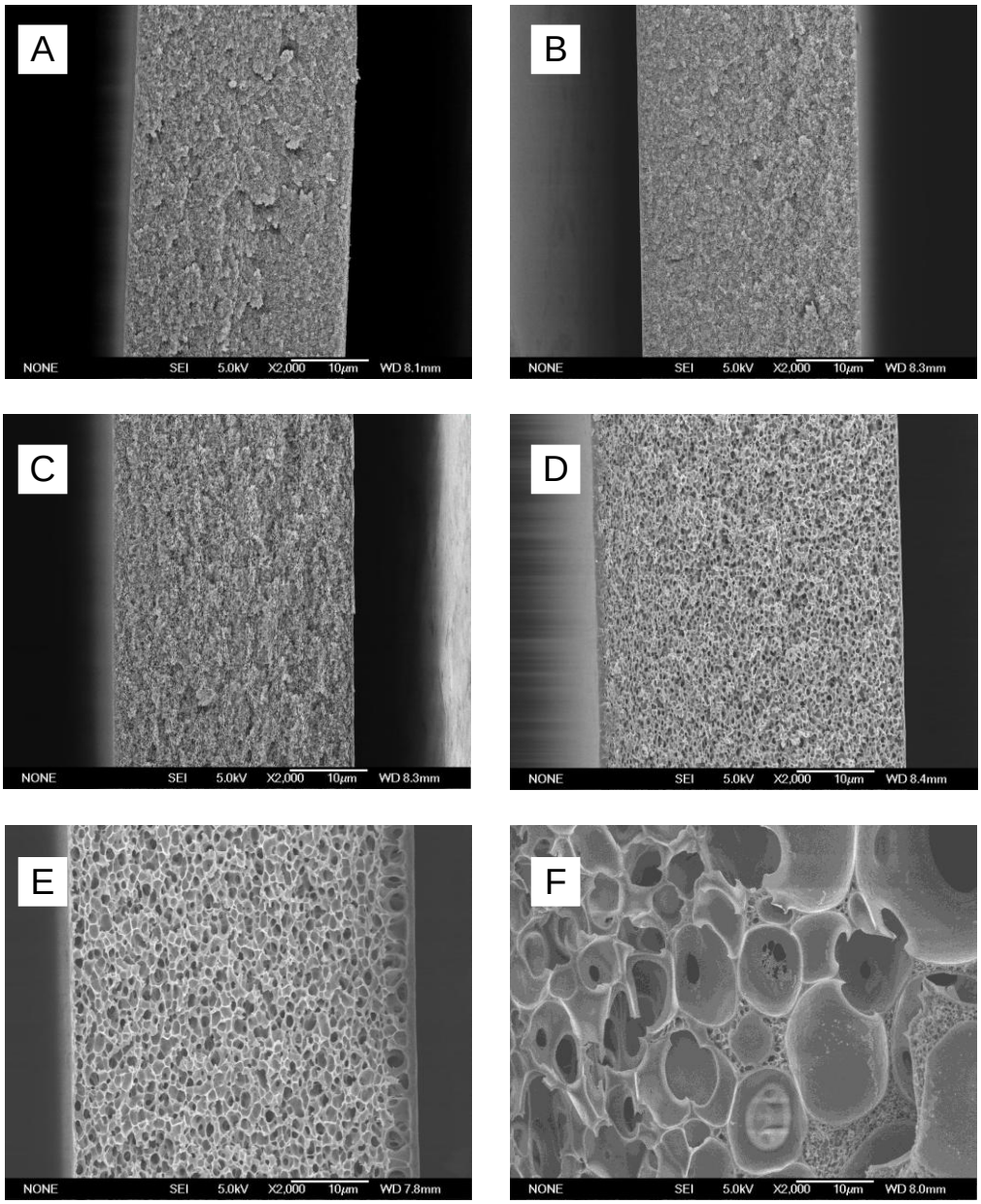

Figure 6.4 FE−SEM images of the cross sections of porous polyimide films BTDA−PPDA/ODA prepared by coagulating for 15 min when 1-butanol content in the non-solvent bath was changed: (A) 1-butanol:DMF (v/v. %)=100:0, (B) 90:10, (C) 80:20, (D) 70:30, (E) 60:40, (F) 50:50. Left and right sides correspond to top and bottom surfaces.

With higher 1-butanol content, immediate phase separation occurs that the formed films contain a dense pore with very small size, as shown in Figure 6.4(A), (B) and (C). In contrast, with lower 1-butanol content, the rate of solvent removal from, along with the rate of 1-butanol entering the cast film is also slowed, which leads to a lower polymer concentration in the polymer rich phase. Therefore, there is a longer time before the film solidifies and larger pores can develop, as can be seen in Figure 6.4(D), (E) and (F).

Another observation from Figure 6.4 is that the pore size increases from the top to the bottom layer of the porous film. When the cast film is exposed first to the precipitation medium, the top layer begins to precipitate immediately. The resulting structure of such a surface layer is finely micro-porous. However, the precipitated surface layer then becomes a barrier that slows down the exchange rate between solvent and non-solvent. Therefore, the two phases formed on precipitation have more time to separate, resulting in the increasing pore size across the film.[57]

In addition, pore size and pore density on the top layer of the porous film affect the electrolyte infiltration into the porous matrix, where the surface of the porous matrix with open and populated pores is easier to be filled up by the electrolyte to allow the fabrication of composite membrane. Experimentally, the surface structure of porous films depends on the exchange rate between solvent and non-solvent during pore-forming period.[74] As shown in Figure 6.5, the density and pore size on the film surface can be controlled by changing 1-butanol/DMF ratio in the coagulation bath. With the 1-butanol/DMF of 80/20, because of high content of non-solvent, the rapid de-mixing occurs, the top surface of porous film shows a fine and populated pore structure, while a dense layer is obtained for the porous film prepared from 1-butanol/DMF of 60/40 due to delayed de-mixing between them. Alternatively, due to moderate de-mixing when

coagulating in 1-butanol/DMF of 70/30, the top surface of porous film exhibits an open and populated pore.

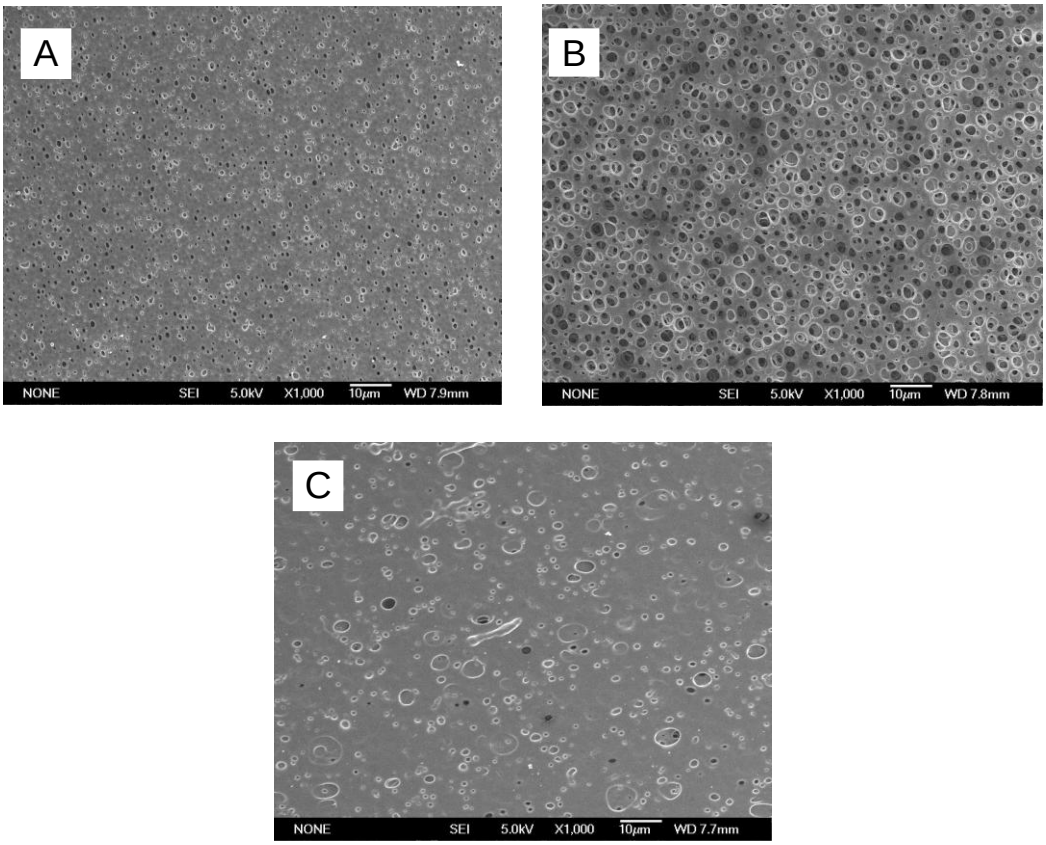

Figure 6.5 FE–SEM images of the top surface of porous polyimide films BTDA–PPDA/ODA prepared by coagulating in different non-solvent baths: (A) 1-butanol:DMF=80:20, (B) 70:30, (C) 60:40.

In addition to the pore size and surface's pore density, porosity is another key property of the porous matrix for preparing the composite membrane. The high porosity of matrix allows us to prepare the composite membrane with higher performance because more proton conducting material could be contained in the resulted composite membrane. The overall porosity of a porous polyimide film can be easily controlled by the polymer content. The porosity increases with the decrease of polymer concentration, as well as by the relative rates at which non-solvent enters and solvent leaves the casting film.

Moreover, from a thermodynamic standpoint, any additive in the cast film will be expected to increase the rate of non-solvent entry and decrease the rate of solvent removal, which favors the formation of a film with high porosity.[74] Therefore, with 16 (wt.%) solid content of casting solution and the presence of the chemical imidization agents (acetic anhydride and pyridine) in the polyimide precursor as additives, high porosity film can be expected. The film porosity was estimated based on Equation (6.1) and the results are shown in Table 6.1. Apparently, the film porosity increases along with the increase of the pore size and has shown a big gap (55 vol.% vs. 80 vol.%) between the porous matrixes prepared at a 1-butanol:DMF (v/v.%) of 20:80 and 30:70. This result can be explained by changing the morphology of porous films from a dense structure (20:80) to an open structure (30:70). Because of the presence of the chemical imidization agents (acetic anhydride and pyridine) in the cast film, a high porosity (80%) was obtained and a value up to 85 (vol.%) can be obtained, referring to the porous matrix prepared at the lowest 1-butanol content (50 vol.%). In addition to the increase in the resulted film porosity, the presence of residual acetic anhydride in the porous matrix makes the wet porous film more hydrophilic and is expected to easily fill it up with Nafion completely in the infiltration process for preparing composite membrane.

It is also found that the pore size of the film is unchanged with the coagulation time when the porous film is prepared by coagulating the cast film in non-solvent bath containing a higher 1-butanol content (from 70 to 100 v/v.%) as shown in Figures 6.6 and 6.7. In contrast, with a lower 1-butanol content in the coagulation bath (from 50 to 60 v/v.%), as can be seen in Figure 6.8, the pore size of the film increases with the increase of coagulation time. These results can be explained by the difference in the exchange rate of solvent and non-solvent according to the amount of solvent (DMF). “In other words, the casting film immediately becomes precipitated when DMF is absent or has low

concentration in a coagulation bath, causing rapid diffusion of 1-butanol into the film. The precipitated polymer becomes solidified easily and the resulting structure is finely microporous from the top to bottom of the porous film. In contrast, when the non-solvent bath contains higher amounts of DMF, the cloud point curves shifts to the polymer-non-solvent axis and the diffusion of non-solvents slows down. The cast film becomes thermodynamically more stable. It takes a longer time to precipitate and reach the point of solidification. The result is the porous film with large pores and the pore size increases when precipitating longer.[73]

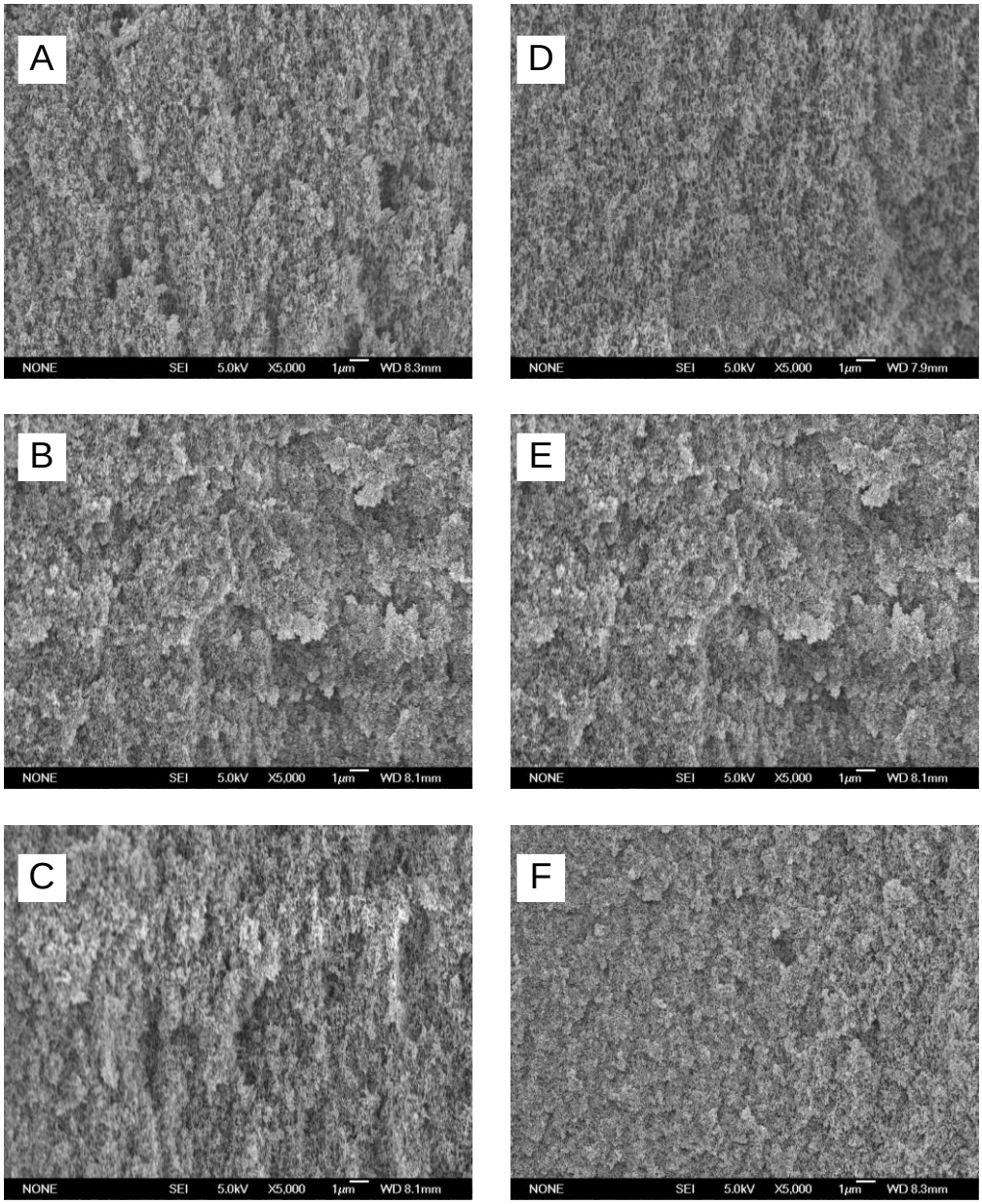

Figure 6.6 FE−SEM images of cross sections at the center of porous polyimide films BTDA–PPDA/ODA prepared when the composition of non-solvent bath and the length of coagulation time were changed (A) 1-butanol:DMF=100:0 for 15 min, (B) 100:0 for 30 min, (C) 100:0 for 60 min, (D) 90:10 for 15 min, (E) 90:10 for 30 min and (F) 90:10 for 60 min.

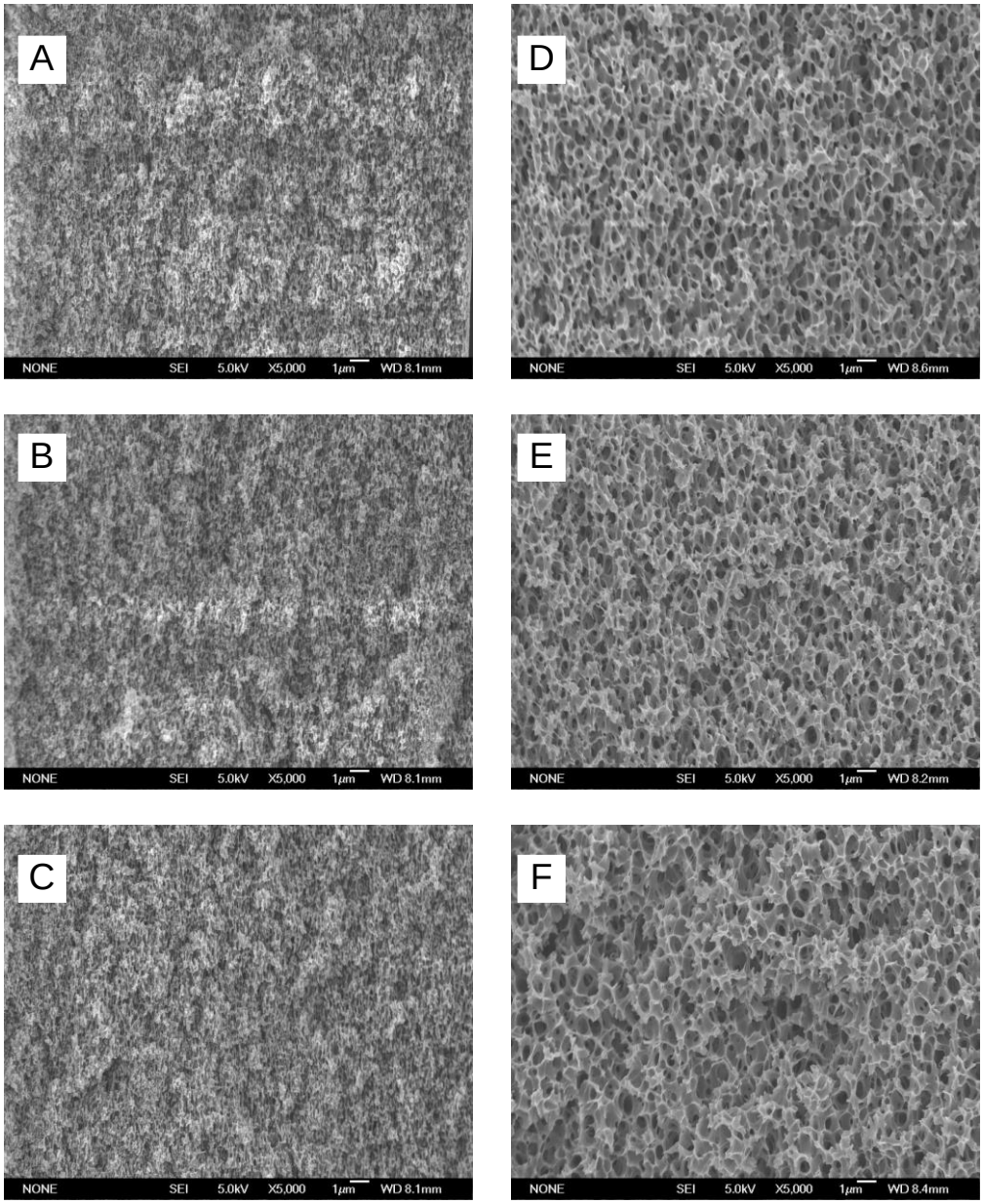

Figure 6.7 FE−SEM images of cross sections at the center of porous polyimide films BTDA−PPDA/ODA prepared when the composition of non-solvent bath and length of coagulation time were changed (A) 1-butanol:DMF=80:20 for 15 min, (B) 80:20 for 30 min, (C) 80:20 for 60 min, (D) 70:30 for 15 min, (E) 70:30 for 30 min and (F) 70:30 for 60 min.

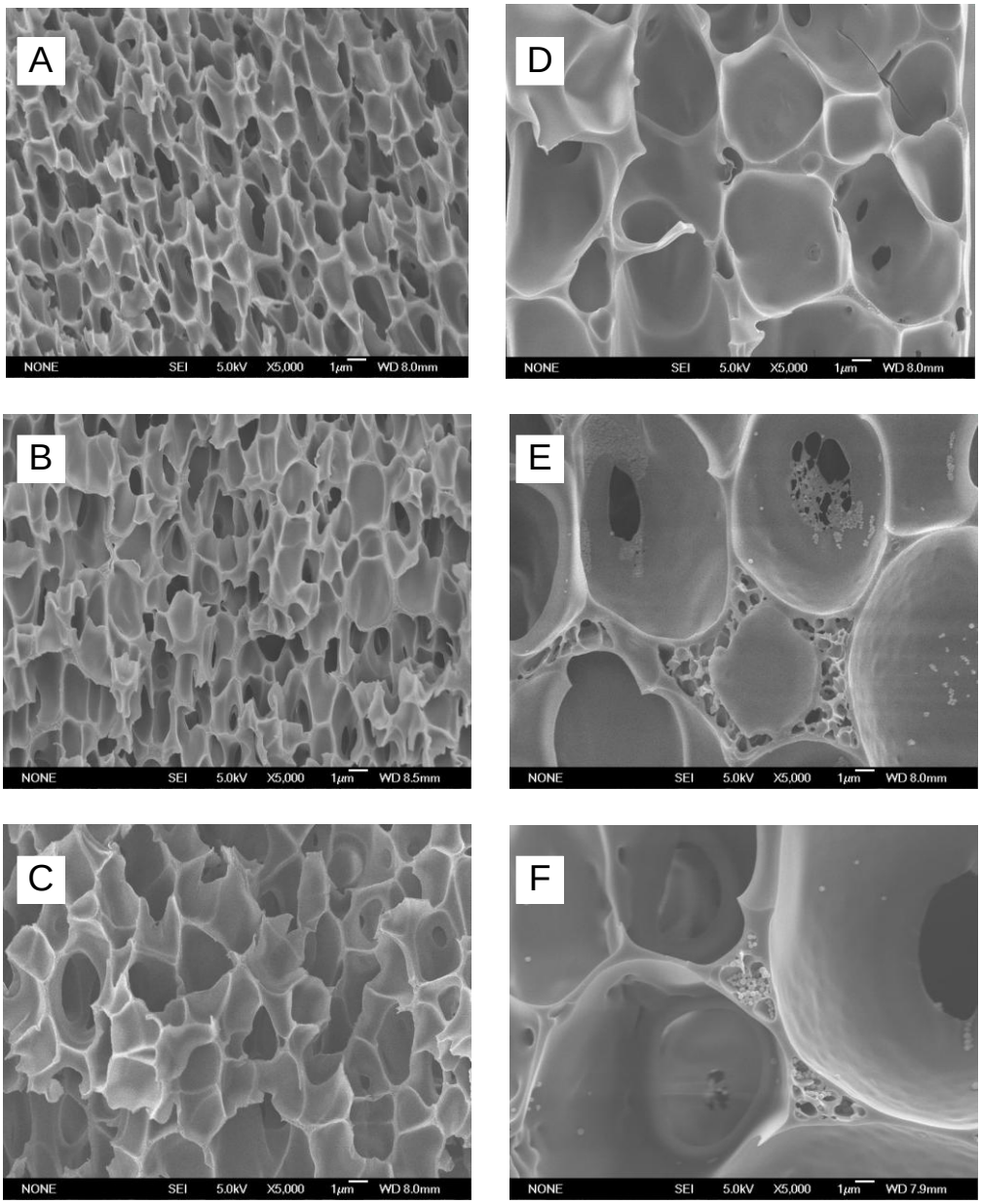

Figure 6.8 FE−SEM images of cross sections at the center of porous polyimide films BTDA−PPDA/ODA prepared when the composition of non-solvent bath and length of coagulation time were changed (A) 1-butanol:DMF=60:40 for 15 min, (B) 60:40 for 30 min, (C) 60:40 for 60 min, (D) 50:50 for 15 min, (E) 50:50 for 30 min and (F) 50:50 for 60 min.

Mechanical strength is one of the important properties for a porous matrix to construct the composite membrane. High mechanical strength allows us to make the membrane thinner, which reduces total membrane resistance, leading to enhanced fuel cell performance. In addition, a high strength of the matrix will be effective to suppress membrane swelling resulting in reduced methanol crossover.

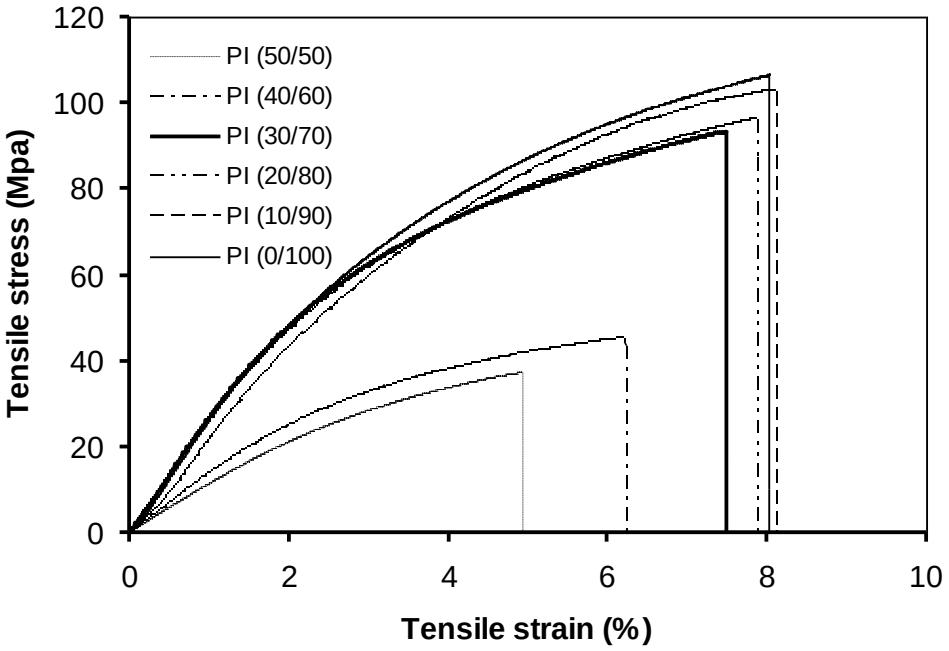

Figure 6.9 Stress vs. strain plots of the porous polyimide film BTDA−PPDA/ODA prepared from different ratios between DMF and 1-butanol.

Apparently, as can be seen in Figure 6.9 and Table 1, the mechanical strength of a porous polyimide films strongly depend on its pore size, which decreases with the increase of pore diameter. With the porous films containing a bigger pore size (1 and 5 μm), they contain macro-voids and are not uniform in pore size, these porous matrixes have lost their structure integrity and lack mechanical strength. In contrast, due to sub-micrometer and uniform pore size of the porous films prepared with higher 1-butanol content, the

films show high strength. In addition, comparing with the porous polyimide matrix prepared by thermal imidization in previous works, the porous matrix fabricated by chemical imidization was shown to have higher mechanical strength because of the damage of polyimide structure when converting poly(amic acid) into corresponding polyimide at high temperatures.

6.4 Conclusion

We have prepared the porous co-polyimide film BTDA−PPDA/ODA based on the chemical imidization of a polyimide precursor with various pore sizes and porosity by changing the ratio between 1-butanol and DMF in the coagulation bath. A wet phase inversion method was applied to develop the porous structure from the cast film. With a lower content of DMF in the non-solvent bath, the pore size of porous films was dense and almost unchanged with coagulation time. When the amount of DMF in the non-solvent bath increases, the pore size of porous films is bigger and increases with the increase of coagulation time. By coagulating the cast film containing 16 wt.% solid content in the non-solvent bath of 1-butanol of 70 (vol.%) and 30 (vol.%) DMF for 15 min, the porous co-polyimide film formed consisted of a highly porous top layer and a spongy type sub-structure with a high mechanical strength of 93.3 (MPa), a pore size of ~0.3 (μm), and a porosity of 80 (vol.%). This porous matrix, which is found to be highly hydrophilic because of the presence of trace acetic anhydride, is thought to be suitable for preparing a composite membrane by filling it with Nafion and other electrolytes.

In next chapter, experiments will be conducted to fill porous polyimide substrates with an electrolyte of Nafion. Characterizations of the composite membrane for DMFC will be conducted, including proton conductivity, methanol crossover, mechanical strength, and fuel cell performance.

Chapter 7 Composite Membrane Based on the Porous Polyimide Matrix Fabricated by Chemical Imidization and Nafion

7.1 Introduction

"A pore-filling electrolyte membrane is composed of a polymer support matrix and a proton conducting material that fills the pores of the matrix. Such a membrane has been confirmed to possess more benefits than others for DMFC application because it offers the possibility to separate the mechanical and electrical properties of the membrane.[25, 76] Depending on the right selection of porous matrix as well as electrolyte, significantly reduced methanol crossover, increased proton conductivity, and higher mechanical strength have been demonstrated.[30, 34] The porous PI is an outstanding support matrix compared with others such as PTFE, CLPE because of its high mechanical strength, ability to suppress membrane swelling, and inertness towards methanol.[27] However, such inertness to almost solvents, and the ability to resist swelling in polymer filling solution led difficulty to infiltrate electrolytes into its pores completely. In addition, the effect of the ion conductivity of electrolytes in micro and nano-pores has been reported, where the confinement of an electrolyte in a nano-pore increases as the pore size becomes smaller because of the orientation of the polymer chains in the pores.[90, 96] On the other hand, the complete infiltration of electrolytes into the substrate to avoid the formation of pores inside the resulting composite membrane is not a trivial thing, which is a major concern for the application of the pore-filling electrolyte membrane.

In chapter 6, the wet porous polyimide film of BTDA−PPDA/ODA with different pore sizes was fabricated. Then, the porous PI film was filled with polyperfluorosulfonic acid (Nafion). Difference from the work in chapter 5, the protocol developed in this chapter

allows an easy infiltration of Nafion ionomer and thus obtained membrane is free from any pore-defect by using a wet porous substrate with acetic anhydride trapped inside the pores during polymer-filling procedure. The effect of pore size of host matrix on the pore-filling capability and composite membrane properties was also characterized.

The composite membrane has shown outstanding properties such as a high mechanical strength, low methanol crossover, high proton conductivity, and less dimensional change between dry and swollen states. Improved fuel cell performance was also demonstrated with this composite membrane. We believe this represents a real breakthrough in the practical development of the membrane for DMFCs.

7.2 Experimental Details

7.2.1 Preparation of Composite Membrane PI−Nafion

The filling polymer Nafion/ethanol suspension was prepared from commercial Nafion solution (5 wt.%, GasHub, Singapore). It was prepared by drying the commercial 5 (wt.%) Nafion solution at 60°C until the solvent is evaporated completely. The dry Nafion was then treated with 25 (wt.%) nitric acid in water at 80°C for 1h following by repeated rinsing with double de-ionized (DDI) water and drying again. After that, the Nafion was put into ethanol and ultrasonicated to facilitate re-dispersion. The formed Nafion/ethanol solution has a Nafion weight ratio of 5 (wt.%).

The porous PI substrate was extended over a round glass plate by a membrane caster; after that, the Nafion/ethanol solution was poured on the surface of the porous film. The glass plate was put in an oven at 60°C for 24h and finally dried in a vacuum oven at

120°C for 12h and then 150°C for 1h. After that, the obtained composite membrane was treated with a common pretreatment procedure using H_2O_2 and H_2SO_4 solutions.[17]

7.2.2 Porous Film and Composite Membrane Characterization

7.2.2.1 Field Emission Scanning Electron Microscope (FE−SEM)

The morphology of the surface and cross-section of composite membranes were observed by JEOL Field Emission Electron Microscope (JSM−6700F). For cross-section observation, samples were fractured under cryogenic conditions using liquid nitrogen. All samples were coated with gold by Auto Fine Coater before images were taken.

7.2.2.2 Fourier Transform Infrared (FT−IR)

The FT-IR spectrum of the thin film was obtained by Spectrometer−PerkinElmer to identify the structure of the porous film and composite membrane.

7.2.2.3 Water Content and Dimensional Stability

Samples of the membranes were weighed (W_1) after immersion in DDI water at 80°C for 24h. Then samples were weighed (W_2) after drying in a vacuum oven at 80°C for 24h. The water content (ΔW) was calculated according to Equation 7.1.[35]

$$\Delta W(\%) = \frac{W_1 - W_2}{W_2} \times 100 \qquad (7.1)$$

Dimensional stability was tested as follows. Membranes around 2.5 cm in diameter were stored in a vacuum oven at 80°C for 24h and the dimension was measured before (L_1) and after (L_2) soaking the samples in DDI water at 80°C for 24h. The dimensional change (ΔL) was calculated using the following Equation 7.2.[35]

$$\Delta L(\%) = \frac{L_2 - L_1}{L_1} \times 100 \quad (7.2)$$

7.2.2.4 Mechanical Strength

Testing was performed using testing machine (Instron 5543) following standard test method for tensile properties of thin plastic sheeting ASTM D 882-02. The samples were prepared in 5 (mm) width and 100 (mm) length with 5 test specimens for each membrane. The testing speed was 10 (mm/min) and the initial gauge length was 50 (mm).

7.2.2.5 Methanol Permeability and Proton Conductivity

The methanol permeability of the membranes was determined using the two compartment diffusion cell technique as reported elsewhere.[17] The proton conductivity of the membrane in the through-plane direction was measured using a potentiostat with a built-in frequency response analyzer (Autolab, Netherlands) in a home-made cell.[89] The cell consists of two Teflon blocks attached with a platinum foil electrode (1.2×1.2 cm) and a platinum lead. The pretreated membrane (1.5×1.5 cm) was sandwiched between these two Teflon blocks held in place with Teflon screws. The impedance measurements were carried out on fully hydrated membranes at different temperatures (room temperature (RT), 50°C, and 80°C) over a frequency range of 250 (kHz) to 150 (kHz). The proton conductivity of the membrane was calculated using the equation $\sigma = L/RS$, where σ, L, R, and S denote the ionic conductivity, the thickness of the membrane, the resistance of the membrane, and the surface area of the electrode, respectively.

7.2.2.6 Single Cell DMFC Performance

Single fuel cell performance test was conducted with an Arbin fuel cell test station. To minimize influence from electrode variation, commercial electrodes (GasHub, Singapore) were used for the membrane electrode assembly (MEA) fabrication and performance test. The electrode consists of a PTFE treated (20 wt.%) carbon paper substrate, a microporous layer with a carbon loading of 1.2 (mg/cm^2), and a catalyst layer. The catalyst layer in the anode contains 40 (wt.%) PtRu/C and Nafion, with a total metal loading of 2.0 (mg/cm^2) (Pt:Ru = 1:1), while that in the cathode contains 40 (wt.%) Pt/C and Nafion, with a Pt loading of 2.0 (mg/cm^2). A MEA with an active electrode area of 5 (cm^2) was obtained by pressing the cathode and anode onto each side of a pretreated Nafion 112 membrane or composite membrane at 140°C and 2.0 (MPa) for 1 min (Hydraulic 3912, Carver, Inc.). The MEA was then assembled into a DMFC single cell. The operation conditions were as follows: anode fuel 1M or 5M MeOH; flow rate, 1.0 (mL/min); oxygen pressure, 0.4 (MPa); and flow rate, 0.25 (L/min). The temperature of the cell was maintained at 70°C.[21] All single cell tests were conducted in triplicates and the results presented here are the average data.

7.3 Results and Discussion

7.3.1 Preparation of Composite membrane PI−Nafion

Porous PI matrixes with various pore sizes were prepared by changing the solvent/non-solvent ratio of DMF/1-butanol and reported previously in chapter 6.

To fabricate successfully a pore-filling composite membrane with a high performance, the porous PI matrix preferentially should have pore sizes on the sub-micrometer scale, or less, to suppress efficiently membrane swelling, maintain high mechanical strength, and enhance proton conductivity. In addition, electrolytes must be able to fill completely all

pores of the porous matrix to make the composite membrane workable. Obviously, composite membranes were successfully prepared from porous matrixes at a 1-butanol:DMF (v/v.%) of 70:30, 60:40, 50:50, as can be seen in Figure 7.1(B),(C),(D), where all pores of the porous matrixes was completely filled with Nafion. In contrast, porous matrixes prepared at a 1-butanol:DMF of 80:20 (v/v.%) could not be infiltrated by Nafion (Figure 7.1A), where two separate layers of the porous matrix and Nafion were observed and micro-pores in the matrix still existed after Nafion infiltration process.

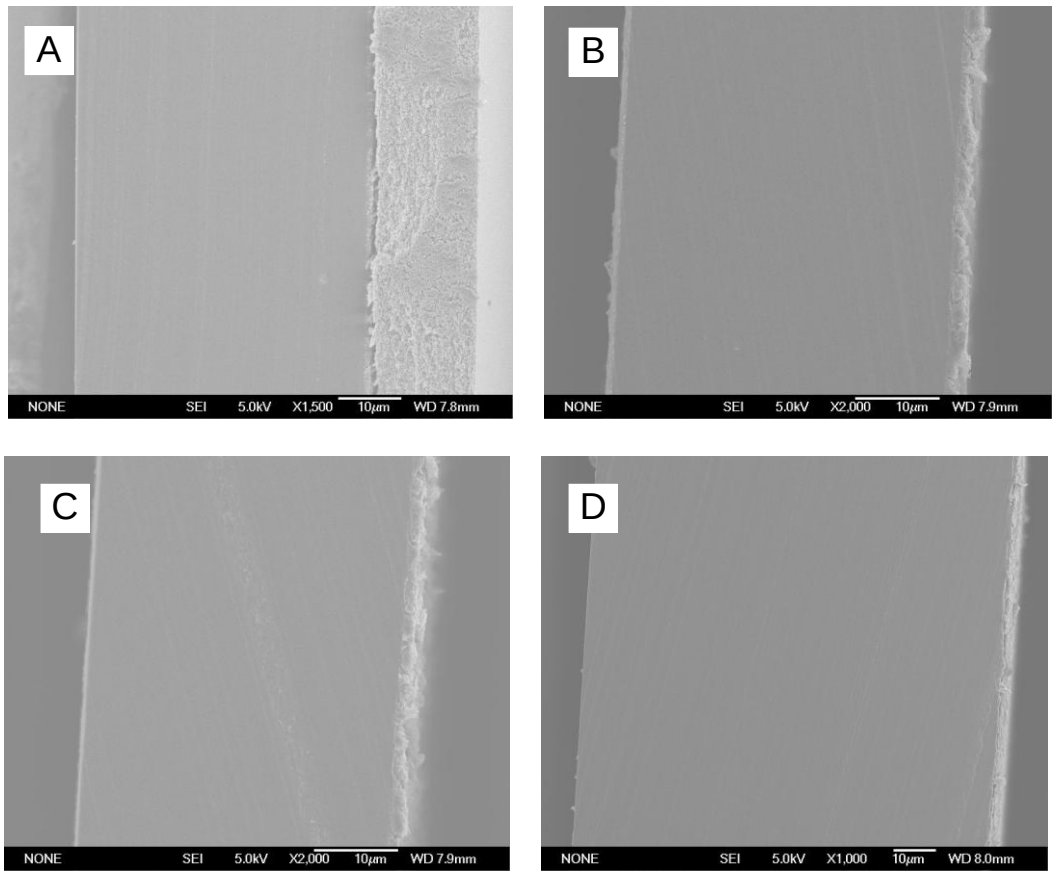

Figure 7.1 FE–SEM images of cross-sections of PI−Nafion composite membranes based on porous PI films prepared with different 1-butanol contents in non-solvent bath with 1-butanol:DMF (v/v.%):(A) 20:80, (B) 30:70, (C) 40:60, (D) 50:50.

Those results indicate that the infiltration depends on pore size of the host matrix. If the pores of the matrix are too small, infiltration can be difficult. Alternately, it is easier to fill the pores by Nafion for the matrixes with larger pore size. However, if the pores of the porous matrix are too large, the blocking of methanol crossover of composite membrane will be less efficient and the mechanical strength of the membrane will usually be lower. Therefore, we only chose the porous matrix with the smallest size while still allowing complete Nafion infiltration, i.e. synthesized at the 1-butanol:DMF ratio of 70:30 (v/v.%), as the porous matrix to fabricate and characterize the composite membrane. As shown in previous chapter, such a substrate exhibits a highly porous structure with porosity of ~80 (vol.%), a pore size of ~0.3 (μm) and a top porous surface.

Other than the pore size effect, for a polymer electrolyte to successfully fill the pores of a host substrate, the viscosity and contact angle on the host substrate of the polymer solution must be low.[97] In this study, to facilitate the subsequent Nafion filling, the commercial 5 (wt.%) Nafion was re-dispersed in ethanol to reduce the viscosity and the contact angle with the porous PI film. In addition, the wet porous PI film was used which has high affinity towards filling polymer because of the presence of residual acetic anhydride in the matrix that makes the wet porous film more hydrophilic. During the process of filling Nafion into the pores of the porous substrate, the gravity force dragged Nafion solution into the wetted pores of the porous PI film and after evaporating solvent, Nafion can completely plug the pores. This use of a wet porous PI film is found to be critical to the formation of composite membrane. If the porous polyimide is completely dried, with all the residual acetic anhydride in the small pores removed, pores will be observed in the composite membrane even if the porous PI is treated again with acetic anhydride before Nafion infiltration. It is believed that, when the fully dried porous substrate is subject to this post-treatment with acetic anhydride, air will usually be trapped

in some of the small pores and make them inaccessible to acetic anhydride. Subsequently the Nafion ionomer will not be able to infiltrate these unwetted pores. Our previous work on the porous substrate synthesis uses thermal imidization. It involved the drying of the porous PI substrate at high temperature and it explained why Nafion cannot fully fill all the pores in that structure. Instead, as shown in Figure 7.1(B), no pore was observed for the composite membrane fabricated with the wet porous PI film and the filling polymer. A smooth morphology was also observed on the top surface of the composite membrane (Figure 7.2B) compared with a porous surface of the matrix (Figure 7.2A) indicating that Nafion was distributed uniformly in the composite membrane.

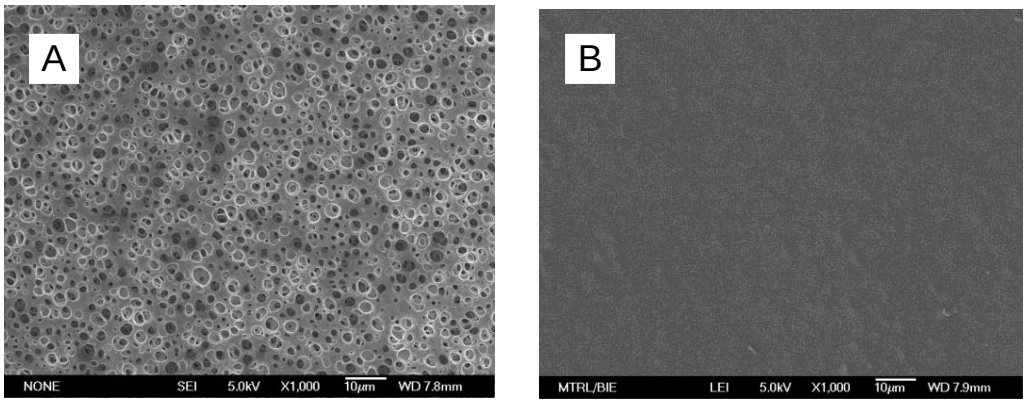

Figure 7.2 FE–SEM images of (A) top surface of porous PI film prepared with 1-butanol:DMF (v/v.%)=70:30 and (B) top surface of composite membrane PI–Nafion.

In addition, the FT–IR spectra PI–Nafion composite membrane (Figure 7.3) also shows an absorption peak at 1,775 (cm^{-1}), indicating the presence of PI in the composite membrane. In the range of 1,400-1,100 (cm^{-1}), two strong vibration bands are present. The band at 1,150 (cm^{-1}) is due to symmetric C-F stretching, while the band at 1,220 (cm^{-1}) is attributed to asymmetric C-F stretching. Moreover, a band at 1,050 (cm^{-1}) was also attributed to S-O stretching of the SO_3 group of Nafion structure.

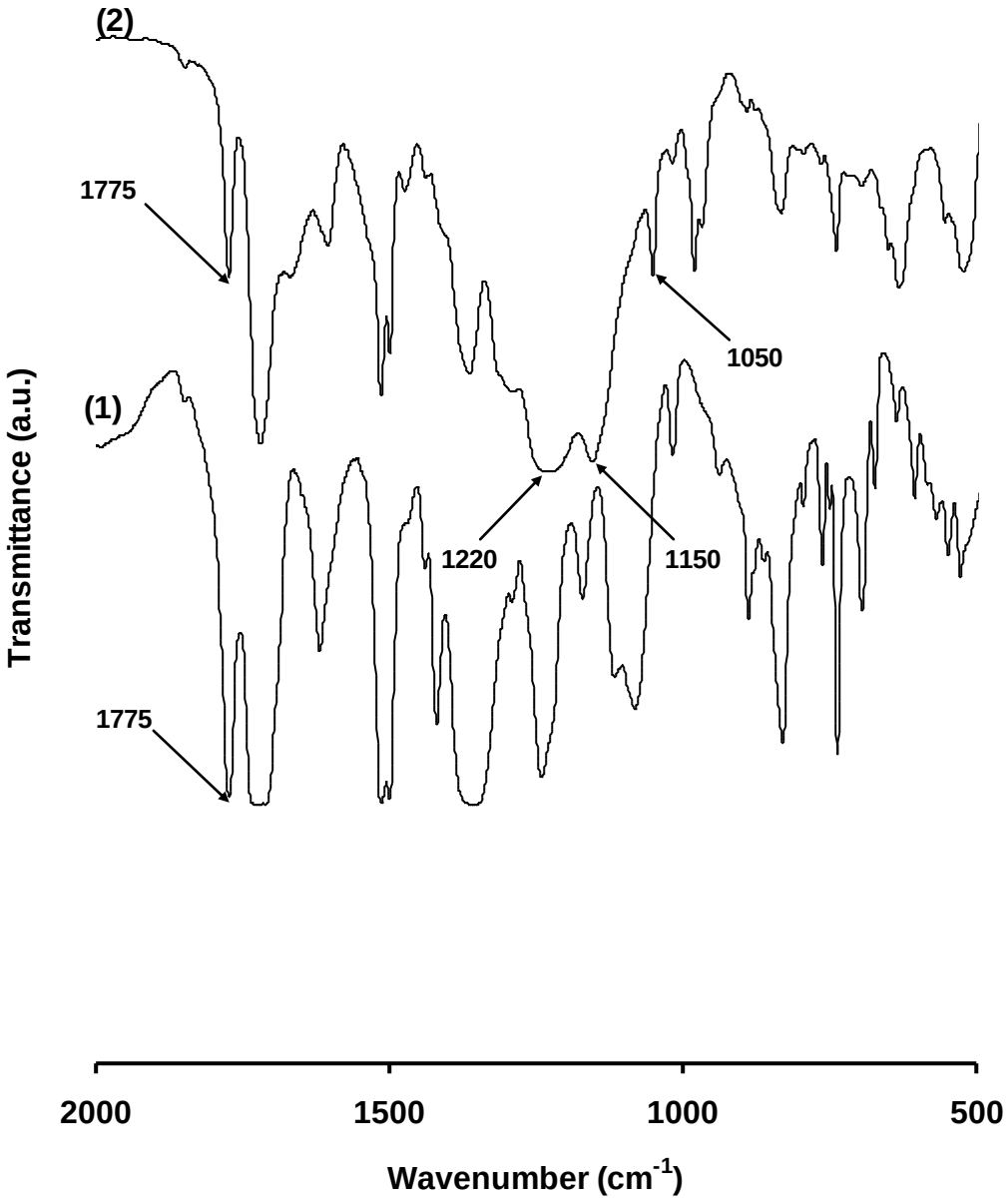

Figure 7.3 FT−IR spectra of (1) polyimide film, and (2) PI−Nafion composite membrane.

7.3.2 Physical and Electrochemical Properties of Membrane

The mechanical strength of membranes affects the durability and performance of a MEA. In this study, due to high mechanical strength of the porous matrix (93.3 MPa), a thin composite membrane of PI−Nafion was constructed successfully. With a thickness of only about 46 (μm) (Table 7.1), it exhibits a much higher mechanical strength than

Nafion 112 membrane (104.5 MPa vs. 26.4 MPa). Benefits of a thinner membrane include reduced total membrane resistance and subsequently increased fuel cell performance.

Table 7.1 Physical Properties of Nafion 112 and Composite Membrane PI–Nafion.

Membrane	Thickness (μm)	Water content (%)	Dimensional change (%)	Mechanical strength (MPa)
Nafion 112	64	15.67	11.85	26.4
PI−Nafion	**46**	**5.92**	**4.75**	**104.5**

The dimensional stability of the membrane is one of the most important properties for practical operation of a fuel cell. Since carbon electrodes do not swell and change in dimension from any water uptake, less damage to the structure integrity of the MEA and improved durability can be expected for those membranes with smaller change in dimension.[77] Table 7.1 also shows the comparison of the PI−Nafion composite membrane and Nafion 112 membrane. After being soaked in water at 80°C for 24h, the PI−Nafion composite membrane shows much lower dimensional change (~1/3 of Nafion 112) and water uptake (~1/3 of Nafion 112). It can be concluded that the strong PI matrix in the composite membrane can effectively suppress the membrane from swelling and prevent the membrane from absorbing excess water, although the volumetric ratio of PI is only 20 (vol.%). Methanol crossover usually occurs in the hydrophilic region of the Nafion polymer which expands with the adsorption of more water.[43] The suppressed water adsorption or less dimensional change in the membrane indicates less expansion of hydrophilic portion (smaller methanol passage). We believe that, in the pore-filling

electrolyte membrane, the host matrix is totally inert to methanol and methanol crossover is mainly through the polymer electrolyte filler, or more specifically, the hydrophilic portion of the Nafion. The fact that composite membrane mechanically prevented Nafion from swelling is expected to lower the methanol crossover. Indeed, as shown in Table 7.2, the measured methanol permeability of the composite membrane is ~80 times lower than that of the Nafion 112 membrane (2.76×10^{-6} cm^2/s vs. 3.36×10^{-8} cm^2/s), although 80 (vol.%) of the membrane is still Nafion polymer.

Table 7.2 Proton conductivity and methanol permeability of Nafion 112 and composite membrane PI–Nafion.

Membrane	Proton conductivity σ (S/cm)			Methanol permeability P (cm^2/s)	Membrane selectivity $\phi=\sigma/P$ (S s/cm^3)
	RT	50 °C	80 °C		
Nafion 112	0.059	0.071	0.079	2.76×10^{-6}	2.14×10^{4}
PI–Nafion	**0.056**	**0.068**	**0.077**	**3.36×10^{-8}**	**1.67×10^{6}**

In this study, we measured the through-plane conductivity for fully hydrated membranes at various temperatures, since it is more representative than the in-plane one for anisotropic membranes.[93, 98] As shown in Table 7.2, proton conductivity of the membranes increases with the increase of temperature as a result of higher proton mobility at higher temperature. At room temperature (RT), the proton conductivity of PI–Nafion composite membrane is only slightly lower than the Nafion 112 membrane (0.056 S/cm vs. 0.059 S/cm). The high porosity of PI support matrix (80 vol.%) minimizes the adverse effect of the non-conducting PI on the conductivity of the resulting PI–Nafion composite membrane. Considering that thinner composite membrane is used

as a result of the improved mechanical strength, the overall membrane resistance of the PI−Nafion composite membrane is actually smaller than Nafion 112 (0.082 vs. 0.108 $\Omega.cm^2$). Table 7.2 also shows the selectivity factor (ϕ), a commonly used quantity to describe a membrane's performance in DMFCs, which is defined as the ratio between the proton conductivity and the methanol permeability. The selectivity (ϕ) of the composite membrane is significantly higher than that of Nafion 112 membrane (1.67×10^6 S s/cm^3 vs. 2.14×10^4 S s/cm^3).

The single cell performance of the MEAs based on the commercial Nafion 112, 117 and PI−Nafion composite membrane using 1M methanol is presented in Figure 7.4. As expected, the MEA with the PI−Nafion composite membrane shows considerably higher performance in comparison with that with Nafion 112 and 117 membranes, because of its lower membrane resistance and reduced methanol crossover. Particularly, the PI−Nafion membrane shows much higher open circuit voltage (OCV) than Nafion 117 and 112 (0.77V vs. 0.67V and 0.55V), although the composite membrane has a smaller thickness. The OCV of a MEA is closely related to the methanol crossover. Higher methanol crossover leads to a lower OCV. The higher OCV for the PI−Nafion membrane then contains that the PI−Nafion composite membrane in the MEA suppressed methanol crossover. This finding is consistent with the ex-situ methanol permeability measurement.

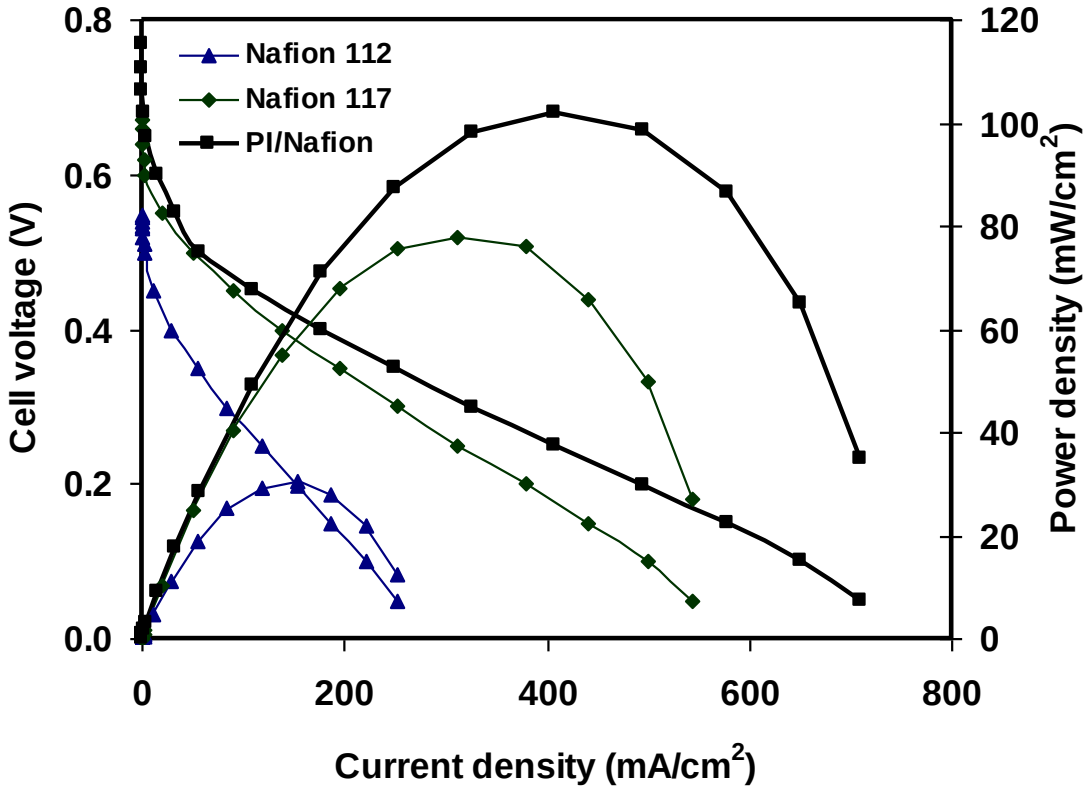

Figure 7.4 DMFC single cell performance of PI−Nafion composite membrane, Nafion 117 and Nafion 112 at 70°C with 1M CH_3OH.

The advantage of significantly reduced methanol crossover with this composite membrane can be clearly seen from the performance test with the feeding of 5M methanol (Figure 7.5).

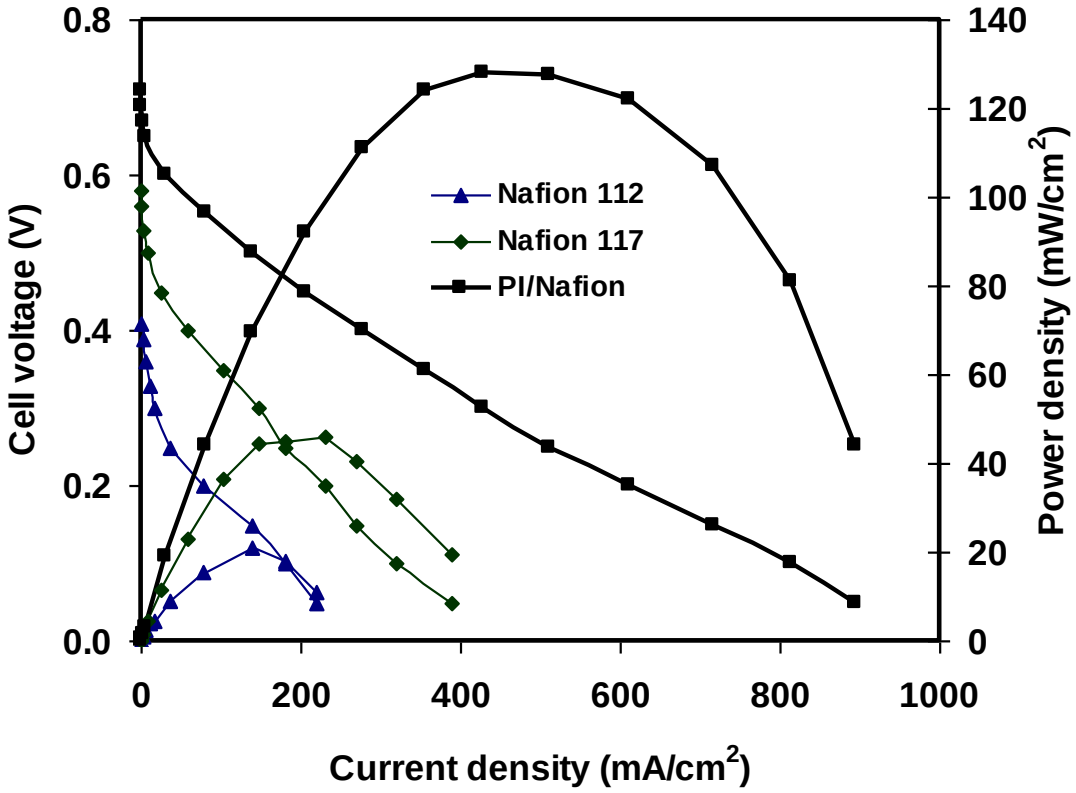

Figure 7.5 DMFC single cell performance of PI−Nafion composite membrane, Nafion 117 and Nafion 112 at 70°C with 5M CH_3OH.

A high fuel concentration is preferred from an application point of view, as it indicates higher specific energy from the power source. At such a high concentration, the maximum power density of the MEA with the pure Nafion 117 and 112 membranes is only 40 (mW/cm^2) and 21 (mW/cm^2), while the maximum power density of the MEA with the PI−Nafion composite membrane is 128 (mW/cm^2) and the OCV of the composite membrane is also much higher than Nafion 117 and 112 (0.71V vs. 0.58V and 0.41V).

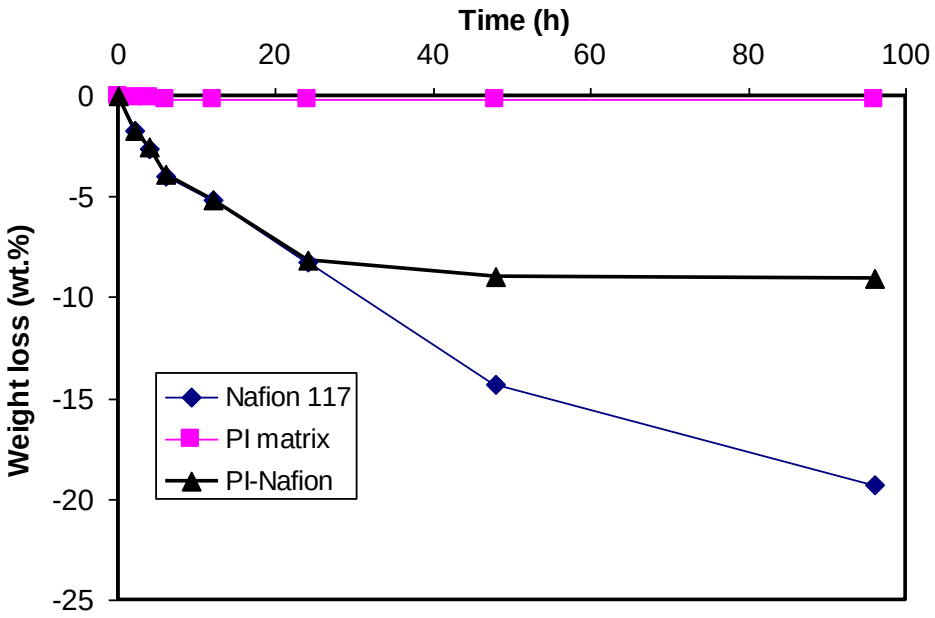

Figure 7.6 Membrane durability test following Fenton procedure of PI matrix, Nafion 117 and composite membrane PI–Nafion.

Finally, the composite membrane's durability was tested following Fenton procedure,[29, 99] where the membrane was exposed to 30 ppm Fe^{2+} and 10 (wt.%) H_2O_2 at 80°C. For comparison, porous PI matrixes and Nafion 117 membrane were also tested and the results are shown in Figure 7.6. Apparently, because of its high mechanical strength and chemical-resistance, the porous PI matrix did not show any weight change even after exposing up to 96h in testing solution. Both Nafion and PI–Nafion composite membranes showed a weight loss under Fenton's test. In other words, these two membranes were subject to decomposition under $OH^{\bullet}$ radicals created by the combination of Fe^{2+} and H_2O_2. The degradation rate of both membranes was similar within the first 24 h treatment. However, while the Nafion membrane showed continued weight loss following further treatment after 24h, the composite membrane PI–Nafion exhibited negligible loss. The results could be explained by the composite structure of the pore-filling electrolyte membrane. Since the surfaces of the composite membrane are covered by a thin layer of

Nafion, these layers show similar degradation rate as Nafion membrane once exposed to Fenton' solution. After the top layers were destroyed, the $OH^{\bullet}$ radical was very difficult to infiltrate into the composite membrane and contact Nafion. Because of the high resistance of the PI matrix to $OH^{\bullet}$ radicals, the PI−Nafion composite membrane showed a higher durability compared to Nafion membrane 117.

7.4 Conclusion

A wet porous PI matrix with high mechanical strength consisting of a pore size around 0.3 (μm) and a porosity of about 80 (vol.%) was successfully filled by an electrolyte of Nafion. We have found a very efficient way for an easy and complete infiltration of the proton conducting polymer into this matrix, which is realized by using a wet porous film with the presence of residual acetic anhydride. The PI−Nafion composite membrane shows excellent properties compared to Nafion-based membrane, such as three times lower in dimensional change, four times higher in mechanical strength, eighty times lower in methanol crossover, and significantly higher in selectivity factor. The improved performance of the DMFCs with PI−Nafion composite membrane is also demonstrated. In particular, due to inertness to chemical attack and preventing the contact between oxidation agent and Nafion material of the porous matrix, the composite membrane PI−Nafion has exhibited a higher durability than Nafion-based membranes. Allowing the use of a very thin membrane and a high methanol concentration, the PI−Nafion composite membrane is very promising as a proton exchange membrane for DMFC. Not limited to Nafion, this approach can be extended to other proton conductors, for whcih even higher proton conductivity can be expected."

To further increase the power density, a composite membrane which works well at a higher temperature is needed. At high temperatures, kinetics of methanol oxidation is

enhanced, leading to improved DMFCs performance. To achieve it, a mixture of acid functionalized zeolite and Nafion will be used as a filler to fill the porous matrix instead of sole Nafion in next chapter. The presence of nanoparticles in the hydrophilic region of the membrane can also help reduce the methanol crossover. Characterization of the composite membrane as a proton exchange membrane for DMFCs will also be conducted in next chapter.

Chapter 8 Nanocomposite Membrane Based on Porous Polyimide Matrix and Sulfonic Acid Functionalized Zeolite BEA Nanocrystals for Direct Methanol Fuel Cells

8.1 Introduction

High methanol permeability and low proton conductivity at high temperature are known as major problems of Nafion-based membranes for DMFC application.[66] The composite membrane based on pore-filling electrolyte is considered as the best membrane to deal with such problems so far because it offers a separation between mechanical and electrical property, which could render the membrane high performance.[25, 77] Our previous works used SPSE and Nafion as electrolytes to infiltrate into the porous PI matrix and the performance of those composite membranes outperformed commercial Nafion membranes.

To further improve the membrane performance, in this chapter, we have synthesized a solid proton conductor with high proton conductivity of sulfonic acid functionalized zeolite BEA nanocrystals (SAZBEA).[100-102] Based on this material and the combination with the porous PI matrix prepared in previous chapters, the PI−Nafion−SAZBEA composite membrane has been successfully fabricated by filling a composite filler of the mixture of Nafion and SAZBEA into the pores of the PI matrix. This composite membrane has shown excellent properties such as extremely low in methanol crossover, high proton conductivity, good mechanical strength and significantly high power density in fuel cell performance.

8.2 Experimental Details

8.2.1 Synthesis of Zeolite Nanocrystals SAZBEA

Sulfonic acid functionalized zeolite BEA nanocrystals (SAZBEA) nanocrystals were synthesized based on previous published method by Holmberg et al.[103] For preparing phenethyl functionalized zeolite BEA (PEBEA) nanocrystals, 76.46 (g) of 35 (wt.%) aqueous tetraethylammonium hydroxide (TEAOH, Sigma−Aldrich) and 2.10 g of aluminum isopropoxide (98 wt.%, Sigma−Aldrich) were mixed well in a 250 (ml) polypropylene (PP) bottle with a magnetic stir bar until the solution becomes clear. 100.50 (g) of aqueous 30 (wt.%) colloidal silica (Ludox HS-30, SiO_2/Na_2O = 90, SiO_2 = 29.90 (wt.%), Na_2O = 0.34 (wt.%), Sigma−Aldrich) was then added. Finally, 0.58 (g) of phenethyl trimethoxysilane (PETMS, 98 wt.%, Sigma−Aldrich) was added to complete the reaction mixture, and the bottle was sealed tightly. It was aged at room temperature for 2 h with strong stirring, and was then heated by a silicone oil bath at 100 °C with stirring for 15 days. The obtained solution was washed three times by centrifugation followed by decanting and redispersion in double de-ionized (DDI) H_2O with ultrasonication. To prepare SAZBEA nanocrystals, the washed PEBEA nanocrystals were dispersed in 96 (wt.%) concentrated sulfuric acid (H_2SO_4) with vigorous stirring to obtain a 2.0 (wt.%) zeolite suspension in sulfuric acid in a PP bottle. This solution was then held at 80°C with stirring for 12h to remove the organic template and add sulfonic acid group to the phenethyl group simultaneously. Finally, the solution was washed by centrifugation as described above until the solution became neutral and the washed SAZBEA was re-dispersed in ethanol.

8.2.2 Preparation of Porous Polyimide Matrix BTDA−PPDA/ODA

A polyimide precursor was synthesized by a polycondensation reaction between a dianhydride (BTDA) and diamines (PPDA and ODA) at a molar ratio of

BTDA:PPDA:ODA (1:0.75:0.25) in DMF at room temperature for 24h to form a poly(amic acid) of 18 (wt.%) solid content. This was then followed by a imidization reaction promoted by acetic anhydride and pyridine with a volume ratio of 2:1 at 60°C for 12h to convert the reactant to the corresponding polyimide containing 16 (wt.%) of solid polyimide.

The polyimide precursor was cast on a round glass surface by spin coating machine (SCS G3, Cookson Electronics) with a spin speed of 900 rpm and a spin time of 30s. The cast film was then coagulated immediately in a non-solvent solution containing 70 (vol.%) of 1-butanol and 30 (vol.%) of DMF at room temperature for 15 min, followed by aging for 5 min in pure methanol and 5 min in DDI H_2O to form a porous film. The porous film was then dried in the air overnight and ready for filling with electrolytes.

8.2.3 Fabrication of Composite Membrane PI−Nafion−SAZBEA

The Nafion/ethanol suspension was prepared by first drying raw Nafion solution (5 wt.%, Gashub, Singapore) at 60°C until all solvents were completely removed. The dry Nafion was then treated with 25 (wt.%) nitric acid solution at 80°C for 1h, followed by repeated rinse three times with DDI H_2O and drying again. The treated Nafion was then put into ethanol and ultrasonicated to form a suspension containing 10 (wt.%) of Nafion. The appropriate amounts of Nafion/ethanol and SAZBEA/ethanol suspension were mixed together by ultrasonicating for 30 min to obtain a mixture of the filling solution.

The porous PI substrate was first extended over a glass plate by a membrane caster. The filling solution was then poured onto the surface of the porous film and the membrane caster was placed in a convection oven at 60°C for 24h. After that, the composite membrane was cured at 120°C for 12h and then 150°C for 1h in a vacuum oven for the

final heat treatment. To prepare the membrane for characterization, it was treated by boiling in a solution of 3 (wt.%) H_2O_2 for 1h then rinsed with boiling water. Then it was boiled in a solution of 0.5M H_2SO_4 for 1h, followed by rinsing with boiling water. Finally, the treated membrane was stored in DDI H_2O overnight and ready for testing.

8.2.4 Material Characterization

8.2.4.1 X−ray Diffraction (XRD)

XRD patterns were obtained by a D8 advance diffractometer (Bruker) using a Cu Kα radiation to investigate the crystallinity of zeolite nanocrystals and verify their survival in the sulfonating process and the preparation of the nanocomposite membrane. The dried samples were mounted onto the holders. The scanning angle ranged from 5° to 40° with a scanning rate of 0.02 (°/s).

8.2.4.2 Fourier Transform Infrared Spectroscopy (FT−IR)

A FT−IR spectrometer (FTS 3100, PerkinElmer) was used to confirm the structures of PEBEA and SAZBEA nanocrystals under the resolution of 0.5 (cm^{-1}). FT−IR samples were prepared by mixing 1 (wt.%) of zeolite BEA with dried KBr and pressing into pellets under a force of 10 metric tons for 30s.

8.2.4.3 Thermoanalysis

A thermogravimetric analyzer (Diamond TG/DTA−TGA, Perkin Elmer) was used to observe the water content, the decomposition of TEAOH and the addition of sulfonic acid groups in the PEBEA nanocrystals. The thermogravimetric analysis was carried out at 10 (°C/min) under an air flow.

8.2.4.4 Membrane Morphology

Both the surface and cross-section of the porous PI film and the composite membrane were observed by JEOL field emission electron microscope (JSM6−700F). For observing the cross-section images, samples were fractured in liquid nitrogen. All samples were coated with a thin layer of gold by an auto fine coater at a current of 20 (mA) for 50s.

8.2.4.5 Transmission Electron Microscopy (TEM)

For the preparation of TEM samples, zeolite BEAs were dispersed in ethanol under ultrasonication for 15 min., then dropped onto a copper grid and dried at room temperature. The thin layer was observed in a TEM (JEOL 2010) operated at 200 (kV).

8.2.4.6 Membrane Durability

The composite membrane's durability was conducted following Fenton procedure,[99] where the membrane was exposed to 30 (ppm) Fe^{2+} and 10 (wt.%) H_2O_2 at 80°C for different lengths of time. The weight loss of the membrane was determined by different masses between before and after exposing to Fenton solution.

8.2.4.7 Methanol Crossover

Methanol permeability of the membranes was measured using the two compartment diffusion technique as reported before.[17]

8.2.4.8 Proton Conductivity

The proton conductivity of the membrane in the through-plane direction was measured by potentiostat (Autolab, Netherlands) in a home-made cell.[93] The cell consists of two Teflon blocks attached with platinum foil electrodes (1.2×1.2 cm) and platinum leads.

The pretreated membrane (1.5×1.5 cm) was clamped between the two Teflon blocks held in place with Teflon screws. The impedance measurements were carried out with a frequency range from 250 (kHz) to 150 (kHz). The proton conductivity of the membrane, σ (S/cm), is defined by Equation (8.1).

$$\sigma = \frac{L}{RS} \qquad (8.1)$$

where S (cm^2), L (cm), R (Ω) denote surface area of the electrode, thickness of the membrane, and resistance, respectively.

For measuring proton conductivity of the solids of PEBEA and SAZBEA nanocrystals, the dried and clean samples were confined in a polycarbonate (PC) cylinder cells under pressure. Then the sample were saturated with DDI H_2O and compressed again before testing.[100, 103]

8.2.4.9 Single DMFC Performance

It was conducted in Arbin fuel cell test station. To minimize the influence from the electrode variation, commercial electrodes (Gashub, Singapore) were used for the membrane electrode assembly (MEA) fabrication and performance test. The electrode consists of a PTFE treated 20 (wt.%) carbon paper substrate, a microporous layer with carbon loading of 1.2 (mg/cm^2), and a catalyst layer. The catalyst layer in anode contains 40 (wt.%) PtRu/C and Nafion, with total metal loading of 2.0 (mg/cm^2) (Pt:Ru = 1:1), while that in cathode contains 40 (wt.%) Pt/C and Nafion, with Pt loading of 2.0 (mg/cm^2). MEA with an active electrode area of 5 (cm^2) was obtained by pressing the cathode and anode onto each side of a pretreated Nafion 117 membrane or composite membrane at 140°C and 2.0 (MPa) for 1 min (Hydraulic 3912, Carver, Inc.). The MEA

was then assembled into a DMFC single cell. The operation conditions were as follows: anode fuel, 1M or 5M methanol; flow rate, 1.0 (mL/min); oxygen pressure, 0.4 (MPa); and flow rate, 0.25 (L/min). The temperature of the cell was at 70°C.

8.3 Results and Discussion

8.3.1 Zeolite Nanocrystals PEBEA and SAZBEA

XRD analysis was first conducted to characterize whether the prepared PEBEA nanocrystals can survive the strong acid treatment.[103] XRD patterns of PEBEA nanocrystals before and after overnight treatment in concentrated sulfuric acid (96 wt.%) at 80°C were shown in Figure 8.1 The characteristic peaks of PEBEA at 8° and 23° existed after the sulfuric acid treatment. This result proved that PEBEA nanocrystals were still stable after the harsh treatment.

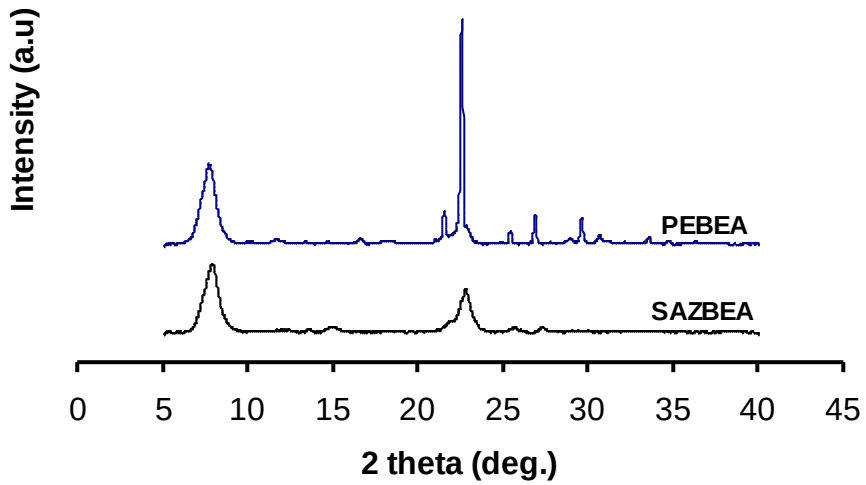

Figure 8.1 XRD patterns of PEBEA and SAZBEA nanocrystals.

Same conclusion can be made from the TEM pictures of the as-synthesized PEBEA and acid treated SAZBEA nanocrystals.[104] As can be seen in Figure 8.2, both SAZBEA and PEBEA nanocrystals have similar shape and size, indicating that the nanocystals survived the concentrated sulfuric acid treatment.

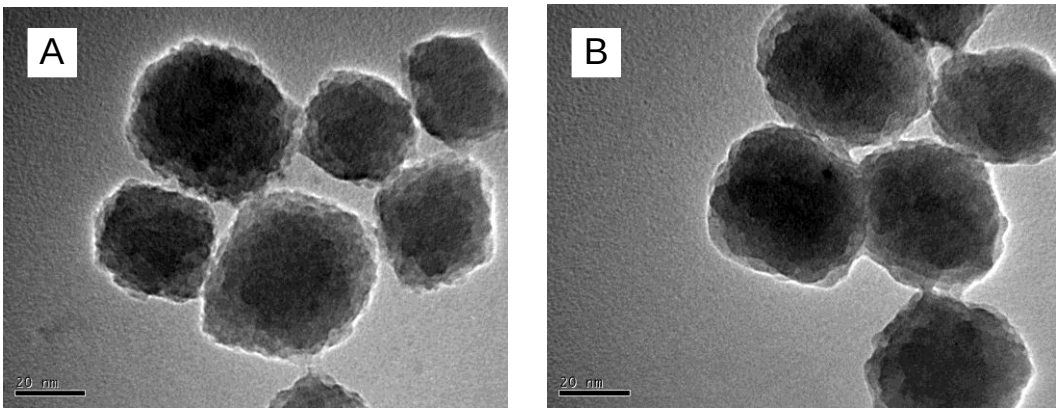

Figure 8.2 TEM images of (A) PEBEA and (B) SAZBEA nanocrystals.

TGA is used to characterize the removal of the structure-directing agent (SDA) in PEBEA nanocrystals and determine the approximate weight percentage of the organic functional group in the functionalized zeolite.[105] As shown in Figure 8.3, there are a large weight loss for PEBEA nanocrystals in the range of 170°C - 370°C (~15 wt.%) that is attributed to the loss of the organic SDA of TEAOH and an additional mass loss (~5 wt.%) at higher temperature (370-470°C) that is assigned to the combustion of the phenethyl (PE) groups. After strong acid treatment, SAZBEA shows a new weight loss in the range of 250-390°C, attributable to HSO_3 groups anchored to the phenyl rings of PE. Thus, the 96 (wt.%) H_2SO_4 acid treatment was effective in simultaneously achieving the organic SDA removal and the sulfonic acid addition.

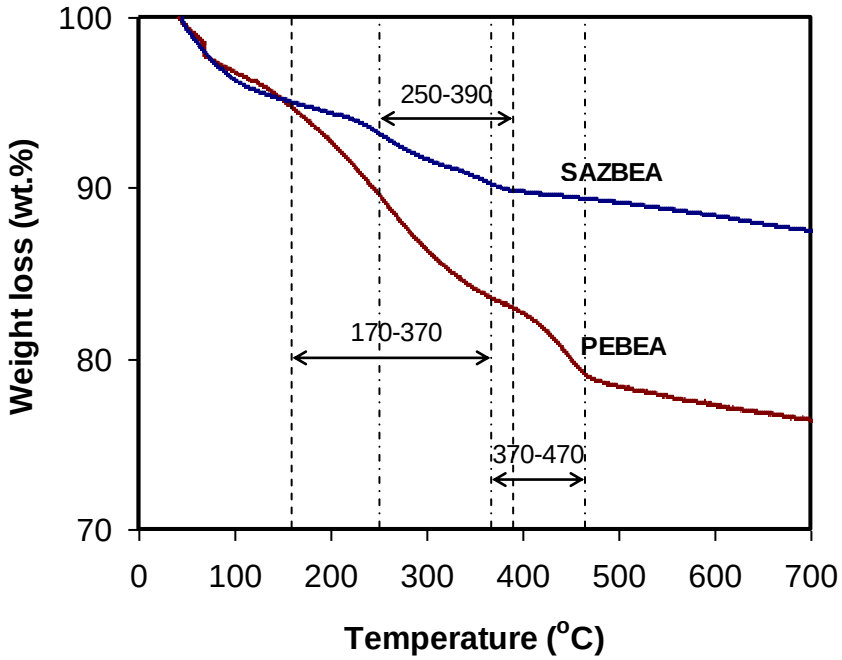

Figure 8.3 TGA curves of PEBEA and SAZBEA nanocrystals.

The success of sulfonation by strong acid treatment was also supported by FT−IR and the proton conductivity measurement.[104].

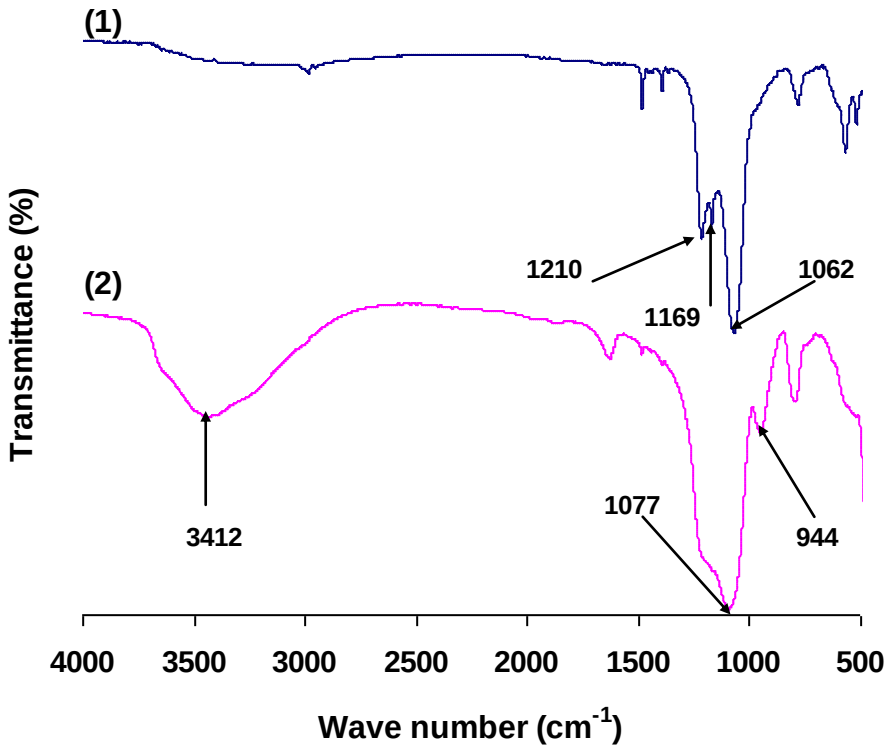

Figure 8.4 FT–IR spectra of (1) PEBEA and (2) SAZBEA.

As shown in Figure 8.4, in addition to absorption peaks at 1062 and 1077 (cm^{-1}) assigned to Si-O stretching, the disappearance of the asymmetric and symmetric stretching of a $(C_2H_5)_4N^+$ group at 1,169 and 1,210 (cm^{-1}) and the appearance of the absorption band of a sulfonic group at 944 (cm^{-1}) have proved the SDA removal of $(C_2H_5)_4N^+$ from PEBEA nanocrystals, as well as the addition of sulfonic group to the phenyl ring. With the introduction of sulfonic group, the proton conductivity of the SAZBEA in fully hydrated condition at room temperature is increased to 2.18×10^{-3} (S/cm), 11 times higher compared to PEBEA (1.89×10^{-4} S/cm).

8.3.2 Composite Membrane Preparation and Its Performance

After the synthesis of SAZBEA nanocrystals, the next task is to fabricate the composite membrane by filling the electrolyte (a mixture of SAZBEA nanocrystals and Nafion

ionomer) into the porous substrate. As shown in Figure 8.5(A) and 8.5(D), the porous PI matrix used to construct the composite membrane consists of a porous top layer and a spongy type sub-structure with a porosity of 80 (vol.%) and a mean pore size of ~0.3 (μm). Here two different amounts of SAZBEA in the filling electrolyte were used, i.e., 5 and 10 (wt.%) of SAZBEA to Nafion solid content. For both cases, the composite electrolyte completely filled up the pores of the supporting matrix, as displayed by the images of cross-sections of composite membranes in Figure 8.5(B) and 8.5(C), and the FE-SEM images of top surfaces of composite membranes in Figure 8.5(E) and 8.5(F). However, the composite membrane fabricated with 5 (wt.%) SAZBEA nanocrystals shows a homogeneous dispersion of nanocrystals on the surface. In contrast, with 10 (wt.%) SAZBEA nanocrystals, a less uniform distribution of nanocrystals was observed both on the surface and in the cross-section, with apparently a SAZBEA nanocrystals rich layer near the surface.

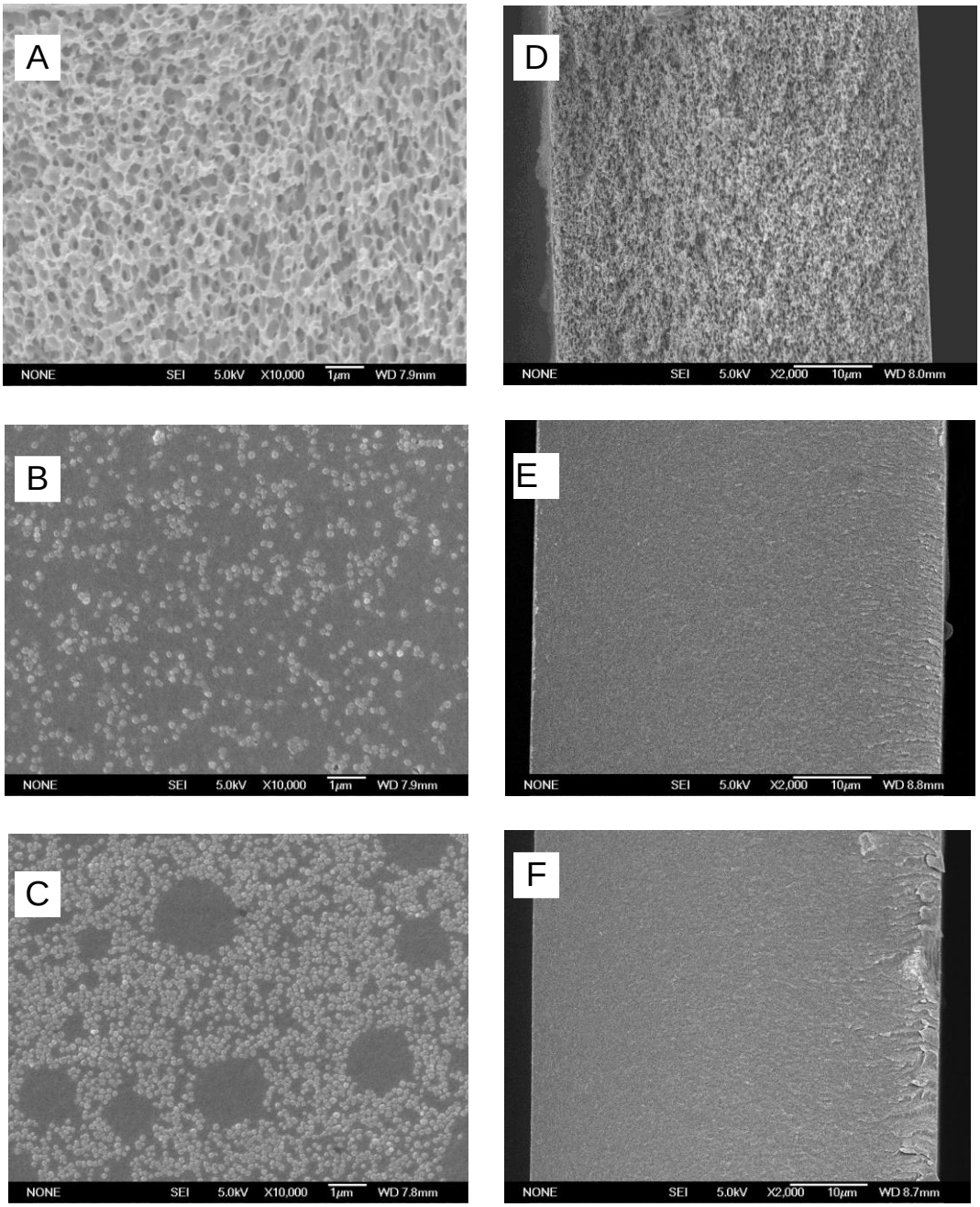

Figure 8.5 FE–SEM images of top surfaces (A), (B), (C) and cross-sections (D), (E), (F) of porous PI matrix fabricated by coagulating the cast film in non-solvent bath containing 70 (vol.%) 1-butanol and 30 (vol.%) DMF for 15 min, PI–Nafion–SAZBEA composite membrane prepared by filling the filler with 5 (wt.%) SAZBEA to Nafion and with 10 (wt.%) SAZBEA to Nafion, respectively.

Mechanical strength of the host matrix is an important factor to produce a good composite membrane. The high strength of the matrix allows the preparation of a thinner composite membrane which can lower the membrane resistance. Table 8.1 compared the mechanical strength of different membranes. As expected, all the composite membranes made from the strong PI matrix shows about 3 times higher mechanical strength than Nafion 117 membrane.

Table 8.1 Physical properties of Nafion 117, composite membrane PI–Nafion, PI–Nafion–5 (wt.%) SAZBEA and PI–Nafion–10 (wt.%) SAZBEA.

Membrane	Water content (%)	Dimensional change (%)	Mechanical strength (MPa)
Nafion 117	15.67	11.85	30.4
PI–Nafion	5.92	4.75	104.5
PI–95 (wt.%) Nafion–5 (wt.%) SAZBEA	**5.85**	**4.71**	**99.4**
PI–90 (wt.%) Nafion–10 (wt.%) SAZBEA	6.15	4.77	91.3

Dimensional stability is one of the key requirements to make new proton exchange membranes for DMFC application. A composite membrane with minimal change in the dimension after the electrolyte filling and under hydrated condition can effectively reduce the methanol crossover by confining the swelling of the filling electrolyte. In the meantime, it is also beneficial for the lifetime of the membrane assembly electrode (MEA), because carbon electrodes do not change in dimension from any water uptake and less damage to the structure integrity of the MEA can be expected. Due to the rigid structure and high mechanical strength of the porous PI matrix, only small change in

dimension between the dry and wet state of the composite membranes was recorded, which is about 1/3 compared with Nafion 117 membrane (Table 8.1).

Membrane durability is the most important issue to be solved before commercializing DMFCs successfully because it affects not only lifetime of MEAs but also the performance of DMFCs. As expected, due to specific structure of the pore-filling electrolyte membrane that an electrolyte is filled into the pores of the porous matrix, the chemical attack agent of the $OH^{\bullet}$ radical is difficult to contact and decompose the electrolyte material, which is confined into the pores. In addition, because of inertness to chemical attack of the host matrix the composite membrane PI–Nafion–SAZBEA exhibited a high durability compared to Nafion 117 membrane (Figure 8.6).

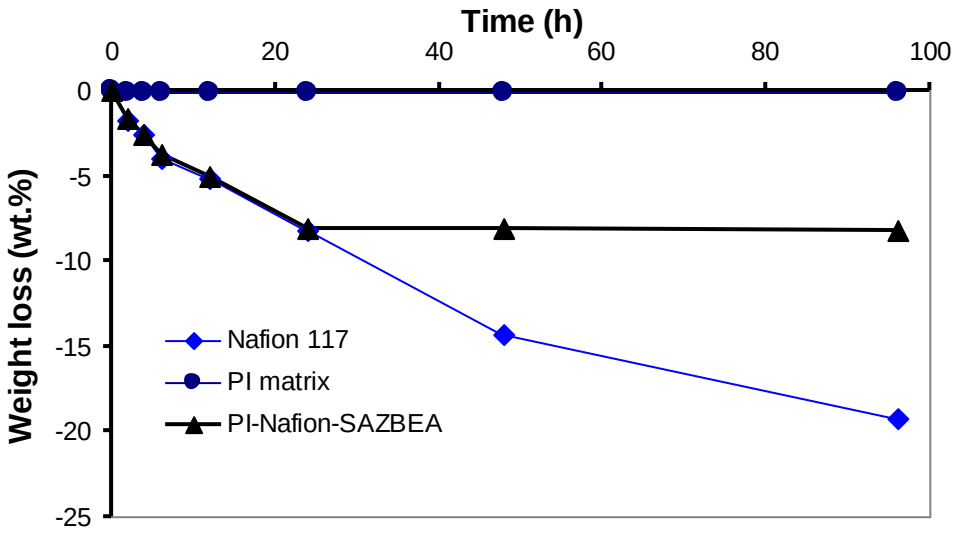

Figure 8.6 Membrane durability test following Fenton procedure of Nafion 117, PI matrix and composite membrane PI–Nafion–5 (wt%) SAZBEA.

The effectiveness of the PI matrix in the reduction of methanol permeability has already been proved in our previous work with the demonstration of PI–Nafion composite membrane. In this study, to further reduce the methanol crossover and increase the proton

conductivity of the membrane, we used a composite filler of Nafion and SAZBEA nanocrystals as proton conducting material and the results were shown in Table 8.2.

Table 8.2 Electrochemical properties of Nafion 117, PI–Nafion, PI–Nafion–5 wt.% SAZBEA and PI–Nafion–10 wt.% SAZBEA composite membranes.

Membrane	Proton conductivity σ (S/cm)			Methanol permeability P (cm^2/s)			Membrane selectivity ϕ=σ/P (S s/cm^3) at RT
	RT	50 °C	80 °C	RT	45 °C	60 °C	
Nafion 117	0.064	0.073	0.082	2.12×10^{-6}	3.29×10^{-6}	4.39×10^{-6}	2.99×10^{4}
PI−Nafion	0.056	0.068	0.077	3.36×10^{-8}	5.04×10^{-8}	6.72×10^{-8}	1.67×10^{6}
PI−Nafion−5 wt.% SAZBEA	**0.062**	**0.072**	**0.083**	**1.15×10^{-8}**	**1.42×10^{-8}**	**1.70×10^{-8}**	**5.39×10^{6}**
PI−Nafion−10 wt.% SAZBEA	0.054	0.067	0.076	5.18×10^{-8}	NA	NA	1.04×10^{6}

With a loading of 5 (wt.%) SAZBEA, the PI–Nafion–SAZBEA composite membrane exhibited a twice lower methanol permeability than PI–Nafion composite membrane (1.15×10^{-8} cm^2/s vs. 3.36×10^{-8} cm^2/s). It is believed that, the nanocrystals in the size range of 40-50 (nm) have been distributed uniformly over the cross-section and located within the hydrophilic region of the Nafion structure, blocked the open pathways of the methanol flow and therefore, led to the reduction of the methanol crossover through the membrane.[21, 22] However, when increasing the SAZBEA content in the filler from 5 (wt.%) to 10 (wt.%), the agglomeration of the nanocrystals near the surface makes it difficult for the nanocrystals to enter the hydrophilic zone of the Nafion structure and the ousted nanocrystals create nanoparticle rich layers with many defects, which are ineffective to prevent the methanol flow through the composite membrane. Therefore, a higher value in methanol permeability was observed (5.18×10^{-8} cm^2/s).

The proton conductivity of the membrane plays the most important role for fuel cell performance in DMFCs. It was confirmed in our past work that the PI−Nafion composite membrane had shown only 5% lower in proton conductivity compared with Nafion 112 (0.056 S/cm vs. 0.059 S/cm), although the volume ratio of PI material in the composite membrane is up to 20%. In this work, with the introduction of 5 (wt.%) of SAZBEA into the filling electrolyte, PI−Nafion−SAZBEA composite membrane shows further improvement in proton conductivity compared with PI−Nafion composite membrane (0.062 S/cm vs. 0.056 S/cm) and it is only slightly lower than that of Nafion 117 membrane (0.064 S/cm) at room temperature, as shown in Table 8.2. Considering the much lower thickness of the composite membrane (50 μm vs. 175 μm), the overall membrane resistance is actually much smaller than Nafion 117. The mechanism behind the improvement in the proton conductivity when introducing SAZBEA into the Nafion structure was explained by Chen *et al*.[106] as follows: in the Nafion membrane, an approximate portion of 20% of the sulfonic acid groups needed for proton conductivity are buried within the hydrophilic interfacial zone between the hydrophobic region of the Nafion backbone and the hydrophilic region of ionic clusters and have not incorporated into the clusters to conduct proton. It was believed that these groups become accessible for ion exchange after the nanocrystals enter this interfacial region, promoting an access of inactive sulfonic acid groups into the ionic clusters. Moreover, the presence of SAZBEA nanocrystals in the hydrophilic region also increased the density of sulfonic acid groups in the membrane, which caused the increase in the proton conductivity. However, a negative effect in the proton conductivity of the resulted composite membrane was observed when increasing the SAZBEA loading in the filler to 10 (wt.%). The proton conductivity was only 0.054 (S/cm) for the composite membrane using the filler with 10 (wt.%) SAZBEA to Nafion content. The reduction of the proton

conductivity of the composite membrane with a higher SAZBEA loading in the filler can be explained by the inhomogeneous dispersion of the nanocrystals and the expected dilution of the high proton conductivity of Nafion (0.064 S/cm) by the low proton conductivity of SAZBEA nanocrystals (2.18×10^{-3} S/ cm).

The temperature dependence of proton conductivity and methanol crossover has been reported in the literatures.[107, 108] The results indicated that the methanol transport and proton conduction in the membrane are activated thermal processes and they both obey Arrhenius correlation. We have examined the temperature dependence on the composite membrane (Table 8.2). At fully hydrated condition, all the composite membranes show similar temperature dependence as Nafion membrane. With further increase in the temperature, the lack of water in the membrane occurs, leading to the decrease of cell performance due to the reduction of proton conductivity of the membrane. However, the composite membrane of PI−Nafion−SAZBEA with the filler containing the nanocrystals of SAZBEA could maintain water content at high temperatures. Thus such a membrane can be used at a higher temperature (~ 130°C).

Due to the extremely low methanol permeability and high proton conductivity of the composite membrane with the filler containing 5 (wt.%) SAZBEA, the single cell DMFC performance with this composite membrane with different methanol concentrations (1 and 5M) at 70°C outperformed Nafion 117 and PI−Nafion composite membrane, as shown in Figures 8.7 and 8.8.

At both methanol concentrations, the PI−Nafion−SAZBEA shows a higher open circuit voltage (OCV) than that of the PI−Nafion composite membrane as a result of a lower methanol permeability. In addition, the PI−Nafion−SAZBEA composite membrane offers a higher value in maximum power density than the PI−Nafion composite membrane. As

fueling DMFCs at the low methanol concentration (1M CH_3OH, the maximum power density increased from 102 (mW/cm^2) for the PI–Nafion to 126 (mW/cm^2) for PI–Nafion–SAZBEA composite membrane, that is about a 24% increase. The benefit of the composite membrane is that it could be used at high methanol concentrations, which is preferred as it indicates a higher specific energy density from the power source.

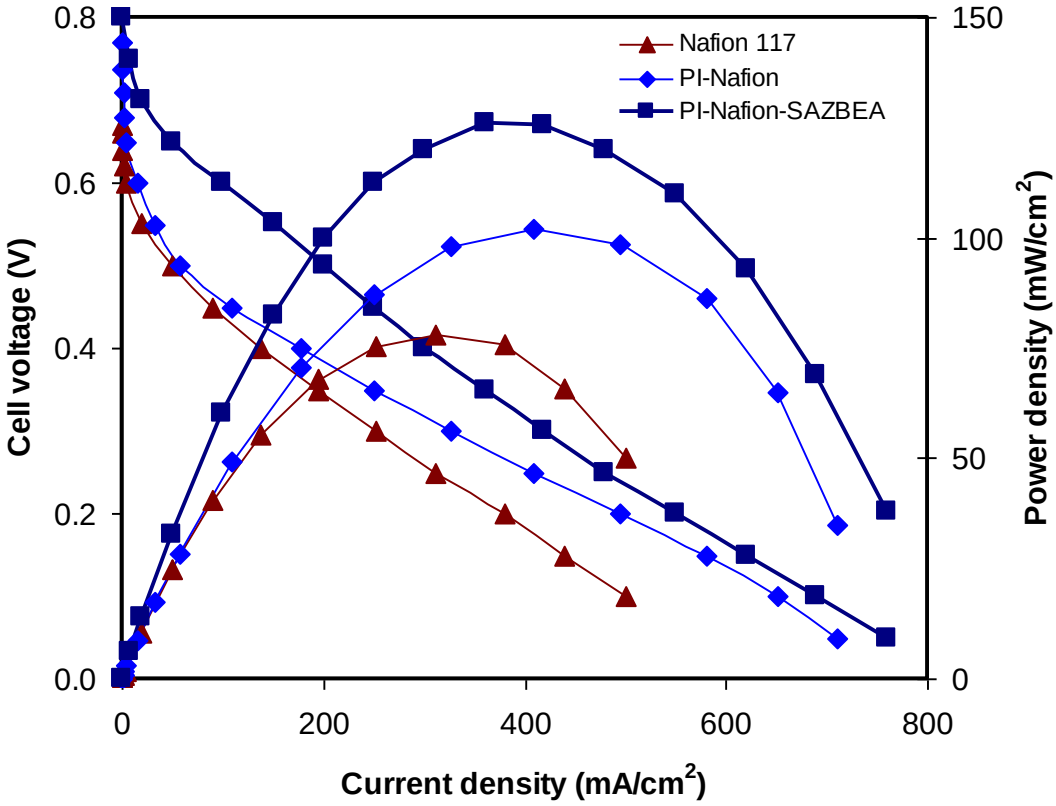

Figure 8.7 DMFC single cell performance of PI–Nafion–SAZBEA composite membrane with 5 (wt.%) SAZBEA to Nafion, PI–Nafion composite membrane and Nafion 117 membrane at 70°C with 1M CH_3OH.

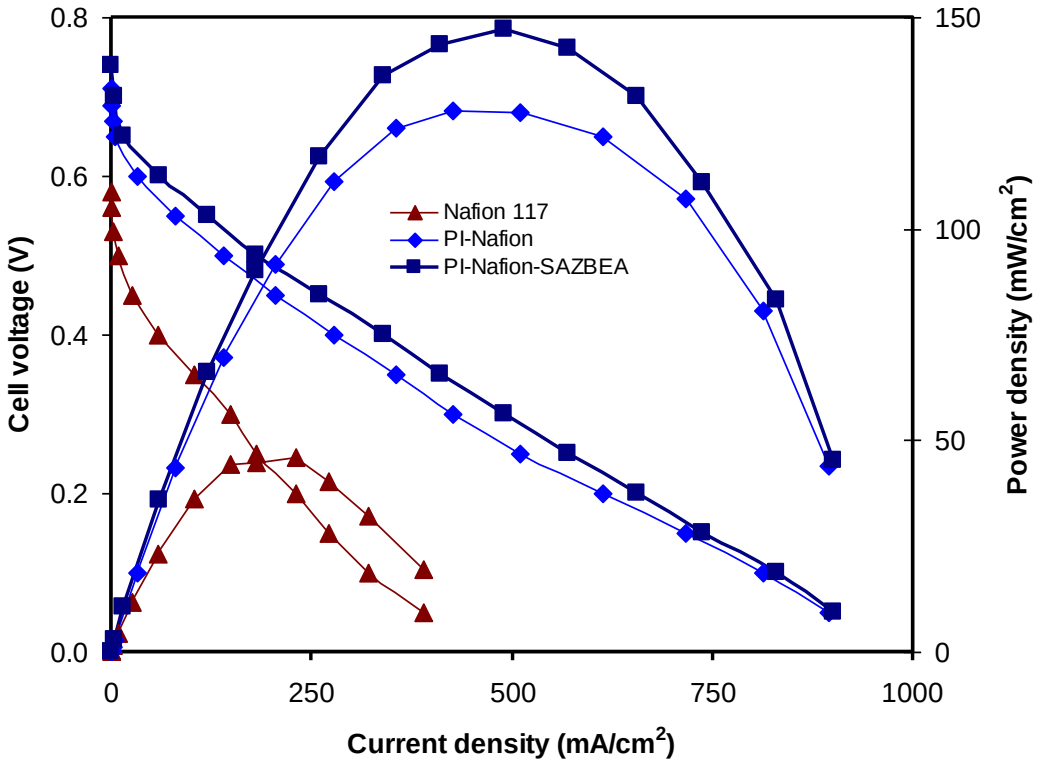

Figure 8.8 DMFC single cell performance of PI–Nafion–SAZBEA composite membrane with 5 (wt.%) SAZBEA to Nafion, PI–Nafion composite membrane and Nafion 117 membrane at 70°C with 5M CH_3OH.

As can be seen in Figure 8.8, when feeding with 5M CH_3OH, the maximum power density of the both composite membranes increases compared with the case of 1M methanol, while a decrease is observed for Nafion 117 membrane. The maximum power density of PI–Nafion–SAZBEA is still higher than that with the PI–Nafion composite membrane (147 mW/cm^2 vs. 128 mW/cm^2). The higher maximum power density of PI–Nafion–SAZBEA composite membrane at higher methanol concentration indicates this composite membrane can be used as a proton exchange membrane in DMFC application.

8.4 Conclusion

The porous PI matrix with high porosity and the sulfonic acid functionalized zeolite BEA nanocrystals containing sulfonic acid groups have been synthesized. Using these materials, the PI−Nafion−SAZBEA composite membrane has been successfully prepared by infiltrating the composite filler of Nafion and SAZBEA nanocrystals into the pores of the support matrix. The composite membrane containing about 20 (vol.%) of PI matrix and 80 (vol.%) of the filler of 95 (wt.%) Nafion and 5 (wt%) SAZBEA nanocrystals shows excellent properties of a proton exchange membrane for DMFCs compared with PI−Nafion as well as Nafion 117 membrane such as extremely low methanol permeability, high mechanical strength, high proton conductivity, high membrane durability and the dimensional stability of membrane in both hydrated and dehydrated state. With high performance for DMFCs, this PI−Nafion−SAZBEA composite membrane is promising as a practical membrane used for DMFC application, particularly with a high methanol concentration.

Although the internal resistance of MEA has not tested yet and such tests will be conducted in future, we expect the MEAs constructed by composite membranes will still have a much lower resistance compared with the MEAs with Nafion membranes in DMFC operation. In addition, we could further speculate that the composite membrane will minimize the tension between the electrode and membrane and offer the possibility of enhanced durability and lifetime, by limiting the swelling of the filling electrolyte with its rigid structure. Of course, real durability tests of MEAs in DMFCs can still be done in the future, but only for demonstration purpose.

Chapter 9 Conclusions and Recommendations

9.1 Conclusions

Porous polyimide films S-BPDA−PPDA/ODA with spongy-type structure and different pore sizes were fabricated in chapter 3 by coagulating a cast liquid film in a non-solvent bath containing a mixture of 1-butanol and NMP with different ratios. The pore size of the porous film is strongly affected by the composition ratio between NMP and 1-butanol. It increases when decreasing 1-butanol content. Because the top surface is semi-porous, the porous film was difficult to be filled with an electrolyte in making a workable membrane. In chapter 4, porous films with different morphologies of spongy and finger types were prepared from cast films containing a non-solvent of 1-butanol or methanol followed by a phase separation in the non-solvents and thermal imidization. The spongy-type structure was obtained when the cast film without additive was coagulated in whatever non-solvent of water, 1-butanol, or a mixture of 1-butanol and DMF with various ratios. Alternatively, due to the effect of the additive, porous films prepared from the cast film containing 1-butanol show a spongy type and a finger type when coagulated in a mixture of 1-butanol/DMF and water respectively. In particular, the methanol-containing cast film after phase separation in water formed a porous film with an ordered finger type (cylinder type) structure. Moreover, the mechanical strength of porous films are strongly affected by their morphologies, where the porous film with a spongy structure and a sub-micrometer pore size exhibited higher mechanical strength than those of cylinder and finger types. In chapter 5, the porous film, consisting of a spongy structure and a porous top layer, with sub-micro-pores, high porosity and mechanical strength was selected as matrix to be filled with an electrolyte of Nafion or SPSE. While this porous matrix was difficult to be filled by Nafion such that separate layers of matrix

and Nafion were observed, SPSE could easily infiltrate into the pores of the matrix and the composite membrane PI−SPSE had been successfully fabricated. The membrane showed better performance in DMFC testing compared to Nafion membrane 1135, including a 16.7% higher OCV and 25% higher maximum power density. To allow the infiltration of Nafion, in chapter 6, the morphology of chemical imidization-based porous polyimides was investigated by coagulating cast films of a polyimide precursor of BTDA−PPDA/ODA in a non-solvent bath which contains a mixture of 1-butanol and DMF with different ratios. The porous films with different pore sizes, a porous/semi-porous top layer and a spongy-type sub-structure were obtained. By avoiding high temperature thermal treatment, the resulted films containing trace of a chemical imidization agent of acetic anhydride are more hydrophilic, which is expected to facilitate the filling with hydrophilic electrolytes, such as Nafion. Using them as support matrixes, in chapter 7, composite membranes based on Nafion filling had been successfully prepared and the membrane constructed from the porous film with a porosity of 80 (vol.%) and pore size of 0.3 (μm) outperformed other composite membranes prepared from those matrixes with a bigger pore size. This composite membrane performed better compared to Nafion membrane 112, including 80 times lower methanol permeability, 4 times stronger mechanical strength. Particularly, such a membrane showed excellent performance for DMFC testing at both 1M and 5M CH_3OH concentrations. Continuing to improve performance of the composite membrane for DMFC, in chapter 8, instead using the electrolyte of Nafion, a mixture of Nafion and sulfonic acid functionalized BEA zeolite (SAZBEA) had been used as the electrolyte and the composite membrane PI−Nafion−SAZBEA had been prepared. Such a membrane further reduced methanol crossover compared to PI−Nafion while maintaining high proton conductivity. In addition to suppressing the swelling by the stiff matrix, these results could be explained by the

presence of nanosized zeolites in the void volume between ionic clusters and fluorocarbon backbones of Nafion, which blocked the methanol flow through the membrane while proton conduction can still proceed. The composite PI−Nafion−SAZBEA membrane containing 5 (wt.%) zeolite showed higher DMFC performance than PI−Nafion, including a 24% higher maximum power density and a 4% higher OCV at methanol-fed concentration of 1M. Even bigger difference was observed when higher methanol concentration of 5M was used, which indicates the potential of using this membrane to DMFC applications.

9.2 Recommendations

The results pointed out in the previous chapters have shown a success of preparing the porous polyimide matrixes with different morphologies and corresponding composite membranes by infiltrating an electrolyte into the substrates. Most of the composite membranes outperformed Nafion-based membranes for DMFCs. Unfortunately, due to resistance to most solvents and low level of swelling during infiltration processes, it is difficult to fill the porous matrix with a proton conducting material to make the composite membrane when the pore size of the matrix becomes too small. Only the matrix with a pore size more than 0.3 (μm) can be successfully infiltrated so far. Experimentally, the mechanical and proton conductivity of the composite membrane based on pore-filling electrolyte would be increased when decreasing the pore size of the matrix. With that in mind and the intention of improving performance of the composite membrane further, a suggestion for future researches would be to prepare the porous polyimide film with a smaller pore size, and allow complete infiltration of a proton conducting material subsequently. To achieve that, other additives being more hydrophilic could be used for synthesizing a polyimide precursor to improve the matrix's infiltration capability along

with its porosity. Other than that, infiltration method also affects the preparation of the composite membrane. Currently, the porous filling is carried out by pouring the electrolyte solution on the surface, followed by heat treatment. In future, the infiltration process could be conducted at high pressure or under vacuum to force the filler to penetrate into the porous matrix. In addition, reducing a total resistance of the membrane is needed to improve the membrane performance. Currently, the composite membrane possesses a thickness of 45 (μm). With a higher mechanical strength of the porous matrix due to the reduction in the pore size, a thinner composite membrane with a lower total resistance while maintaining high mechanical strength is expected to be made. Another way to improve the performance of the membrane is to enhance the proton conductivity and reduce the crystal size of the acid functionalized zeolite, which currently is about 2.3×10^{-3} (S/cm) in conductivity and 40 (nm) in size. In addition, the proton conductivity of PI−Nafion−SAZBEA composite membrane at different humidity conditions and its fuel cell performance at high temperature of 140°C for DMFC will be conducted in the future. Finally, not limited to SPSE, Nafion, and the mixture of Nafion and zeolite, this approach could be extended to other electrolytes possessing better properties or different functions (e.g. anion conducting membrane) to construct the composite membrane.

REFERENCES

1. *EIA Annual Energy Outlook 2009*. DOE/EIA-0383 (2009).
2. Hart, D., *Sustainable energy conversion: fuel cells -- the competitive option?* Journal of Power Sources, 2000. **86**(1-2): p. 23-27.
3. Shukla, A.K., A.S. Aricò, and V. Antonucci, *An appraisal of electric automobile power sources.* Renewable and Sustainable Energy Reviews, 2001. **5**(2): p. 137-155.
4. Chalk, S.G., J.F. Miller, and F.W. Wagner, *Challenges for fuel cells in transport applications.* Journal of Power Sources, 2000. **86**(1-2): p. 40-51.
5. Hoogers, G., *Fuel Cell Technology Handbook*. 2003: CRC Press.
6. Scott, K., W.M. Taama, and P. Argyropoulos, *Engineering aspects of the direct methanol fuel cell system.* Journal of Power Sources, 1999. **79**(1): p. 43-59.
7. Nordlund, J. and G. Lindbergh, *Temperature-Dependent Kinetics of the Anode in the DMFC.* Journal of The Electrochemical Society, 2004. **151**(9): p. A1357-A1362.
8. Adjemian, K.T., et al., *Silicon Oxide Nafion Composite Membranes for Proton-Exchange Membrane Fuel Cell Operation at 80-140[degree]C.* Journal of The Electrochemical Society, 2002. **149**(3): p. A256-A261.
9. Jiang, R. and D. Chu, *Comparative Studies of Methanol Crossover and Cell Performance for a DMFC.* Journal of The Electrochemical Society, 2004. **151**(1): p. A69-A76.
10. Kulikovsky, A.A., *On the Nature of Mixed Potential in a DMFC.* Journal of The Electrochemical Society, 2005. **152**(6): p. A1121-A1127.
11. Liu, F. and C.-Y. Wang, *Mixed Potential in a Direct Methanol Fuel Cell.* Journal of The Electrochemical Society, 2007. **154**(6): p. B514-B522.

12. Ren, X., T.E. Springer, and S. Gottesfeld, *Water and Methanol Uptakes in Nafion Membranes and Membrane Effects on Direct Methanol Cell Performance.* Journal of The Electrochemical Society, 2000. **147**(1): p. 92-98.

13. Devanathan, R., *Recent developments in proton exchange membranes for fuel cells.* Energy & Environmental Science, 2008. **1**(1): p. 101-119.

14. Hickner, M.A., et al., *Alternative Polymer Systems for Proton Exchange Membranes (PEMs).* Chemical Reviews, 2004. **104**(10): p. 4587-4612.

15. Kreuer, K.D., *On the development of proton conducting polymer membranes for hydrogen and methanol fuel cells.* Journal of Membrane Science, 2001. **185**(1): p. 29-39.

16. Mauritz, K.A. and R.B. Moore, *State of Understanding of Nafion.* Chemical Reviews, 2004. **104**(10): p. 4535-4586.

17. Tricoli, V., *Proton and Methanol Transport in Poly(perfluorosulfonate) Membranes Containing Cs[sup +] and H[sup +] Cations.* Journal of The Electrochemical Society, 1998. **145**(11): p. 3798-3801.

18. Sone, Y., P. Ekdunge, and D. Simonsson, *Proton Conductivity of Nafion 117 as Measured by a Four-Electrode AC Impedance Method.* Journal of The Electrochemical Society, 1996. **143**(4): p. 1254-1259.

19. Baglio, V., et al., *Composite Mesoporous Titania Nafion-Based Membranes for Direct Methanol Fuel Cell Operation at High Temperature.* Journal of The Electrochemical Society, 2005. **152**(7): p. A1373-A1377.

20. Kannan, A.G., N.R. Choudhury, and N.K. Dutta, *In situ modification of Nafion® membranes with phospho-silicate for improved water retention and proton conduction.* Journal of Membrane Science, 2009. **333**(1-2): p. 50-58.

21. Chen, Z., et al., *Nafion/Zeolite Nanocomposite Membrane by in Situ Crystallization for a Direct Methanol Fuel Cell.* Chemistry of Materials, 2006. **18**(24): p. 5669-5675.

22. Holmberg, B.A., X. Wang, and Y. Yan, *Nanocomposite fuel cell membranes based on Nafion and acid functionalized zeolite beta nanocrystals.* Journal of Membrane Science, 2008. **320**(1-2): p. 86-92.

23. Takahiko Nakano, S.N.H.K., *Preparation of novel sulfonated block copolyimides for proton conductivity membranes.* Polymers for Advanced Technologies, 2005. **16**(10): p. 753-757.

24. Yasuhide Okazaki, S.N.H.K., *Proton-conductive membranes based on blends of polyimides.* Journal of Polymer Science Part B: Polymer Physics, 2007. **45**(11): p. 1325-1332.

25. Yamaguchi, T., et al., *A Pore-Filling Electrolyte Membrane-Electrode Integrated System for a Direct Methanol Fuel Cell Application.* Journal of The Electrochemical Society, 2002. **149**(11): p. A1448-A1453.

26. Yamaguchi, T., H. Kuroki, and F. Miyata, *DMFC performances using a pore-filling polymer electrolyte membrane for portable usages.* Electrochemistry Communications, 2005. **7**(7): p. 730-734.

27. Yamaguchi, T., F. Miyata, and S. Nakao, *Polymer Electrolyte Membranes with a Pore-Filling Structure for a Direct Methanol Fuel Cell.* Advanced Materials, 2003. **15**(14): p. 1198-1201.

28. Yamaguchi, T., F. Miyata, and S.-i. Nakao, *Pore-filling type polymer electrolyte membranes for a direct methanol fuel cell.* Journal of Membrane Science, 2003. **214**(2): p. 283-292.

29. Yamaguchi, T., et al., *An Extremely Low Methanol Crossover and Highly Durable Aromatic Pore-Filling Electrolyte Membrane for Direct Methanol Fuel Cells.* Advanced Materials, 2007. **19**(4): p. 592-596.

30. Yamamoto, D., H. Munakata, and K. Kanamura, *Synthesis and Characterization of Composite Membrane with Three-Dimensionally Ordered Macroporous Polyimide Matrix for DMFC.* Journal of the Electrochemical Society, 2008. **155**(3): p. B303-B308.

31. Nakajima, H., et al., *High Temperature Proton Conducting Organic/Inorganic Nanohybrids for Polymer Electrolyte Membrane.* Journal of The Electrochemical Society, 2002. **149**(8): p. A953-A959.

32. Sasajima, K., H. Munakata, and K. Kanamura, *Properties of Composite Membrane Consisting of 3DOM Silica Matrix Filled with Sulfonated Poly(1,4-phenylene ether ether sulfone) at Various Ratios.* Journal of The Electrochemical Society, 2008. **155**(2): p. B143-B147.

33. Wang, L., et al., *Sulfonated polyimide/PTFE reinforced membrane for PEMFCs.* Journal of Power Sources, 2007. **167**(1): p. 47-52.

34. Nishimura, H. and T. Yamaguchi, *Performance of a Pore-Filling Electrolyte Membrane in Hydrogen-Oxygen PEFC.* Electrochemical and Solid-State Letters, 2004. **7**(11): p. A385-A388.

35. Hara, N., et al., *Rapid Proton Conduction through Unfreezable and Bound Water in a Wholly Aromatic Pore-Filling Electrolyte Membrane.* The Journal of Physical Chemistry B, 2009. **113**(14): p. 4656-4663.

36. Liu, F., et al., *Nafion/PTFE composite membranes for fuel cell applications.* Journal of Membrane Science, 2003. **212**(1-2): p. 213-223.

37. Larminie, J. and A. Dicks, *Fuel Cell Systems Explained*. 2003: John Wiley & Son Ltd, England.

38. Stanis, R.J., et al., *Evaluation of hydrogen and methanol fuel cell performance of sulfonated diels alder poly(phenylene) membranes.* Journal of Power Sources. **195**(1): p. 104-110.

39. Wang, Z.-B., et al., *Investigation of the performance decay of anodic PtRu catalyst with working time of direct methanol fuel cells.* Journal of Power Sources, 2008. **181**(1): p. 93-100.

40. Manoharan, R. and J. Prabhuram, *Possibilities of prevention of formation of poisoning species on direct methanol fuel cell anodes.* Journal of Power Sources, 2001. **96**(1): p. 220-225.

41. Jiang, R. and D. Chu, *Water Crossover: A Challenge to DMFC System I. Experimental Determination of Water Crossover.* Journal of The Electrochemical Society, 2008. **155**(8): p. B798-B803.

42. Guo, J.W., et al., *Development of PtRu-CeO2/C anode electrocatalyst for direct methanol fuel cells.* Journal of Power Sources, 2006. **156**(2): p. 345-354.

43. Zawodzinski, J.T.A., et al., *Water Uptake by and Transport Through Nafion[sup [registered sign]] 117 Membranes.* Journal of The Electrochemical Society, 1993. **140**(4): p. 1041-1047.

44. Yang, J.H. and Y.C. Bae, *Methanol Crossover Effect for Direct Methanol Fuel Cells: Applicability of Methanol Activity in Polymer Electrolyte Membrane.* Journal of The Electrochemical Society, 2008. **155**(2): p. B194-B199.

45. Kim, Y.J., et al., *Evaluation of a palladinized Nafion(TM) for direct methanol fuel cell application.* Electrochimica Acta, 2004. **49**(19): p. 3227-3234.

46. Antonucci, P.L., et al., *Investigation of a direct methanol fuel cell based on a composite Nafion®-silica electrolyte for high temperature operation.* Solid State Ionics, 1999. **125**(1-4): p. 431-437.

47. Ye, X., H. Bai, and W.S.W. Ho, *Synthesis and characterization of new sulfonated polyimides as proton-exchange membranes for fuel cells.* Journal of Membrane Science, 2006. **279**(1-2): p. 570-577.

48. Okamoto, K.-i., et al., *Methanol permeability and proton conductivity of sulfonated co-polyimide membranes.* Journal of Membrane Science, 2005. **258**(1-2): p. 115-122.

49. Penner, R.M. and C.R. Martin, *Ion Transporting Composite Membranes.* Journal of The Electrochemical Society, 1985. **132**(2): p. 514-515.

50. Liu, C. and C.R. Martin, *Ion Transporting Composite Membranes.* Journal of The Electrochemical Society, 1990. **137**(2): p. 510-515.

51. Kricheldorf, H.R., O. Nuyken, and G. Swift, *Handbook of Polymer Synthesis*, ed. Second. 2004: CRC Press.

52. Kawakami, H., M. Mikawa, and S. Nagaoka, *Gas transport properties in thermally cured aromatic polyimide membranes.* Journal of Membrane Science, 1996. **118**(2): p. 223-230.

53. Kim, I.C., et al., *Preparation of soluble polyimides and ultrafiltration membrane performances.* Journal of Applied Polymer Science, 2000. **75**(1): p. 1-9.

54. Huang, C., et al., *High strength electrospun polymer nanofibers made from BPDA-PDA polyimide.* European Polymer Journal, 2006. **42**(5): p. 1099-1104.

55. Mazoniene, E., et al., *(Co)polyimides from commonly used monomers, and their nanocomposites.* Progress in Solid State Chemistry, 2006. **34**(2-4): p. 201-211.

56. Kawakami, H., J. Anzai, and S. Nagaoka, *Gas transport properties of soluble aromatic polyimides with sulfone diamine moieties.* Journal of Applied Polymer Science, 1995. **57**(7): p. 789-795.

57. Baker, R.W., *Membrane Technology and Applications*. 2000: McGraw-Hill.

58. Shimizu, H., H. Kawakami, and S. Nagaoka, *Membrane formation mechanism and permeation properties of a novel porous polyimide membrane.* Polymers for Advanced Technologies, 2002. **13**(5): p. 370-380.

59. Matsuyama, H., et al., *Studies on phase separation rate in porous polyimide membrane formation by immersion precipitation.* Journal of Applied Polymer Science, 2003. **90**(1): p. 292-296.

60. Wang, X., M. Waje, and Y. Yan, *Methanol Resistant Cathodic Catalyst for Direct Methanol Fuel Cells.* Journal of The Electrochemical Society, 2004. **151**(12): p. A2183-A2188.

61. Lasch, K., L. Jörissen, and J. Garche, *The effect of metal oxides as co-catalysts for the electro-oxidation of methanol on platinum-ruthenium.* Journal of Power Sources, 1999. **84**(2): p. 225-230.

62. Wang, J., et al., *Promoting the current for methanol electro-oxidation by mixing Pt-based catalysts with CeO2 nanoparticles.* Journal of Power Sources, 2007. **170**(2): p. 297-302.

63. Lee, C.H., et al., *Electrooxidation of methanol on Pt-Ru catalysts supported by basal plane graphite in phosphoric acid solution.* Journal of Power Sources, 2000. **86**(1-2): p. 478-481.

64. Jeon, M.K., et al., *Investigation of Pt/WC/C catalyst for methanol electro-oxidation and oxygen electro-reduction.* Journal of Power Sources, 2008. **185**(2): p. 927-931.

65. Shukla, A.K. and R.K. Raman, *Methanol-Resistant Oxygen-Reduction Catalysts for Direct Methanol Fuel Cells.* Annual Review of Materials Research, 2003. **33**(1): p. 155-168.

66. Tricoli, V., N. Carretta, and M. Bartolozzi, *A Comparative Investigation of Proton and Methanol Transport in Fluorinated Ionomeric Membranes.* Journal of The Electrochemical Society, 2000. **147**(4): p. 1286-1290.

67. Ren, X. and S. Gottesfeld, *Electro-osmotic Drag of Water in Poly(perfluorosulfonic acid) Membranes.* Journal of The Electrochemical Society, 2001. **148**(1): p. A87-A93.

68. Barragán, V.M., et al., *Transport of methanol and water through Nafion membranes.* Journal of Power Sources, 2004. **130**(1-2): p. 22-29.

69. Alberti, G. and M. Casciola, *Composite Membranes for Medium-Temperature PEM Fuel Cells.* Annual Review of Materials Research, 2003. **33**(1): p. 129-154.

70. Lee, C.H., C.H. Park, and Y.M. Lee, *Sulfonated polyimide membranes grafted with sulfoalkylated side chains for proton exchange membrane fuel cell (PEMFC) applications.* Journal of Membrane Science, 2008. **313**(1-2): p. 199-206.

71. Sasaki, T., et al., *High thermal stable thermoplastic-thermosetting polyimide film by use of asymmetric dianhydride (a-BPDA).* Polymer, 2005. **46**(18): p. 6968-6975.

72. Vandezande, P., et al., *High throughput study of phase inversion parameters for polyimide-based SRNF membranes.* Journal of Membrane Science, 2009. **330**(1-2): p. 307-318.

73. Kim, J.H., et al., *Phase behavior and mechanism of membrane formation for polyimide/DMSO/water system.* Journal of Membrane Science, 2001. **187**(1-2): p. 47-55.

74. Porter, M.C., *Handbook of Industrial Membrane Technology*. 1990: Noyes Publications, New Jersey.

75. Mayo, D.W., F.A. Miller, and R.W. Hannah, *Course Notes on the Interpretation of Infrared and Raman Spectra*. 2004: John Wiley & Son, Inc., New Jersey.

76. Munakata, H., D. Yamamoto, and K. Kanamura, *Three-dimensionally ordered macroporous polyimide composite membrane with controlled pore size for direct methanol fuel cells.* Journal of Power Sources, 2008. **178**(2): p. 596-602.

77. Munakata, H., D. Yamamoto, and K. Kanamura, *Properties of composite proton-conducting membranes prepared from three-dimensionally ordered macroporous polyimide matrix and polyelectrolyte.* Chemical Communications, 2005(31): p. 3986-3988.

78. Chi-Yuan Huang, W.-Y.C., *Chemical surface treatment of poly(tetrafluoroethylene) powder.* Angewandte Makromolekulare Chemie, 1993. **209**(1): p. 9-23.

79. P. Santhana Gopala Krishnan, C.Z.C.Y.S.C.J.W.C.C., *Preparation of Nanoporous Polyimide Films from Poly(urethane-imide) by Thermal Treatment.* Macromolecular Materials and Engineering, 2003. **288**(9): p. 730-736.

80. Nunes, S.P. and K.-V. Peinemann, *Membrane Technology in the Chemical Industry*. 2006: Wiley-VCH, Germany.

81. Taketani, Y., S. Nagaoka, and H. Kawakami, *Fabrication of three-dimensionally ordered microporous membrane by wet phase separation.* Journal of Applied Polymer Science, 2004. **92**(5): p. 3016-3021.

82. Chun, K.-Y., et al., *Effects of solvent on the pore formation in asymmetric 6FDA-4,4'ODA polyimide membrane: terms of thermodynamics, precipitation kinetics, and physical factors.* Journal of Membrane Science, 2000. **169**(2): p. 197-214.

83. Haufe, S. and U. Stimming, *Proton conducting membranes based on electrolyte filled microporous matrices.* Journal of Membrane Science, 2001. **185**(1): p. 95-103.

84. Ren, X., et al., *Methanol Transport Through Nation Membranes. Electro-osmotic Drag Effects on Potential Step Measurements.* Journal of The Electrochemical Society, 2000. **147**(2): p. 466-474.

85. Tricoli, V. and F. Nannetti, *Zeolite-Nafion composites as ion conducting membrane materials*, in *Electrochimica Acta*. 2003. p. 2625-2633.

86. Der-Jang Liaw, B.-Y.L.K.-L.S., *Preparation and characterization of new polyimides derived from 2,2-bis[4-[2-(4-aminophenoxy)ethoxy]phenyl]sulfone.* Polymers for Advanced Technologies, 1999. **10**(1-2): p. 13-19.

87. S. P. Jiang, Z.L.Z.Q.T., *Layer-by-Layer Self-Assembly of Composite Polyelectrolyte-Nafion Membranes for Direct Methanol Fuel Cells.* Advanced Materials, 2006. **18**(8): p. 1068-1072.

88. Cable, K.M., K.A. Mauritz, and R.B. Moore, *Anisotropic ionic conductivity in uniaxially oriented perfluorosulfonate ionomers.* Chemistry of Materials, 1995. **7**(9): p. 1601-1603.

89. Buchi, F.N. and G.G. Scherer, *Investigation of the Transversal Water Profile in Nafion Membranes in Polymer Electrolyte Fuel Cells.* Journal of The Electrochemical Society, 2001. **148**(3): p. A183-A188.

90. Vorrey, S. and D. Teeters, *Study of the ion conduction of polymer electrolytes confined in micro and nanopores.* Electrochimica Acta, 2003. **48**(14-16): p. 2137-2141.

91. Liu, Y., et al., *Reinforced and self-humidifying composite membrane for fuel cell applications.* Journal of Membrane Science, 2009. **330**(1-2): p. 357-362.

92. Slade, S., et al., *Ionic Conductivity of an Extruded Nafion 1100 EW Series of Membranes.* Journal of The Electrochemical Society, 2002. **149**(12): p. A1556-A1564.

93. Silva, R.F., M. De Francesco, and A. Pozio, *Tangential and normal conductivities of Nafion® membranes used in polymer electrolyte fuel cells.* Journal of Power Sources, 2004. **134**(1): p. 18-26.

94. Yildirim, M.H., et al., *Impregnated membranes for direct methanol fuel cells at high methanol concentrations.* Journal of Membrane Science, 2009. **328**(1-2): p. 127-133.

95. Roderick, W.R. and P.L. Bhatia, *Action of Trifluoroacetic Anhydride on N-Substituted Amic Acids1,2.* The Journal of Organic Chemistry, 1963. **28**(8): p. 2018-2024.

96. Oren, Y., V. Freger, and C. Linder, *Highly conductive ordered heterogeneous ion-exchange membranes.* Journal of Membrane Science, 2004. **239**(1): p. 17-26.

97. Brack, H.P., et al., *A contact angle investigation of the surface properties of selected proton-conducting radiation-grafted membranes.* Journal of Membrane Science, 2003. **214**(1): p. 1-19.

98. Gardner, C.L. and A.V. Anantaraman, *Studies on ion-exchange membranes. II. Measurement of the anisotropic conductance of Nafion®.* Journal of Electroanalytical Chemistry, 1998. **449**(1-2): p. 209-214.

99. Merlo, L., et al., *Resistance to peroxide degradation of Hyflon® Ion membranes.* Journal of Power Sources, 2007. **171**(1): p. 140-147.

100. Tsuji, K., C.W. Jones, and M.E. Davis, *Organic-functionalized molecular sieves (OFMSs): I. Synthesis and characterization of OFMSs with polar functional groups.* Microporous and Mesoporous Materials, 1999. **29**(3): p. 339-349.

101. Jones, C.W., K. Tsuji, and M.E. Davis, *Organic-functionalized molecular sieves (OFMSs):: II. Synthesis, characterization and the transformation of OFMSs containing non-polar functional groups into solid acids.* Microporous and Mesoporous Materials, 1999. **33**(1-3): p. 223-240.

102. Jones, C.W., K. Tsuji, and M.E. Davis, *Organic-functionalized molecular sieves as shape-selective catalysts.* Nature, 1998. **393**(6680): p. 52-54.

103. Holmberg, B.A., et al., *Synthesis and proton conductivity of sulfonic acid functionalized zeolite BEA nanocrystals.* Microporous and Mesoporous Materials, 2005. **80**(1-3): p. 347-356.

104. Schoeman, B.J., et al., *The Synthesis of Discrete Colloidal Crystals of Zeolite Beta and their Application in the Preparation of Thin Microporous Films.* Journal of Porous Materials, 2001. **8**(1): p. 13-22.

105. Jones, C.W., et al., *Organic-functionalized molecular sieves. III. Shape selective catalysis.* Microporous and Mesoporous Materials, 2001. **42**(1): p. 21-35.

106. Chen, T.-Y. and J. Leddy, *Ion Exchange Capacity of Nafion and Nafion Composites.* Langmuir, 2000. **16**(6): p. 2866-2871.

107. V. Tricoli, N. Carretta, and M. Bartolozzi, *A Comparative Investigation of Proton and Methanol Transport in Fluorinated Ionomeric Membranes*, Journal of The Electrochemical Society, 2000. **147**(4): p. 1286-1290.

108. M.P. Godino, et al., *Study of the Activation Energy for Transport of Water and Methanol through a Nafion Membrane*, Chemical Engineering Journal, 2009. **152**: p. 20-25.